Johannes W. Judex

Diss. No. 18865

Grass for Power Generation

GRASS FOR POWER GENERATION –

Extending the Fuel Flexibility for IGCC Power Plants

JOHANNES W. JUDEX

DISS. ETH N° 18865

– Grass for Power Generation –
Extending the Fuel Flexibility
for IGCC Power Plants

A dissertation submitted to

ETH ZURICH

for the degree of

Doctor of Sciences

presented by

Johannes W. Judex

Dipl.-Ing. TU-Berlin

Born on
July 6th 1977
Citizen of Germany

accepted on the recommendation of

Prof. Dr. Alexander Wokaun
Prof. Dr. Massimo Morbidelli
Dr. Serge M. A. Biollaz

2010

Contents

Abstract

The situation of the current electrical power production is characterised by a trend to use more and more alternative energies and the fact that the European power plant fleet is ageing. Since the electrical consumption is expected to increase further, old power plants which are to be switched off need to be replaced. There are two main candidates of large power plant types being discussed:

✧ natural gas combined cycle plants

✧ nuclear power plants

Nuclear power plants are not suited to implement alternative energies, whereas combined cycle power plants can be equipped with a biomass gasifier. In this way an IGCC power plant is designed, which can fully or partially run on biomass. There is also a need to employ additional biomass feed stock types like annual plants. In this work grass is studied as additional energy resource for IGCC applications. Being able to use grass as supplementary feed stock would increase the fuel flexibility of IGCC power plants.

✧ A review of the chemical and physical properties of grass as solid fuel was carried out. Grass contains a very large number of different inorganic elements mostly in minor amounts. It revealed that in addition to the elements causing corrosion in gas turbines at least Sr and Ba are found in grass. Both show similar corrosiveness to the known alkalis K and Na. Earth alkali elements (Mg, Ca) also being known for depositions and corrosion enhancement, are present in critical amounts in the fuel. It is unsure whether the positive effects (binding sulphur or vanadium) or the negative effects (deposition, surface damage) will prevail. The generally low energy density can be avoided by on-field densifica-

tion or immediate pyrolysis. The water content can be expected to be lower than for all other biomasses owing to good drying properties and the possibility of on-field drying.

✧ For the integration into IGCC power plants the grass must be thermally gasified. A lab-scale fluidised bed gasification reactor was designed and put into operation. Air blown gasification experiments were conducted with grass and thereby the stability of the process and emission of contaminants, relevant for gas turbine applications, was analysed (i. e. K, Na, Mg, Ca, Pb, V).

✧ Gasification experiments were carried out between 700 and 750 °C for fuel to air ratios between 0.17 and 0.35. Different bed materials (dolomite, SiO_2, Al_2O_3) were tested: dolomite was excluded after first trials, because it appeared unsuitable for fluidised bed applications due to its mechanical weakness. Silica sand was used for 700 °C only since the ash melting behaviour of grass together with silica indicated agglomeration above 700 °C. The experiments at this temperature were conducted without bed agglomeration or defluidisation. Alumina bed material was used for 700 and 750 °C, since the ash melting behaviour of grass together with alumina proved to be less critical at higher temperatures. A 10 h run was conducted to see if unstable situations in the gasification process can occur. All experiments succeeded without any defluidisation or agglomeration. Axial temperature profile measurements proved an isothermal behaviour. The axial devolution of the superficial gas velocity is evident but still moderate. Despite the low temperature of 700 to 750 °C, the tar concentration is lower than for fluidised bed wood gasification given in literature.

✧ The contaminants in the gas phase where analysed by means of a dedicated sampling train and an ICP-OES device. It was shown that by applying a hot gas filter at 400 °C all the contaminant concentrations aside from potassium and sodium were low enough to satisfy the gas turbine limits. Sodium was found in concentrations higher than the allowed limit for mono-fuel applications. The concentrations are low enough if a cofiring approach with natural gas is targeted. Potassium could not be quantified at the given concentration level due to the insensitive response of the ICP-OES to potassium. Secondary measures other than hot gas clean up to reduce contaminants were not employed.

✧ A novel single pellet gasifier was designed and commissioned in order to investigate the transient gasification of a single pellet. The reactor showed similar characteristic as the fluidised bed with respect to gas devolution, fuel size and heating rate of the fuel. The experiments proved to be fully reproducible. By means of a surface ionisation detector, the alkali emission for different grass pellets was monitored qualitatively. The results revealed that around 90 % of the alkalis are emitted during the combustion phase of the char. The remaining 10 % are released due to the volatilisation during the pyrolysis and gasificaition. Leaching and doping with potassium and sodium of the grass influenced the emission during the combustion phase much stronger than during the volatilisation. The implementation of a hot gas filter at 400 °C resulted in a heavily reduced alkali emission. The results indicated, that the passing alkali fraction is released during the pyrolysis, wheras the larger fraction emitted from the char combustion could be separated.

Grass is by any means suitable to be gasified in a fluidised bed gasifier. Hot gas filtration at 400 °C is sufficient if the cofiring concept is followed. However, secondary measures are required to further reduce the sodium concentration if the mono-fuel concept is chosen.

Kurzfassung

Die momentane Situation der Elektrizitätsproduktion ist gekennzeichnet durch die Tendenz steigender Anteile an erneuerbaren Energien sowie eine stetige Veralterung des europäischen Kraftwerksparks. Kraftwerke, die altersbedingt vom Netz genommen werden, müssen durch neue und effizientere Kraftwerke ersetzt werden. Da ein weiterer Anstieg des Elektrizitätskonsums erwartet wird, müssen zudem zusätzliche Kraftwerke geschaffen werden. Zur Zeit sind zwei Kraftwerkstypen vorzugsweise in der Diskussion.

✧ Erdgas gefeuerte Gas- und Dampfkraftwerke (GuDs) und

✧ Atomkraftwerke der neusten Generation

In Atomkraftwerke können keine erneuerbaren Energien im Sinne eines Ersatzes implementiert werden. Im Gegensatz dazu können in GuDs Biomassevergaser integriert werden, die beliebige Teile des ansonsten verwendeten Erdgases duch sogenanntes Syngas ersetzen können. Die Vergaser werden heute in der Regel mit Kohle betrieben, lassen aber die Möglichkeit offen auch Biomasse einzusetzen.

Aufgrund der zum Teil mangelnden Verfügbarkeit herkömmlicher Biomasse (Holz, Restholz) besteht die Notwendigkeit zusätzliche Ressourcen wie z. B. jährige Pflanzen auf ihre Eignung zu prüfen.

In dieser Arbeit wird die Eignung von naturbelassenem Gras für den Einsatz in GuDs mit integrierter Vergasung überprüft. Die Möglichkeit Gras als Brennstoff zu nutzen würde die Brennstoffflexibilität für zukünftige Anlagen erhöhen. Folgende Bereiche und Themen wurden deshalb in der vorliegenden Dissertation bearbeitet:

✧ Eine Übersicht über die physikalischen und chemischen Eigenschaften von Gras als fester Brennstoff wurde herausgearbeitet

und vergleichend mit anderen festen Bioenergieträgern dargestellt. Gras enthält eine vergleichbar grosse Anzahl an anorganischen Elementen, die meisten davon jedoch in geringen Mengen. Zusätzlich zu den bekannten Elementen wie K, Na, Mg, Ca oder V, die zu Beschädigungen an der Gasturbine führen, sind in der Vergangenheit im Gras Barium und Strontium nachgewiesen worden, die eine ähnliche oder stärkere Korrosivität zeigen als die oben erwähnten Alkalimetalle. Insgesamt sind besonders die Alkali- und Erdalkalimetalle im Gras in kritischen Mengen vorhanden. Aus der Übersicht geht nicht hervor, ob z. B. bei Elementen wie Ca das Binden von Schwefel als positiver Effekt oder eine höhere Emission und letzlich Ablagerung und Oberflächenzerstörung überwiegen werden. Die im Vergleich zu verholzter Biomasse niedrigere Energiedichte von Gras kann teilweise durch das Trocknen auf dem Feld und schnellstmögliche Verdichtung zu Ballen oder Pellets oder durch Pyrolyse kompensiert werden. Durch eine Feldtrocknung kann ein geringerer Wassergehalt erwarten werden, als bei herkömmlichen biogenen Brennstoffen.

✧ Für die erfolgreiche Integration in ein GuD mit integrierter Vergasung muss das Gras effizient und problemlos vergast werden können. Um dies zu demonstrieren wurde eine luftbetriebene Wirbelschichtvergasungsanlage im Labormassstab (5kW) aufgebaut und betrieben. Verschiedene Experimente wurden durchgeführt, um die Prozessstabilität zu demonstrieren, sowie die für die Gasturbine relevante Störstoffemission (K, Na, Mg, Ca, Pb, V) nachzuweisen.

✧ Vergasungsexperimente wurden für Luft-Brennstoffverhältnisse zwischen 0.17 und 0.35 und Temperaturen zwischen 700 und 750 °C durchgeführt. Verschiedene Bettmaterialien (Dolomit, SiO_2, Al_2O_3) wurden getestet: Dolomit wurde nach den ersten Versuchen ausgeschlossen, da die mechanische Beanspruchung in der Wirbelschicht das Material aufrieb und der verbleibende Staub ausgetragen wurde. Siliziumoxid wurde für Experimente bis 700 °C verwendet, da aufgrund des hohen Kaliumgehaltes von Gras für höhere Temperaturen die Gefahr der Bettagglomeration gegeben ist. Bei dieser Temperatur konnten jedoch alle Experimente ohne Defluidisierung oder Bettagglomerationen durchgeführt werden. Aluminiumoxid wurde für Temperaturen bis 750 °C verwendet, da für diese Temperatur noch keine Gefahr der Ascheschmelze ge-

geben ist. Ein $10\,h$ Langzeitversuch wurde durchgeführt, um für eine längere Zeitspanne die Prozessstabilität zu demonstrieren. Alle Experimente wurden ohne Probleme wie Defluidisierung oder Ascheagglomerationen durchgeführt. Durch axiale Profilmessungen wurde eine gute thermische Durchmischung nachgewiesen. Trotz der niedrigen Prozesstemperatur ist der Teergehalt niedriger als für die in der Literatur angegebene Wirbelschichtvergasung für Holz.

✧ Die Störstoffe in der Gasphase wurden mit Hilfe eines eigens dafür optimierten Probenahmesystems und eines ICP-OES online und offline analysiert. Durch die Anwendung eines Warmgasfilters bei $400\,°C$, waren alle Störstoffkonzentrationen mit Ausnahme von Kalium und Natrium niedrig genug, um die Gasturbinenrichtlinien einzuhalten. Die Konzentration von Natrium war geringfügig zu hoch, um die Grenzwerte für ein rein grasbetriebenes GuD (Graskraftwerk) einzuhalten. Kalium konnte aufgrund der geringen Sensitivität des Messgerätes nicht nachgewiesen werden. Die Nachweisgrenze war zudem zu hoch, um eine ausreichend niedrige Konzentration für ein Graskraftwerk zu messen. Alle Konzentrationen sind jedoch ausreichend niedrig, um ein GuD zu betreiben, in dem $10\,\%$ des Heizwertes durch die Vergasung von Gras, der Rest durch Erdgas zur Verfügung gestellt wird. Sekundärmassnahmen um die Störstoffkonzentration zu beeinflussen, wurden mit Ausnahme des Warmgasfilters nicht eingesetzt. Solche Massnahmen müssen jedoch eingesetzt werden, um die Grenzwerte für ein Graskraftwerk zu erreichen.

✧ Ein neuartiger Einpellet–Reaktor wurde konstruiert, um die transiente Vergasung eines einzelnen Pellets zu beobachten. Der Vergaser zeigte eine ähnliche Charakteristik wie die Wirbelschicht hinsichtlich der Brennstoffgrösse, Heizrate und Gasentwicklung während der Pyrolyse. Durch die Verwendung eines Oberflächenionisierungssensor (engl. SID) konnte die Alkali (K + Na) Emission qualitativ während der Vergasung und Verbrennung eines einzelnen Pellets dokumentiert werden. Die Ergebnisse ergaben, dass die Hauptemission der Alkalien ($90\,\%$) während der Restkoksverbrennung stattfindet. Die verbleibenden $10\,\%$ werden während der Trocknung, Pyrolyse und Vergasung freigesetzt. Das Auswaschen der Alkalien aus dem Gras sowie das Zusetzen von Alkalien zu dem Gras führte in beiden Fällen hauptsächlich zur

Beeinflussung der 90 % aus dem Reskoks freigesetzen Alkalien. Der Einsatz eines Warmgasfilters bei 400 °C führte erwartungsgemäss zu einer stark reduzierten Alkaliemission. Die durch den Filter passierenden Alkalien stammten aus dem kleinen Anteil, der während der Pyrolyse freigesetzt wird.

Die vorliegenden Untersuchungen haben eindeutig gezeigt, dass sich Gras zur Vergasung in einer Wirbelschicht bei moderaten Temperaturen bis 750 °C sehr gut eignet. Eine Warmgasfiltration des Rohgases bei 400 °C ist ausreichend, wenn das Gas im obigen Sinne in einer Co-Verbrennung mit Erdgas verwendet werden soll. Zusätzliche Sekundärmassnahmen sind jedoch erforderlich, wenn das Gas in einem Graskraftwerk verwendet werden soll.

Nomenclature

Symbol	Unit	Explanation
Latin symbols		
c_p	$kJ/(kg\,K)$	Specific heat
g	m/s^2	Standard gravity
HHV	MJ/kg, MJ/m^3	Higher heating value
ΔH_R^0	$MJ/kmol$	Standard enthalpy of formation ($25\,°C, 1\,bar$)
LHV	MJ/kg, MJ/m^3	Lower heating value
$\dot{M}_i$	kg/s	Mass flow of the component i
$\tilde{M}$	g/mol	Molar mass
$\dot{V}_i$	m^3/s	Volume flow of the component i
$\dot{Q}_i$	W	Energy flow of the component i
T	K	Kelvin temperature
u_{mf}	m/s	Minimum fluidisation velocity
w	kg/kg	Water content
x_i	%, ml/m^3	Gas phase concentration
y_i	$\mu g/l$	Contaminant concentration in the solvent
Abreviations		
ATP		Adenosine triphosphate
CCA		Chromium copper arsenate
CPC		Condensation particle counter
DL		Detection limit
DS		Dry substance
ECN		Energieonderzoek Centrum Nederland
eDaB		elemental Data Base
FC		Fixed carbon
FID		Flame Ionization Detector
FP		Flow point
GC		Gas chromatograph
GE		General Electric Power
HTSG		High Temperature Steam Generator
ICP-OES		Inductively coupled plasma optical emission spectrometry
IGCC		Integrated gasification combined cycle
MP		Melting point
MS		Mass spectrometer
pH		Potentia Hydrogenii (measure of the acidity or basicity)

PM1		Particulate matter smaller than 1 μm
PSI		Paul Scherrer Institute (research institute in Switzerland)
RDF		Residue Derived Fuel
RWE		Rheinisch-Westfälisches Elektrizitätswerk
SDBS		Spectral database for organic compounds
SID		Surface ionisation detector
SP		Sinter point
TCD		Thermal Conductivity Detector
TGA		Thermo gravimetric analysis
VM		Volatile mater
VTT		Valtion Teknillinen Tutkimuskeskus (Technical Research Centre of Finland
XPS		X-ray Photoelectron Spectroscopy

Greek symbols

Φ		Eccentricity factor
Ψ_C	–	carbon conversion
ϵ_{mf}		Void fraction at minimum fluidisation
ϵ		Emission factor for radiation calculations
η_C	–	cold gas efficiency
η_H	–	hot gas efficiency
η	Pa s	dynamic viscosity
ϑ	°C	Celsius temperature
λ	–	air to fuel ratio, equivalence ratio
ν	m^2/s	Kinematic viskosity
ρ_i	kg/m^3	density of the component i
σ		Stefan-Boltzmann constant
ϕ	kg/kg	Ratio of exhaust gas flow to fuel gas flow
ξ_i	kg/kg	Mass ratio of component i

Dimensionless numbers

Ar	–	Archimedes number
Nu	–	Nusselt number
Re	–	Reynolds number
Gr	–	Grashof number
Pr	–	Prandtl number

Subscripts and unit extensions

AR	as received
at	By atomis, mainly as %at
da	dry ash
el	electrical
FP	Flow point
MP	melting point
SP	Sinter point
th	thermal
vol	By volume, mainly as %vol
w	By weight, mainly as %w

Introduction

Renewable energy is not a topic for green activists anymore for quite
some time. Companies like Nuon start to introduce biomass into their
large size power plants [1]. In many countries the power plant fleet
is ageing and compensation is needed. This is an excellent chance
to introduce biomass into the power plant installations. There are
mainly two reasons: firstly this strategy would lessen the dependency
on fossil fuels, which are finite and emit much CO_2; and secondly the
compensation for CO_2 emissions will be reduced.

In the age of considerable increase of alternative energy in power pro-
duction, the shortage of wood as energy resource in Europe is becoming
more evident. The Pulp and Paper Industry in Germany [2] depicts that
the extensive use of wood for energy production increases its market va-
lue, which in return locally raises the production costs of paper. On the
other hand paper price is traded on international markets. Production
of paper in this situation will become less profitable. A phenomenon
arising from the shared exploitation of resources. The material will go
the the technology that generates the largest revenue.

The consequence is the increased search for additional biomass feed
stocks. Annual plants are a family of feed stocks gaining more and
more interest. Among those, agricultural residues as well as energy
crops play a major role. A neglected part of this family is native grass.
It becomes available due to a steady increase in preserving the cultural
landscape.

In some regions grass may be available as energy resource and could
be used as such if adequate characterized. At this moment grass is
considered to be one of the more difficult and least economical biomass
fuels due to its low bulk density and high amount of inorganic com-

ponents. The idea of gasifying grass for energy production has been followed before [3–5] but not consequently.

The usage of grass can be positively linked to environmental issues [6]. Erosion is a problem, which can be addressed by planting energy crops and grass [7; 8]. Reduced nitrate leaching was observed by Christian and Riche [9] when miscanthus was established. Those plants reach a very fast cover of exposed soil. It was also reported that growing perennial grasses in suitable places can remove CO_2 from the atmosphere into constant soil carbon [10–12] (via root material) and subsequent increase in soil carbon [13]. This again improves soil quality by preventing leaching of essential nutrients. Plants can also be used to retrieve contaminations from industrial soils. The elements they bind, can be extracted later on in thermal processes [14].

Mostly native grass is considered to be used in fermentation processes (e. g. [15]). The product consists of roughly 60% CH_4 and 40% CO_2, which must be separated in order to get a feeding allowance into the existing natural gas grid. The technologies are not yet as sophisticated as they should be. The slip stream of methane in the exhaust line is far too high [16] – between 2 and 10 % – that could lead to second thoughts about the ecological impact of the concept. Fritsche et al. [17] reported that the energy potential of grass can be used more efficiently when being combusted. Also, the floor space required for a fermentation unit of an equal energy output, is beyond those for equivalent thermal units. This is mainly based on the much longer residence time of the fuel and thus a larger plant for the same output. Around $50\,MW_{th}$ of methane is planed to be produced in Güstrow (D) on a site with $20\,ha$ space floor [1]. The Skyve gasification plant uses approx.. $1\,ha$ for an output of $14\,MW_{th}$. Raising the output to $50\,MW_{th}$ would increase the space floor by a factor of 3.5 max. The carbon conversion is also much lower compared to thermal units. But still the technology is competitive being much simpler and easier to implement.

Another option is the combustion [18]. It produces only heat for steam applications including steam turbines. Steam turbines show a lower efficiency than gas turbines. This option is not considered here on purpose because the process should produce a maximum of electrical energy. At this time the state of the art technology is an IGCC plant (section 1.1). Fuel cell technologies for gasification applications are still

---

[1]http://nawaro.ag

not fully developed and therefore not available on the market. Also, the given efficiencies normally do not include the production of the fuel gas and can not be compared as they come.

At this time woody biomass is characterised and reviewed very nicely in various publications [19–26]. Some publications deal with special types of plants to study their use as biomass feedstock [27–29; 10]. These are mostly of local interest. Only a few already try to tackle the biomass feedstock of natural grassland species [3; 4; 20; 30]. In 1993 fluidised bed gasification experiments were carried out for ryegrass [3]. In 1995 some experiments were conducted to proof the feasibility of the gasification of alfalfa residues in a fluidized bed gasifier [4]. In 1997 modelling of a B-IGCC power plant was taken up to investigate the economic feasibility of various solid fuels among, which verge grass was a candidate [31]. The author calculated net efficiency of the combined cycle being 39 % by using an Aspen Plus$^{®}$ model. The chosen gas turbine was a GE LM 2500 with a gasifier input of almost 70 MW_{th}. Being ten years old, these results would likely improve due to better system efficiencies. Grass was assumed to be partially availabe as waste product.

Being a neglected fuel so far, there is still need to a much more detailed analysis of the grass as fuel and the gasification process with grass. This thesis especially aims to the characterisation of grass as fuel for the application in integrated gasification combined cycles. This includes the characterisation of the fuel, the stability of the gasification process and the contaminant monitoring in the product gas. A dedicated sampling system was used especially capable of collecting not only tars and water but also aerosol particles to a high degree. See the next graph for a visualised structure of the thesis.

Visualised structure of this thesis

Chapter 1
IGCC power plants and gas
turbine requirements
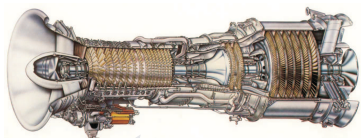
General Electric LM2500 Gas Turbine

Chapter 2
Characterisation of grass as fuel
for power generation. Elemental
analysis and technical implications
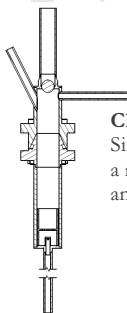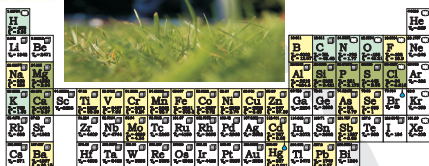
Chapter 5
Single pellet gasification with
a novel reactor. First tests
and online alkali monitoring

Chapter 3
Sampling system to support
online analysis of permenaent
gases and contaminants

Chapter 4
Fluidised bed gasification
experiments of grass. Stability,
and contaminant analysis
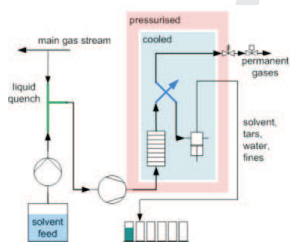
Scope

The scope of this thesis by summarising the introduction is split into three distinct parts:

✧ the properties of grass and the corresponding impacts on gasification and subsequent combustion

✧ the stability of grass gasification for various conditions

✧ the monitoring of the concentrations of the contaminants in the product gas

The first part is covered by a literature review about grass, its physical and chemical properties with regard to gasification and gas turbine application. By this review grass is also compared to other types of solid fuel such as wood, agricultural residues, energy crops ans coal.

The second part requires the construction of a fluidised bed gasification reactor seeming best suitable. With this reactor experiments are carried out to prove or disprove that stable operation of grass gasification is possible.

The third part requires the further development and characterisation of an appropriate sampling system to be able to monitor the contaminants in the raw gas continuously.

Chapter 1

IGCC power systems with grass

1.1 IGCC power plants

An IGCC (Integrated Gasification Combined Cycle) power plant consists of three major units. The classic gas turbine cycle, the steam turbine cycle, which draws its energy out of the exhaust gas of the gas turbine and the gasification island that provides the combustible gas to the gas turbine (figure 1.1) [32]. The natural gas fired combined power plant – as a base case – shows efficiencies up to 60 % (see figure 1.4). The major draw back in the past was the comparably high specific cost for the installation. Today this technology offers new opportunities due to the increase of the overall efficiency. Additionally, there is a tendency of the suppliers to incorporate gasification technologies in order to be able to offer an entire power plant, which decreases the costs.

Figure 1.2 shows a brief history of IGCC installations (detailed numbers in [33–38]). The first demonstration unit was built in Lünen, Germany in 1972. The installation used the Lurgi gasifier and a Siemens V93 gas turbine – the plant size was 163 MW_{el}. The next installation followed in 1984 in Cool Water, USA. The gas turbine was delivered by GE[1]. The gasifier was an entrained flow type Texcao. Famous coal IGCC installations are Buggenum (253 MW_{el}) in Netherlands, Puertollano (300 MW_{el}) in Spain or Wabash River (262 MW_{el}) in the US. The

---

[1]General Electric Power
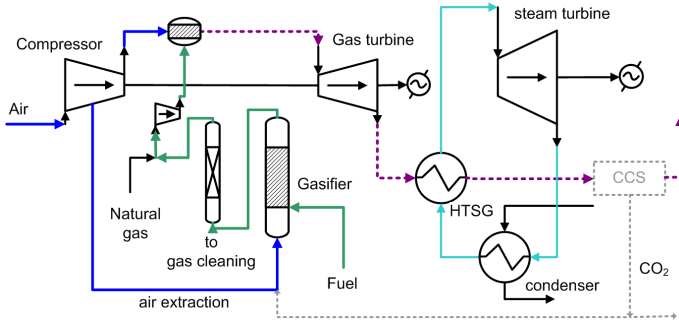
Figure 1.1: *Simplified process flow of an IGCC power plant with optional CCS*

first biomass IGCC (B-IGCC) plant was set up in Värnamo, Sweden in 1993 by Sydkraft. The gas turbine was a typhoon type from Alstom. The thermal power of the pressurised circulating fluidised bed gasifier was 18 MW_{th}. Many plants followed most with coal gasifiers – some as big as 700 MW_{el}. From the graph it can be derived, that the importance of IGCC power plants is still growing. Current IGCC proposals usually include the promise to be »*carbon capture ready*«. This aims to decrease the CO_2 emission, which will safe expenses for CO_2 penalties. This on one hand makes the installation more attractive, but on the other hand reduces the overall efficiency due to the additional unit. Plans for the future have been proposed and partially started. Examples are: Siemens [39] plans large plants with its newly bought gasification technology now called SFG (former Future Energy GSP) in China. Nuon[2] started to built its »Magnum« plant in Eemshaven, Netherlands [40; 1]. It is planned to be finished by 2011 and is supposed to run partially on biomass. The biomass portion will be increased from year to year with the goal of replacing natural gas. RWE[3] began planning an IGCC-CCS plant (with carbon capture and sequestration) in 2008 [38]. It is planned to be commissioned in 2015.

1.2 Options to integrate grass into existing power plants

The general options to integrate biomass into an IGCC installation are listed below:

---

[2] Dutch energy electricity company now owned partially by Vattenfall
[3] Rheinisch-Westfälisches Elektrizitätswerk AG

1
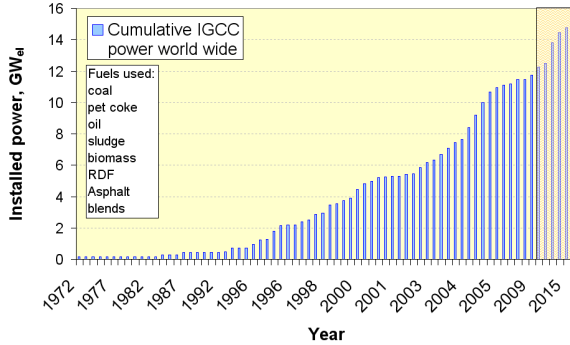
Figure 1.2: *History of IGCC power plant installations. Not all power plants depicted here are still running*

⬦ mono-fuel type: building a new B-IGCC like Värnamo. This usually limits the size of the power plant, due to the limited fuel supply.

⬦ cofiring type: building a new natural gas combined cycle and include a gasifier, which replaces certain amounts of the natural gas energy.

⬦ retrofitted type: retrofit an existing combined cycle plant with a biomass gasifier.

⬦ blending type: blend a coal or waste gasifier of an existing IGCC plant with biomass supplies.

The mono-fuel plant clearly is the option with the most limited size due to the comparably low availability of grass.

Building a new plant and integrating the gasifier from the start would certainly yield on optimised infrastructure and a larger plant size.

Retrofitting an exiting plant with a gasifier is a matter of space, because for energetic reasons the gasifier installation should be located close the bottoming cycle.

Blending an existing coal fired IGCC plant with grass depends on the type of gasifier. It is, e. g., by all means possible to feed grass into an entrained flow reactor, where the low melting point of the ash is even welcome. It is however difficult to feed grass into an existing fluidised

bed gasifier running at temperatures up to 900 °C, and hereby risking bed agglomeration.

As history and science showed, a mono-fuel plant needs adopted turbine burners due to the difference in combustion properties between syngas and natural gas [41]. But this type also yields the lowest emission impacts. In contrast, a blend of natural gas with up to 20 % hydrogen and CO can be burned in a standard burner without modification [42]. For short termed introduction of grass – with a comparably limited availability – into future installations the option to blend the syngas with natural gas will likely to be more successful. Otherwise the plants will be too small to replace a substantial part of the aging power plant fleets (see section 1.6).

From the point of the gasifier the contaminant emission only is relevant. From the point of the gas turbines there are only two types of plants which differ in their gas composition. For the above reasons only the mono-fuel and cofiring type will be considered further in this thesis enclosing the other two types automatically.

1.3 Manufacturers implementation of syngas into gas turbine cycles

Adopted low LHV gas burners have been available for quite some time now and were successfully installed e. g. in Värnamo. Now the major gas turbine manufacturers like GE [34], Siemens [43] or Alstom [44] put much effort in developing syngas burners capable of burning not only syngas but also various blends of syngas and natural gas. As it is reported by Brdar and Jones [34] GE already has a burner, that is capable of changing blends under full load. The difficulties are mainly the content of H_2 in the gas. Hydrogen does stabilize the flame up to a certain amount, which is related to its high laminar flame speed (fast flame propagation). When using premixed combustion, there is a limit for the H_2 concentration, when the flame flashes back into the burner nozzle at this point the burner has to be modified [42]. The reacted gas should enter the turbine quickly to avoid early cooling; the combustion chamber must be shorter for short flames. At the other end the flame becomes long (slow flame propagation) if less hydrogen is in the gas and the reactions are not fully completed when the gas enters the turbine

blades. The burner must be modified accordingly to flame properties being expected from the entire range of different blends.

The hydrogen content in air blown gasification usually does not exceed 15 %. For the combustion set this is a moderate concentration even more if mixed with natural gas. The proposed mixture of 10 % LHV (44 % vol) would lead to a mixture like the one listed in table 1.1 column 3. As it will be obvious the hydrogen content is very moderate. The table lists only the major components. The blend though was calculated including the minor components C_2H_2, C_2H_6, C_3H_6 from the gasifier and C_3H_6, C_3H_8 from the natural gas grid. The blend now can not be considered as low LHV fuel anymore. As it was reported in Judex et al. [45] this mixture can be processed in normal gas turbine combustors without any modifications. It is therefore suitable to retrofit existing natural gas combined cycles.

% LHV syngas blend	5.00	10.00	15.00	20.00	25.00
CH_4	70.64	55.32	45.72	39.14	34.36
CO	3.04	4.68	5.70	6.41	6.92
H_2	3.30	5.08	6.20	6.96	7.52
C_2H_4	0.23	0.35	0.42	0.48	0.51
CO_2	5.53	8.51	10.39	11.67	12.60
N_2	16.41	25.29	30.84	34.65	37.42
LHV, MJ/m^3	26.90	21.79	18.59	16.40	14.80

Table 1.1: *Example of syngas/ natural gas blends based on the gasification experiments (dry) and commercial natural gas*

1.4 Gas turbine restrictions

It is very difficult to get coherent data on gas turbine requirements, since it always depends strongly on the type of turbine, age, manufacturer and experience of the operator. This is probably the reason why the published data is so heterogeneous e. g. in [46; 47; 31; 48–52]. From table 1.2 it can be concluded that in the first step of research, elements like given in reference [52] (Na, K, Pb, V, Ca, Mg) should be monitored more closely. An then secondary measures can be applied. For further analysis the data given by [52] only is taken into account. It is the most restrictive data found in literature. It may be that a different manufacturer allows higher concentrations of contaminants.

The numbers are given as concentrations in the fuel flow. The value depends on the effective flow at the turbine inlet (combustion chamber outlet see figure 1.3). Thus, the table gives different values for different ratios of turbine inlet flows to fuel flows φ as defined by equation (1.1).

Configuration $\longmapsto$		GE**	cofiring	GE**	mono-fuel
λ assumed $\longmapsto$		–	2	–	3.8
$\varphi \longmapsto$		50	18*	12	4.5*
K + Na	mg/kg_{fuel}	0.3	0.108	0.072	0.027
Pb	mg/kg_{fuel}	1	0.36	0.24	0.04
V	mg/kg_{fuel}	0.5	0.18	0.12	0.02
Ca	mg/kg_{fuel}	2	0.72	0.48	0.08
Mg	mg/kg_{fuel}	2	0.72	0.48	0.08

Table 1.2: *Gas turbine specifications and inlet limits (*interpolated [52], **as published)*
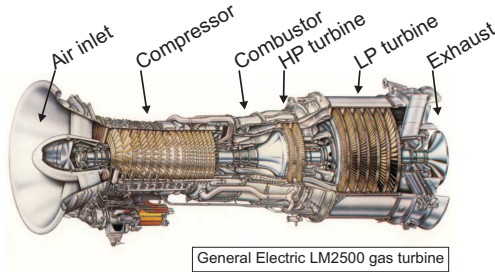
Figure 1.3: *GE LM2500 aero derivative gas turbine [53] (HP: high pressure, LP: low pressure)*

$$\varphi = \frac{\text{exhaust gas flow, } kg/h}{\text{fuel gas flow, } kg/h} \qquad (1.1)$$

To get appropriate numbers for φ for the cases of cofiring and mono-fuel, λ must be assumed. The interpolated columns were calculated for the 10 % LHV mixture ($\varphi = 18$) and mono-fuel ($\varphi = 4.5$). The air to fuel ratio in the gas turbine was proposed to be $\lambda = 2$ ($\varphi = 18$). This is a good value for syngas mixtures. Increasing the combustion air would lead to higher tolerances of the elements. For a mono-fuel plant with

a low LHV gas, the limits are more restrictive, since φ will be much smaller. The combustion air was proposed to yield $\lambda = 3.8$ according to the B-IGCC plant in Värnamo.

From the fuel review in the first part of this work it was derived, that additional elements with similar corrosiveness can be part of grass (figure 2.18). It is strongly suggested that these elements are monitored as well though no restrictions are given at the moment. As a first approximation the alkali type elements (Li, Ba, Sr) can be set below the restrictions for potassium and sodium as well. Since the limits are set as a sum this now means the sum of all five elements should not exceed the given limit.

Sulphur is an element, which is not limited by GE. This is justified by the argument that sulphur levels up to 1 % does not cause any problems in the gas turbine as long as alkalis are restricted [52]. Sulphur may be a problem for downstream units like the heat recovery steam generator. Still Roberge [54] reports alloy degradation by simple H_2S penetration into the alloy.

The manufacturers want to make sure that their turbines run with the lowest possible risk. Hence the limits are set rather low. Potassium is much more restricted than sodium [52] though sodium seems to be more corrosive then potassium [55] and volatilises in equal amounts. Vanadium, calcium and magnesium are elements mainly known from oil driven turbines. Sodium and potassium instead can also be present in the combustion air or process steam (Cheng cycle). This can become a problem especially if the plant is located close to the sea. In natural gas usually only sodium can be found.

Particulate matter can cause deposits and erosion. There is a dependency of the combustion temperature and the particle size when particle based deposits can occur [56]. The empirical study taking into account experience from running gas turbine units revealed that the higher the combustion temperature, the lower the limits for the particle size must be in order to avoid depositions.

1.5 Relevance of the restricted elements and condensibles

Sodium and potassium   Together with sulphur alkalis can lead to severe sulphidation attacks through the deposition of the alkali melts on the turbine. The reported compound is usually Na_2SO_4 and K_2SO_4.

The melt destroys the protective oxide layer of the alloys and the alkalis react with the unprotected metal (see [57; 54] for more information).

Magnesium and calcium Magnesium and calcium are mainly responsible for depositions in lining and valves, which may also hinder flawless operation of the installation. Calcium is also known to be able to damage the protective oxide layers in steel [54]. This makes subsequent active corrosion more easy to take place. Magnesium melts have been reported to destroy zirconium. It is also known to be existent in alkali melts that are responsible for corrosion.

Lead and vanadium Vanadium pentoxide (V_2O_5) with a low melting point can be formed after the combustion of V_2O_3, which is a possible component in the gasification product. In the turbine, the molten vanadium is considered to cause severe damage. Lead is also a corrosive element if it gets into contact with the metal surface [54].

Particles Particles can lead to fouling and erosion of hot gas parts as well as plugging and erosion of nozzles and valves. Normally this problem is solved by dedusting the gas. Since dedusting is a standard installation and hot gas filtration is a proven technology [56], hot gas particulate removal will be included as part of the sampling system. The temperature will be set to be 400 °C which corresponds to a study of Siemens [58]. The study was about retrofitting a NGCC into an IGCC. Here the syngas was proposed to be cooled down to 370 °C before entering downstream units. The exhaust heat can be used in the bottoming cycle.

Tars Tars can lead to depositions in the lines or in the nozzle before the burner if gas is cooled below their dew points. This is usually not critical if the gas can be kept above 400 °C.

Corrosion can be considered a three component mechanism. Firstly the corrosive elements need to precipitate on a surface as a melt, then the protective oxide layer must be cracked and last the oxidation of the metal compounds can take place with subsequent removal of material [57; 54].

1.6 Power scales and biomass supply

To get a better impression of the meaning of cofiring in terms of power plant size and availability, the following figure 1.4 was created. The replacement of 10 % of the gas turbine input heat with syngas would result in a figure as depicted in the graph. The diagram shows the efficiency of combined cycles over the ISO base load[4] output as given by [59]. The brown dots mark combined cycle plants as offered by a supplier. The two fitting curves mark the trend for aero derivative turbines (upper left line) and heavy duty turbines (lower right line). On the right hand side the biomass amount is given to replace the named 10 % LHV of NG in each of the given plants (green squares).
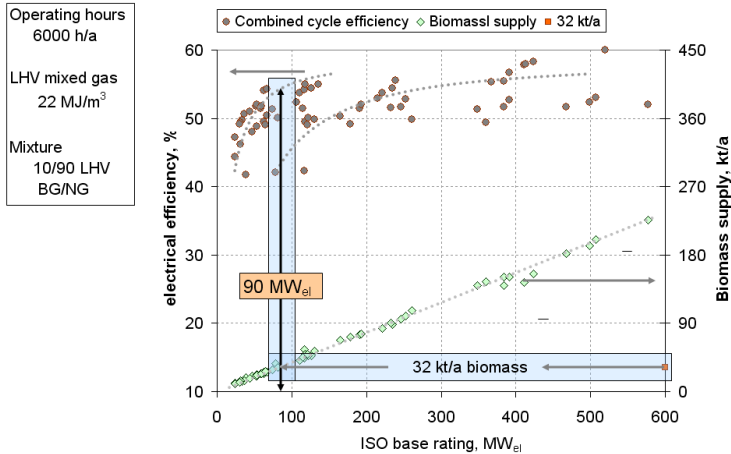
Figure 1.4: *The meaning of blending 10 % LHV of syngas into a natural gas combined cycle*

As it was calculated from a GIS analysis (section 2.5), a reasonable amount of grass is $32\,kt/a$. This amount is depicted on the right hand axis. The resulting size of a possible combined cycle plant could be around $90\,MW_{el}$. The gas turbine can either be an aero derivative or a heavy duty turbine with latter having a lower efficiency. From figure 1.5 it can be derived, that the specific costs for both installations are comparable. Still aero derivative turbines offer the advantage of a

---

[4]data corrected for fixed output conditions, T, p, moisture

high load and flow flexibility. Especially the flow flexibility is an important feature when blends of natural gas and syngas are used. Changing the blend involves significant differences in turbine inlet flows, which the turbine and burner must be able to cope with.
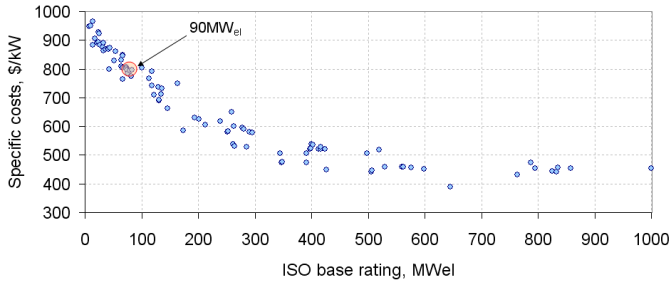
Figure 1.5: *Specific costs of combined cycle installations 2008 [59]*

Chapter 2

Grass for power generation – a view on the fuel

In the first part of chapter 2 general findings, thoughts and the availability of grass will be discussed. Whereas in the second part the physical and chemical properties of grass are given based on extensive literature research. The investigated elemental composition and properties are collected in a database and evaluated subsequently.

2.1 Why do we need to know ?

The general characterisation of the fuel is a necessary task since the possible fluctuations of characteristic properties will always exceed the possible variations in such experiments.

The elemental composition of solid fuels strongly influences the process of gasification and combustion. While some elements like hydrogen or carbon add to the process in a positive way, most of the others have negative effects or both. They can influence the process by decreasing or increasing the ash melting point, harming downstream components by fouling, deposition or/and corrosion and finally by polluting the environment when being emitted. The successful introduction of grass as an energy carrier, depends strongly on the knowledge of the fuel and the capability of the available technologies.

The gas turbine technology is highly developed nowadays. This includes special materials that allow higher entrance temperatures but also are much more sensitive to contaminants. This especially affects contaminants coming from the gasification unit. Trying to feed gas turbines with biomass syngas implies a extensive knowledge of both the gas and the fuel. Otherwise gas turbine manufactures would never agree to conduct real tests, which is a necessary step before implementation of the technology.

Eventually the argument of the importance of grass as an energy carrier is a fundamental task. There are countries, which possess enough grass for a substantial contribution but others that do not. Yet, to prepare the path to such a technology this characterisation is necessary.

2.2 Thoughts about climate change and CO_2

The common opinion about renewable energy is that the fuel itself has to be regenerative. But the crucial point is rather how fast the produced CO_2 can be fixed into biomass again. Oil and coal too are likewise renewable – if certain environmental conditions are set–, only the time until the carbon cycle is closed, is much longer compared to biomass, see figure 2.1. The characteristic feature, which is relevant is the residence time of the carbon dioxide in the atmosphere. This part of the carbon cycle is the most important when discussing climate change.
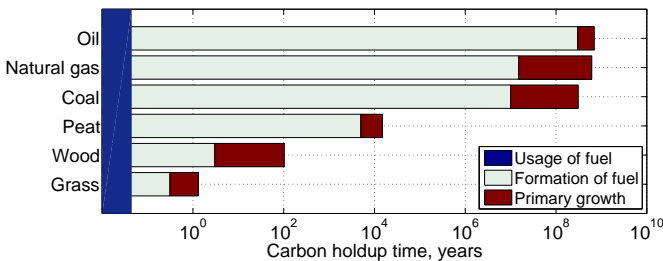
Figure 2.1: *Simplified stations of carbon during a life cycle*

The faster this part of the cycle is accomplished the lesser problems will occur. The conclusion is that the basis can not be "if" the carbon will be bound again but rather how much time it needs. Hence the

expression renewable is rather defined by time than by properties. To be totally consequent if a stable CO_2 concentration in the atmosphere needs to be maintained only as much CO_2 may be emitted as it can be fixed again immediately.

The situation we face is an enrichment of CO_2 in the atmosphere ($380\,ml/m^3$ rising) caused by the intensive use of fossil fuels. The belief, that switching to renewable energies would solve that problem is wrong. By using alternative energy resources we are just able to hold a status-quo in terms of current CO_2 level in the air. To resolve that problem completely, carbon from the atmosphere (CO_2) has to be stored away permanently. Ideas like carbon removal from the exhaust of power plants by using algae or other technologies, which transfer the gaseous CO_2 into solid carbon mostly conceal one important point: Having the carbon fixed, the obvious thing is to use it again by selling a carbonaceous product. This would finance the expenses of the plant but the carbon is released again eventually. Storing away the solid carbon would end up in a plant that would cost a lot of money but produces hardly anything worth selling. Something in between as proposed by Reed [1] could be: using the volatiles and storing the carbon rich char in soils. This would also lead to carbon enrichment respectively improvement of the soil quality.

In terms of CO_2 emissions even biomass can not be considered as alternative as long as fossil fuels were used to harvest and process the material [60]. But going to alternative energy supply is not a matter of instant switching but rather of stepwise and reasonable replacement as well as increase in efficient energy use. There is one fundamental rule that any process applied to the resource will consume a part of it and thereby energy will be lost.

Obviously the biomass with the shortest cycle is annual and perennial grasses as well as algae, where the retention time of carbon in air reaches one or less than a year.

2.3 Definition and classification of energy grass

To proceed with the definition of energy grass it must be known that there is already an expression for dedicated energy plants. *Energy crops* is an expression mostly used in terms of specially grown C4 plants

---

[1]http://www.biomassec.com/

optimized in yield of biomass like Miscanthus, Panicum (switchgrass), Phalaris (canary grass), Sorghum, Arundo Donax and Pennisetum pur-pureum (bana grass) [61]. Those plants have low or middle fertilizer and water requirements and high biomass yields. Energy grass should not include dedicated energy crops or agricultural residues, which are already pooled in a technical expression. Figure 2.2 displays the clas-sification of the three terms for young biomass products for energy use as it will be used in this context.

DEDICATED ENERGY CROPS	AGRICULTURAL RESIDUES	ENERGY-GRASS
Grown for the reason of energy production. - Miscanthus - Switchgrass - Reed Canary - Sorghum - Hemp ...	Residues and waste from agricultural and food industry. - Straw - Husk - Shells - Corncob - Sheath - Shuck ...	Herbaceous products from open grassland - recreation areas - low value pasture - sport areas - streetside greenings - crop rotatation ...

Figure 2.2: *Definition and separation of the term energy grass*

Energy grass can be understood as herbaceous plants that grow in natural grassland cultures, but is not fertilized and is not harvested for a variate of reasons. Still it bears chemical energy, which could be used for power or fuel production.

The big difference between energy crops and energy grass is the fact, that the first ones are cultivated in mostly monoculture, which must be taken care of, while the other one is only maintained showing a blend of some 30 and more species. Dedicated cultivation of grass is pointless since energy crops would be much more suitable for this task. More about energy crops can be read elsewhere [61; 10]. It is of course obvious that some species (e. g. Alfalfa/ Lucerne) can be sorted as energy-crop and energy grass at the same time at different places, depending on whether it is cultivated or not.

Grassland contains three major groups of plants: grasses (approx. 2/3), legumes and herbs (approx. 1/3). The majority of the grass leads to the general expression grassland regardless of the other two types. Some titles use herbaceous biomass; this refers mainly to the herbs. Since

grass gives the major contribution, other expressions should be avoided to make sure everybody talks of the same subject [62]. In the Phylis database from ECN[2] [63] the term *verge grass* was used to express an undefined blend of grassland genotypes.

On this note the simple term »*grass*« will be used in the further context.

2.4 Availability: literature digest

The occurrence and availability of grass is still uncertain at the moment and can only be estimated. A study from BFE[3] [64] reports around 1'000 *kha* grassland area in Switzerland, from which a biomass yield of around 5'000 *kt DS/a* is derived[4]. This is most likely too optimistic because normal extensive grassland cultures produce between 1 and 3 *t DS/ha* [6; 17]. This would rather yield an annual biomass of around 2'000 *kt DS/a*. Florine et al. [30] reported a biomass yield of up to 8 *t DS/ha* in the US. This is hardly achievable without fertilizing the soil or otherwise using a soil having a huge storage of nutrients at this time. A comparable scenario for Germany calculates with 3 *t DS/ha* having a potential area of roughly 315'000 *ha* in 2010 [17]. Another scenario from Germany Raab et al. [65] reports 20 % excess grassland provoked by the cutback of the cattle number and the transition from extensive grassland to cultivated cattle feed [17]. The development shows that more and more areas are freed of feed production because the stock of cattles decreases continuously. The remaining cattles produce more milk and therefore need more concentrated feed. The protection of species on the other hand forces a maintainance strategy for these areas (Offenhaltungsflächen).

In Switzerland a first estimation gives a total area of low usage grassland of around 26 *kha* [66; 67] and another ten *kha* of other areas of biomass maintenance.

Not all of the reported biomass can be efficiently used, since there are losses from storing, transporting and preprocessing. Mass loss due to rain can be up to 20 % (see section 2.7.2).

---

[2]Energy research Centre of the Netherlands
[3]Bundesamt für Energie
[4]DS: dry substance

The cost of supply can be estimated between 80-90 €/t DS (2006), Rösch and Raab [68]. Slightly higher numbers were reported by El-trop et al. [69]. In Switzerland the current hay price (2009) is around 270 CHF/t DS[5]. Rentizelas et al. [70] reports that storage and hand-ling accounts for around 50 % of the total costs of logistic. Worley and Cundiff [71] calculated a total delivery cost of hay type sorghum of around 57$ (1996). Cundiff et al. [72] computed delivery costs for switchgrass without harvest handling of around 19$ (1997). Harvest and storage costs account between 20 and 30$ (1996) [73]. Storage consumes space even more when the material – as it is the case here – is delivered only once maybe twice a year. This is the reason why the density (see section 2.7.1.2) is the most important parameters for pre-treatment. Simulations of logisitical and storage concepts always depend on a few very sensitive assumptions like moisture of the fuel, drying expenses or constant availability of the material. The results must always be discussed critically.

The plant growth follows an expected curve of slow progressive increase at the beginning, when the leaves are few and small followed by a high production period when the leaves have optimal number and coverage and a slowing down period, when leaves and plants start to grow into each others zone of light, soil and moisture (see figure 2.3) [74; 75]. The mortality rate equals the production rate until another parameter limits the growth.
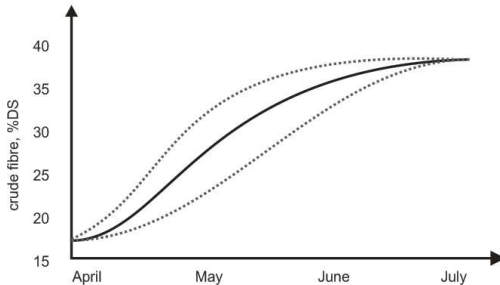
Figure 2.3: *Development of crude fibre (celluloses, lignin) during spring re-produced from [74]*

---

[5]www.agrigate.ch

The main increase in biomass is normally found in late spring (figure 2.3). Followed by the summer recession when the temperature gets hot, the soil dry and the humidity is low. This leads to hindered water and nutrient uptake.

The number of possible cuttings do depend on the type of vegetation and soil. For extensive grassland usually two cuttings per year can be done. A distinct higher or lower usage will lead eventually to a lower output. Different species have different regenerations abilities after being injured by mowing or animals. This results in different regenerations times, which in return determines the interval of the possible swath [76]. The production rate – if the system is maintained properly – is normally increased by doing regularly cuttings [77].

There is a distinct limitation of utilization regarding the swath. After the mowing the reservoir of NPK[6] must be built up again and the plants must unfold their leaves to be able to produce biomass. If the grassland is cut too often the harvest will become poor [76]. Late harvest and lower cut frequency can improve the biomass yield [78]. It must be noted, that the species and richness change after each cutting.

Figure 2.4 illustrates a possible concept of how the grass can be taken economically to a power plant. The green dots represent the harvested areas, the orange dots mark the primary processing plants where the grass is condensed to a high degree. The big red dot is a central power plant where the processed grass will be transformed into electrical energy.

2.5 Availability: GIS analysis for Switzerland

A GIS[7] study for Switzerland has been conducted [80], though it was not a main issue of this thesis. It was conducted on behalf of the BFE and together with and managed by J.-L. Hersener (Ingenieurbüro HERSENER). It revealed the grass yield for selected areas. The locations were chosen along the infrastructure, where the construction of a GT combined cycle plant seemed reasonable. In the north of Switzerland (Gösgen) an area of about $27\,kn$ radius produces a grass yield of about $32\,kt/a$ of grass (figure 2.5). This would correspond to a gasifier size of about $20\,MW$ input. The mean transport length would correspond do

---

[6]Sodium-Phosphorus-Potassium
[7]Geographical Informations System
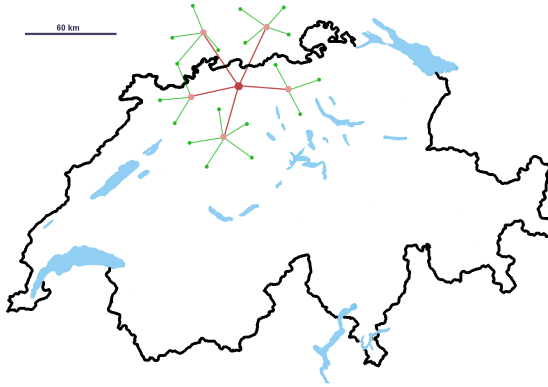
Figure 2.4: *Provision concept for Switzerland as suggested by Ganko et al.*
[79] for Poland

approx. 30 *kn*. Other authors calculated with only 20 *kn* [69] so 30 *kn*
can be considered rather an upper limit.
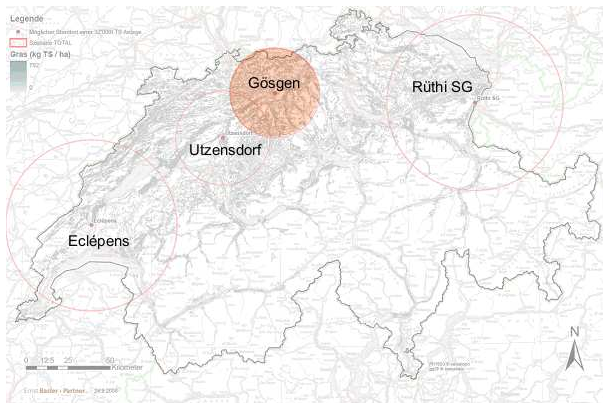
Figure 2.5: *GIS analysis for grass in Switzerland [80]. Each circle yields*
about 32 kt DS/a of grass.

For the analysis the georeferenced statistics (Arealstytistik) for Swit-
zerland was used and evaluated with various filters like tilt, sunshine,
precipitation, altitude, exposition and soil suitability. Due to this filters
grassland, which is qualified for cattle food was excluded. Grassland

with an exceeding tilt, altitude and so on compared to a boundary value were excluded too. Detailed information can be taken from [80].

For the type of grass mentioned above the logistical concept of transportation from the field to some place is already established. At the moment the harvest is either transported to farmland where it is ploughed in the soil for enrichment or it is used if suitable for feeding or finally it is disposed. The effort left is the redirection of the material to a central processing point. This is a minor change in the logistical structure and the stimulus for the owner to do it.

From this analysis it becomes obvious, that for Switzerland the availability is a very critical parameter. As is was stated before the plant size, which can be expected for the cofiring concept is about 90 MW_{el}. Replacing a substantial part of the current power plant fleet would rather aim to sizes larger than 500 MW_{el}. Especially for Switzerland, where the areas that are available for such plants are rather scarce. Still grass can be used in a mixture together with agricultural residues. This would yield a bigger amount of available fuel, much more likely to satisfy the named size.

2.6 Critical observations - energy vs. food

We must always be aware of the fact, that there is no resource or arable land that is not under stress of being exploited by competing faculties [81] – Forrest land is lost to agricultural land, which intensively used is eventually lost being unproductive. Giving priority to one interested party is most of the time not a matter of reason but rather of money. Political guidelines are responsible for not letting economy become unreasonable and unsustainable. There is exactly such a situation for natural grassland. There are several options how to use it, among which are: the bio fibre industry, biogas producers, soil improvement and not least feed extender. The latter is loosing more and more importance because of the increase in high potential cattle needing high value feed.

Within the last two year the discussions about energy vs. food surfaced rapidly. Grain, soya and corn prices increased based on the usage of those food stocks for biofuels. This effect was enhanced by people who started trading with those values [82]. Bio-fuel dedicated energy plants bear more environmental threats than their title suggests [83–85].

The change in land-use conceals light to heavy long term consequences, which are not easily visible. This includes carbon release from forest clearing or breaking of soil surfaces, which subsequently must count as additional CO_2 release and soil degradation.

Grass should not be competing with food in terms of used acres. There are quite a number of areas, where grass has to be maintained but growing high quality feed or other usage is not possible or not allowed. Good feed for cattle are not equally good as fuel. It contains much raw protein and thus nitrogen and minerals being not wanted in the gasification process. Extensive grassland cultures (not fertilized) normally show a high amount of species (high diversity) but also fail high biomass yields. The quality for feed is very poor. In contrast fertilized grassland shows high biomass yield, good nutrition values but low number of species [62].

In addition, plants rich in nitrogen show unfavourable drying mechanisms [77]. Further does extensive grassland cultures cope with low nutrient contents. This will reduce the amount of alkali elements in the fuel. All this leads to the conclusion that extensive grassland products are more suitable for gasification than the intensive ones.

There is one thing to be noted: using grass for energy production has complex effects leading to unexpected situations. One is that agriculture may start to produce grass which completely misses the point of the idea, but may be more profitable than to feed it to the cattle in times when energy costs are climbing high enough; another one if grass is left on the ground rotting, the fermentation process produces CO_2 and also methane, which is even worse in terms of climate impact [86].

2.7 Common properties and their impact on thermal processing

Natural grass differs significantly from wood and coal with respect to certain elements. There are three major points, which cause problems in almost all steps of processing.

- ✧ material structure (pre-processing)
- ✧ elemental composition (process management)
- ✧ hazardous products (post-processing)

Thus structural, physical and chemical properties must be identified and characterised, which will be done in the following sections.

Remarks on the graphs The graphs in this section show comparisons of various fuels. The data was collected from published data and inserted into a database now referred as eDaB[8]. The square mark shows the algebraic average values; additionally the median is plotted as a diamond mark. The data itself is printed as dots in order to see the distribution clusters. The numbers in brackets show the number of data available for each element in the specified group. All numbers refer to dry biomass unless specified otherwise.

Dry biomass is assumed to be not completely dry, but dry with respect to an appropriate method of drying. Not many authors give the applied procedures or uncertainties together with the published data. For this reason no error bars or confidence regions can be told. The data shall give an impression of the level and range to be expected.

Demolition wood is not included in the data, since it contains additional compounds from impregnation or colouring. Such feedstocks need special care when thermally processed.

2.7.1 Material

Material properties are macro-physical properties like fibre structure, storage density and other bulk properties. These properties are relevant for harvest engines, pre-processing units and storage facilities but less relevant for the gasification process [87].

2.7.1.1 Lignin and cellulose

Annual or perennial plants have low lignin contents due to the lack of the secondary wall of the cells. Lignification takes primarily place in the secondary wall of the cells, which hardens and stiffens the material when plants grow old. The primary walls of the cells instead show lower lignin contents and are thus much more fragile against environmental influences. As Ghetti et al. [88] stated, the difference of the bonding of the two materials lead to different devolatilisation behaviour. As mentioned before fuel containing less lignin is expected to produce less

---

[8]elemental Data Base

char [89]. This is enhanced by catalytic char reactions if an increased alkali content is given [90; 91]. This was tested mostly by doping char with certain alkali components such as K_2CO_3. In contrary, it was reported by DeGroot and Richards [92]; von Scala [93] that with increased alkali content the char production rate is increased The higher cellulose content and light structure of grass will result in a fast and high volatilization [94], which in return enables a lower process temperature and subsequent sensible heat loss through the exiting gas flow. Though von Scala [93] stated that the heating rate does not have an influence on the char formation, Williams and Besler [89] observed otherwise. The heating rate as well as the end temperature had a significant effect on the fraction left after the process.

Biomass containing more lignin will likely produce more liquid during fast pyrolysis [95], since the majority of heavier molecular weight derived compounds present in pyrolysis oil originate from the lignin monomers present in the biomass. Since grass contains less lignin than wood it must be specifically tested if the path via pyrolysis oil is reasonable.

2.7.1.2 Density

The density of the fuel or bulk density influences on one hand the economy of the logistics and on the other hand the handling of the feed into the power plant. Thready material like straw and grass are harvested loose and normally transported as bales or other compressed forms. Decreasing the void fraction both enhances the handling and the logistics economy.

If the material is compressed to clusters the density increases to $150\,kg/m^3$ at least [69] (table 2.1). On site pelletizing was successfully tried in the 90es [61] but terminated because of the lack of profitability in those days [96]. The pellets produced this way showed a density of 800-$1200\,kg/m^3$. Rabier [97] reported similar values. A centralised pellet manufacturer communicated to need around 4 % of the fuel energy – straw in this case – to produce a high quality pellets (including milling and drying)[9]. Other types of equally high density fuels are pyrolysis oil or slurry (mixed oil and coke), or torrefied pellets [98].

---

[9]http://www.buhlergroup.com

State	Density, kg/m^3	Reference
On site	1.4 (kg/m^2)	calculated
Fresh (grass)	50	[7]
Standard Fill (chaffed grass)	85-100	[21]
Dried and chopped grass pellets	170-380	measurement
Bale (grass)	120-150	[7]
Compact roll	350	[61]
Bale (straw)	800-1200	[96]
Dust (crops)	150	[99]
Pellets (bulk straw)	540-660	[23]
Pellets (single, straw)	1100	[97]
Pellets (agricultural)	950-1250	[97]
Pellets (grass)	1300	measurement
Oil (rape)	920	[99]
Pyrolysis oil (general)	1200-1300	[100]

Table 2.1: *Typical densities of different states of grass and comparable fuels in* kg/m^3

2.7.2 Mass loss and stability

To ensure continuous operation of the power plant, storage of the fuel is unavoidable. But there are several steps, at which mass loss of the solid material can occur, thus as little steps as possible should be ensured.

1 harvest losses due to pick up efficiency

2 respiration and crumble losses due to on field drying

3 leaching losses due to rain on cut material

4 storage losses due to hygroscopic behaviour of the material (fungi, bacteria)

5 abrasion losses due to mechanical exposure during transport

Most problems can be addressed by enhancing the processes of drying, preprocessing and compacting.

Harvest loss can not be avoided since pick up efficiencies can not be 100 %. It is directly linked to the time given for the harvest. Respiration losses can be reduced by drying the material as quick as possible below 38 % moisture. Then respiration activity of plants is very low. But bacterial degradation still goes on until the grass is at least as dry as 15 % moisture. But if the grass is too dry before being transported crumble losses will increase [77]. Tedding is still the most simple way

to dry grass. To increase the drying rate the grass must be bruised as much as possible to free the water from within the plant. The unbruised plant will close its stomata shortly after being cut and thus the intracellular water ill not be driven out easily. When stored in natural form the material can take up moisture again due to its hygroscopic behavior [101]. In a highly humid atmosphere funghi and bacteria will then start to decompose the material.

Leaching as mentioned above has two effects the first one is reduction in material, which is negative and second a large part of nutrients and minerals are lost which is only negative if the material is used as feed for cattle. Instead it is a highly appreciable result if used as feed for energy production for two reasons: lower nutrient removal from the soil and lower contaminants in the gas stream. Watson (taken from [102]) reported some numbers for rain losses listed in table 2.2.

Treatment	Loss DS (%)
No rain - mechanical losses	14.7
Rain	23.7
1-2 showers (1-20 *mm*)	18.9
5-6 showers (12-63 *mm*)	27.1

Table 2.2: *Losses of dry substance (DS) during haymaking [102]*

During transport of the solid material, whether as pellets or packed, abrasion losses will occur. In general it can be noted that less losses will occur, when the material is more compacted [61]. It will also use less storage space, which is economically interesting. The abrasion of pellets was studied by Obernberger and Thek [23]. The results show a significant loss of mass if the pellet quality is low – it can be as high as 20 % with an average value is 4 %.

If the fuel is processed to pyrolysis oil or even slurry, losses are significantly reduced. But then long term stability of the fluid must be considered [103]. Producing slurry has some other advantages: the density is comparably high (table 2.1), which in return decreases the necessary storage and transport volume; biological degradation (mass loss) can only take place slowly; liquid fuel is much easier to transport than solid or rather fibrous fuel. But the demand on the material of the storage facility is much higher since pyrolysis oil is very aggressive (pH 2.8 [100]) and toxic.

The bio-degradation rate of pyrolysis oil is around 50 % within 28 days, which means that it is degraded if spilt twice as fast as fossil oil [104]. This is an important environmental aspect, since accidents where oil is lost through damage is almost unavoidable as history shows.

2.7.3 Physical analysis

The physical properties are properties that define the material in terms of weight, state of aggregation, energy content, melting point, volatility in other words thermal and material attributes.

2.7.3.1 Energy content

Energy in biomass is derived from solar energy. Photosynthesis transforms the energy in solar radiation into solid biomass or phytomass. The maximum efficiency that can be theoretically obtained is around 5 % [105] (exergy analysis). Experimental studies [106] showed around 4 %. The Energy content of biomass is expressed either as HHV (Higher heating Value) or LHV (Lower Heating Value). The difference is the state of aggregation of water (H_2O) after combustion. If the energy of the steam can be recuperated as usable heat the HHV is obtained. If the steam must be discharged only the LHV can be obtained.

There are several empirical formulas to calculate the energy content of biomass. The most familiar one is probably the formula of Boie (equation (2.1)) where C, H, O are the mass fractions of the elements in the biomass.

$$LHV, MJ/kg = 34.8\ C + 93.9\ H - 10.8\ O \qquad (2.1)$$

Other formulas return the HHV of Biomass like the one published by Channiwala and Parikh [107] (N: Nitrogen content, Ash: ash content from proximate analysis):

$$HHV, MJ/kg = 34.91\ C + 117.83\ H - 10.34\ O$$
$$-1.51\ N + 10.05\ S - 2.11\ Ash \qquad (2.2)$$

Typical LHV values of dry biomass are around 17 MJ/kg, where the difference between LHV and HHV depends on the available hydrogen.

The hydrogen forms water vapour, which stores the enthalpy of evaporation. Oasmaa et al. [100] gives the correlation equation (2.3) to calculate the LHV from the HHV

$$LHV, J/g = HHV, J/g - 218.13 \; H \; (w\,\%) \tag{2.3}$$

Grass normally shows slightly lower LHV values than wood because of its higher ash content. Oil or lignin containing plants show higher heating values since the heating value for cellulose is much lower (17 MJ/kg) than for oil (36 MJ/kg, $C_{40}H_{44}O_6$) and lignin (29 MJ/kg, $C_6H_{10}O_5$) [20].
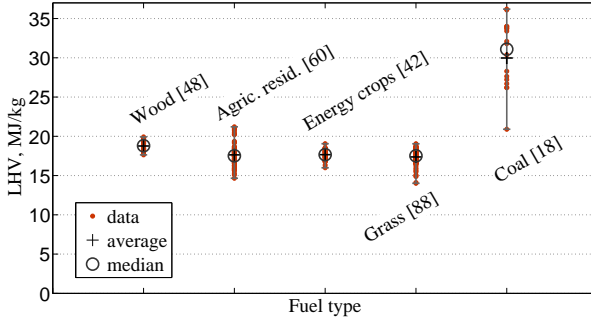
Figure 2.6: *LHV of various fuels from eDaB*

Carbon is the main energy carrier followed by hydrogen as indicated in table 2.3. This is one reason why a good carbon conversion is such an important factor.

Element	mass fraction kg/kg	molar fraction mol/kg	Energy of combustion MJ/kg ([108])
H_2	0.0298	27.56	-6.67
C	0.4848	40.36	-15.88

Table 2.3: *Energy content of elements*

When gasified the energy content is reduced according to the cold gas efficiency of the process. This is normally below 80 %. The produced raw gas is called low LHV gas (Schwachgas) referring to its low energy

content (usually between 3 and 6 MJ/m^3). To run a gas turbine around its ISO rating, higher flow rates must be realised. This can lead to serious changes in flow patterns. Generally aero derivative gas turbines seem to be much more suitable for this application since they can cope better with changes of the gas flow than heavy duty turbines [109]. Low LHV gas (from 2.5 MJ/m^3) can be burned in gas turbines [110] (ALSTOM burner). There are gas turbines especially adapted for the use of low LHV gas (GE LM2500 [31]). In Värnamo a gas turbine was used from European Gas Turbines LTD that aparently is a subcompany of ALSTOM power now. The gas turbine was provided with different syngases from wood, bark or straw. New turbines are made of high tech material and elaborate coatings in order to increase the inlet temperature. The fuel requirements are getting even more strict for this type of turbines.

2.7.3.2 van Krevelen diagram

The following diagram shows the process of coalification of biomass. It was set up by Prof. van Krevelen [111] to reconstruct the mechanisms of coalification by the sub-processes dehydrogenation, dehydration etc.
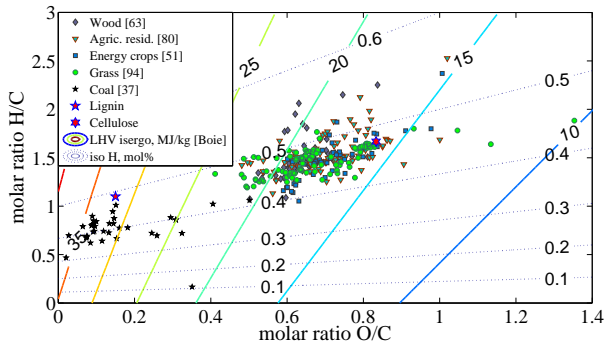
Figure 2.7: *van Krevelen Diagramm*

It was also extensively used to evaluate the quality of fossil fuel resources. High quality fuel is always on the lower left side of the diagram showing a high carbon content like anthracite. So called low LHV fuels

(see [56]) show a much lower carbon content, is rather found way up and on the right hand side in the diagram with a high oxygen content.

The coloured thick isolines mark the lines of constant LHV calculated from the formula of Boie equation (2.1). Though this equation is over-ruled in the meantime and replaced by better ones (see section 2.7.3.1), it only needs the C, H, O amount to get an good suggestion of the LHV.

The dashed blue lines are the isolines for constant hydrogen content. The 0.5 line marks CH_2O being a simple carbohydrate. Around $95\,\%$ of the plants (dry matter) consists of carbohydrates [112] as depicted by the graph.

In the diagram one can track the process of drying, which is the removal of H_2O. For any oxygen removed two hydrogen atoms are removed as well. The direction the fuel will be shifted is accordingly to the lower left corner, if CO_2 is released the fuel shifts to the upper left corner, if CO is released the fuel shifts straight to the top and so on.

2.7.3.3 Water content

The water content further reduces the LHV and thus the efficiency, since more water vapour leaves the system carrying away energy. The reduction is given with the following formula:

$$LHV, MJ/kg = LHV_{wf}(1 - w) - \Delta h^{LV} w \qquad (2.4)$$

Where the index wf means »$water\,free$«, w is the water content defined as

$$w = \frac{M_{H_2O}}{M_{H_2O} + M_B} \qquad (2.5)$$

and h^{LV} is the heat of vaporization.

Typical water contents for wood are 10-50 % (up to $50\,\%$ if newly cut) [20], for grass before drying or torrefaction it would rather be around 50-70 % [112]. In contrast, the effort to dry the material is much less for grass than for wood based on the open structure of grass. $40\,\%$ water content would reduce the LHV to 55 %. It becomes just zero when the heat of evaporation equals the HHV at around 90 % water content.

The other term to express the water fraction in the fuel is moisture. Its referred to the dry substance (DS) instead of the wet substance (WS) equation (2.6). This definition leads to the result, that the moisture can very well exceed 100 % whereas the water content can not.

$$w = \frac{M_{H_2O}}{M_B} \tag{2.6}$$

The water content strongly influences the ability of the material to be stored. More than 15 % moisture will lead to bio-degradation of the material and development of fungi and bacteria. This would end in a significant loss of biomass or even auto ignition. Hence it is unavoidable to dry the energy grass before storing [7].
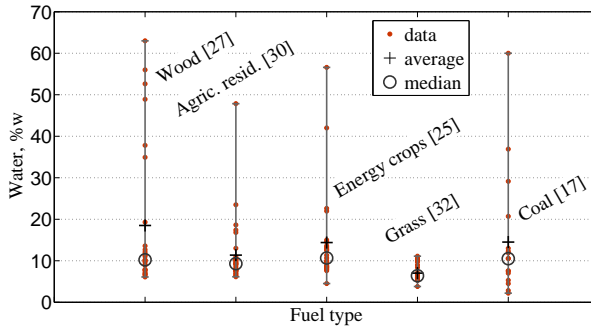
Figure 2.8: *Water content as received for different fuels from eDaB*

Figure 2.8 depicts some values for the water content as received. Grassland material shows one of the lowest moistures of all. This is simply due to the drying on field. Most likely it was dried on field before being transported. The *DIN 51 718* explains the procedure of drying. It takes place in a drying oven at $106 \pm 2\,^\circ\mathrm{C}$ at atmospheric pressure until the weight does not change any more.

2.7.3.4 Volatile matter and fixed carbon

Volatile matter is the weight fraction of the material that evaporates during the process based on the applied temperature. The ISO norm *ISO DIN 51720*[113] says the sample has to be coked at $900\,^\circ\mathrm{C}$ for 7

minutes. The sample must be cooled down in an exsiccator to prevent it from drawing moisture and is then weighed.

The volatility strongly influences the reaction kinetics in the gas phase and thus the composition of the product gas. A range of values for the volatile fraction is given in figure 2.9
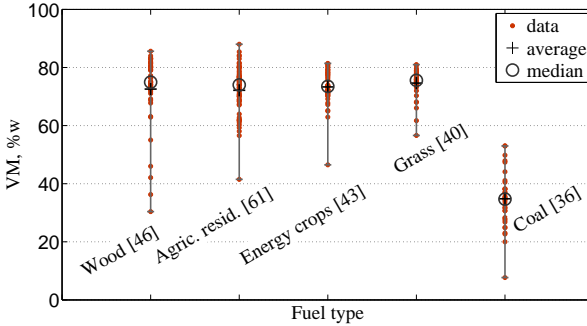
Figure 2.9: *Volatile matter for various fuels from eDaB*

The interpretation of this data is very difficult since it can not be assumed, that all data have been acquired under consistent temperature and pressure. Some authors report 950 °C, most do not even specify the parameters or norm of their tests. The residue is called coke and consists of fixed carbon (FC) (figure 2.10) and ash [113] (figure 2.12).

The FC content in grass can be expected to be lower than in other types of biomass. The high alkali contents will lead to an improved char decomposition. Corresponding to the high volatility the FC content must be lower than for coal.

The amount of FC, is quite relevant to the residence time of the particles in the reactor since the char reactions are the limiting step in the gasification process [114]. The carbon conversion is obviously much dependent on the completeness of the char reactions. Higher temperature and addition of steam will lead to more efficient and faster char reactions. Grass based on its low lignin content is suspected to produce a low char yield and therefore lower gasification temperatures and a higher throughput may be feasible.
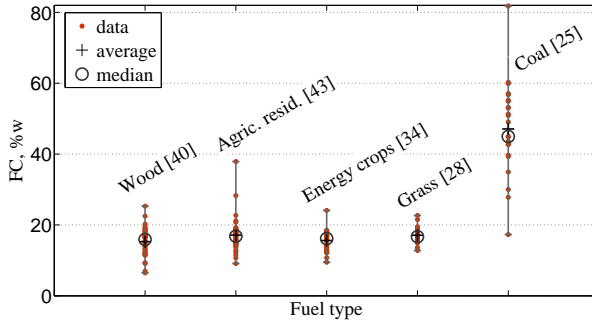
Figure 2.10: *Fixed carbon for various fuels from eDaB*

2.7.3.5 Volatilization diagram

The volatilization diagram (figure 2.11) shows the part of the fuel that gasifies according to section 2.7.3.4 versus the carbon plus ash content. These two are the main contributors to the remaining coke. The volatile matter is a very important parameter providing information about the reactivity of the fuel.
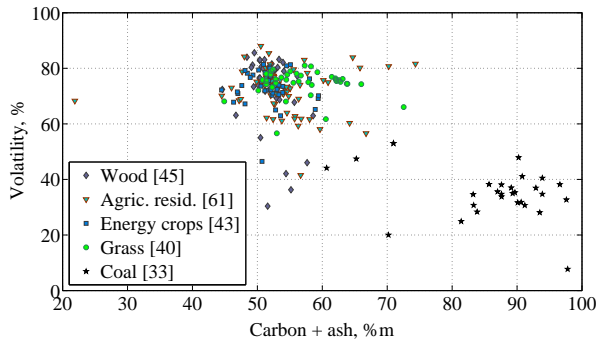
Figure 2.11: *Volatility of various fuels from eDaB*

31

2.7.3.6 Ash content and melting behaviour

The average ash content is higher in grass compared to other biomass based on its high content of inorganic compounds (mainly Si and K). The elements are normally bound in mineralized complexes. The major part is given by SiO_2 and K_2O. Depending on the process management and additives the elements will be partially bound to the ash. The other part will leave the reactor with the gas as either particle or gas.
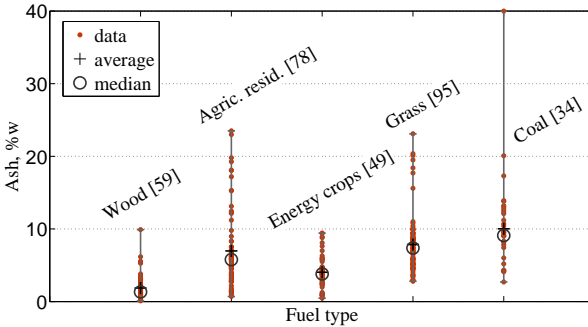
Figure 2.12: *Ash contents in various fuels from eDaB*

Graph 2.12 shows, that the amount of ash in grass is not necessarily higher than in some coals but still higher than in wood. Figure 2.13 gives the ash components distribution for grass. The high amount of silicon and potassium is significant different from other fuels.

The amount of ash also influences the efficiency of the cycle. Larger amounts of ash will lead to a higher effort for ash removal and higher particle or dust entrainment and thus better and more expensive dust removal units. It also request a higher throughput of biomass to reach the given energy output. This is especially important for plants where downstream components are dependent on a constant input stream.

Ash fractioning is one way to achieve a separation of the elements, which may be recycled as fertilizer from those that should be retained like heavy metals [115].

Ash can be used in two ways: either to be recycled as fertilizer then the best way is hot gas filtration above 800 °C, which also results in emission of heavy metals and alkalis into the gas turbine or engine [116]. Another
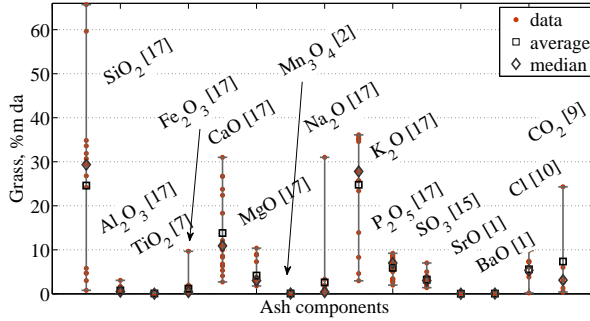
Figure 2.13: *Ash components for energy grass from eDaB*

option is to use the ash as sorbent for gas cleaning, then the heavy metals are bound to the ash and can not be used without additional conditioning.

The melting point of ash is quite important for the process because this is when slagging and sintering starts. When the slag cools down it becomes a very hard glass like material that is very hard to remove. In entrained flow gasification slagging is wanted, for it shields the units wall from the immense heat the process needs (e. g. GSP gasifier [117]).

It must be noted that for ash there is no homogeneous melting point. It already starts at a certain temperature when most grains are still solid. For coal there is a definition to determine the ash melting numbers: DIN 51730 [118]. For biomass a new standard will be defined, which should be released soon by the CEN[10]. An cuboid of ash is positioned in a heater and optically recorded. Then the temperature is increased continuously. The characteristic temperatures are defined by the shape of the particle.

A rough estimation of the melting point (MP), begin of sintering (SB) and flow point (FP) was given by Hartmann et al. [20] in equations ((2.7)) to ((2.9)) elements in %w). The calculated temperature ϑ can deviate by as much as 100 °C from the real one. This is based on the hetero-

---

[10]European Committee for Standardisation

geneous form of the ash particles and also on the fact that process ash melts over a range of temperatures not at a fixed one.

$$\vartheta_{MP}, {}^{\circ}C \;=\; 1172 - 53.9\ K + 252.7\ Ca - 788.4\ Mg \qquad (2.7)$$

$$\vartheta_{SB}, {}^{\circ}C \;=\; 1159 - 58.7\ K + 237.9\ Ca - 743.8\ Mg \qquad (2.8)$$

$$\vartheta_{FP}, {}^{\circ}C \;=\; 1369 - 43.4\ K + 192.7\ Ca - 698\ Mg \qquad (2.9)$$

The equations indicate, that the components K, Ca and Mg turned out to be the main influencers of the melting point. Since these components are more abundant in grass than in wood, the melting and sintering point is lower but not as low as expected. Using this equation for grass the melting point of grass is still as high as 1077 °C. Agglomeration experiments of lucerne (alfalfa) gasification showed a lower temperature of 840 °C [119].
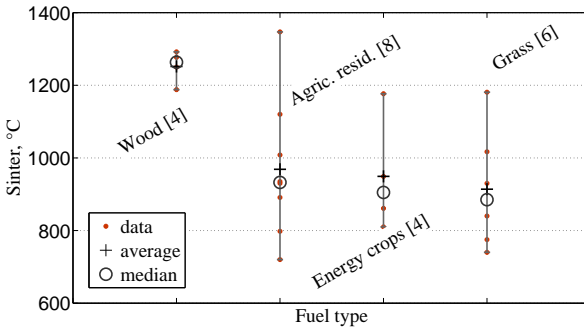
Figure 2.14: *Sintering point of various ashes from eDaB*

It seems a remarkable point that equation (2.7) state a lower ash melting point for higher Mg content, whereas the melting temperature of MgO is quite high (table 2.4). The ash composition is normally determined after soft combustion of the fuel. This means the elements are fully oxidised. In gasification processes these elements are most likely not fully oxidised but rather form other minerals like potassium silicate.

Öhman et al. [119] reported some behaviour of agglomeration in a fluidized bed reactor. One of the materials used was lucerne showing similar elemental composition as a natural grass blend. The molten ash
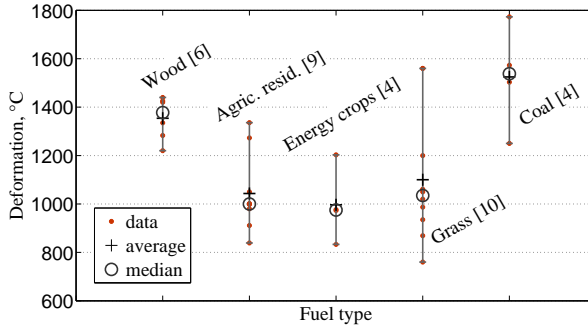
Figure 2.15: *Deformation point of various ashes from eDaB*
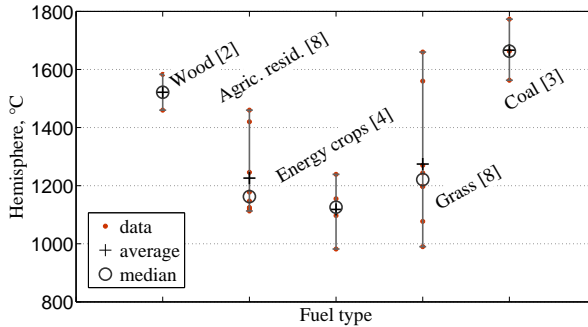
Figure 2.16: *Hemisphere point of various ashes from eDaB*

particles seem to consist of several layers showing varying composi-
tions. The main components responsible for the melting were alkali
silicates, like K_2SiO_3, $MgCa_3Si_2O_8$, $K_2Si_2O_5$ and potassium chloride.
This result shows clearly, that equations (2.7) to (2.9) assume a suffi-
cient abundance of silicon and calcium. The equations are a result of a
multi component analysis, where those elements did not seem to have
a major influence because their amount was not limiting.

Moilanen [121, recited] reported that pressure has a negative influence
on the ash melting behaviour. Pressurized gasification seems to carry
a greater risk of ash agglomeration for a given temperature.

35
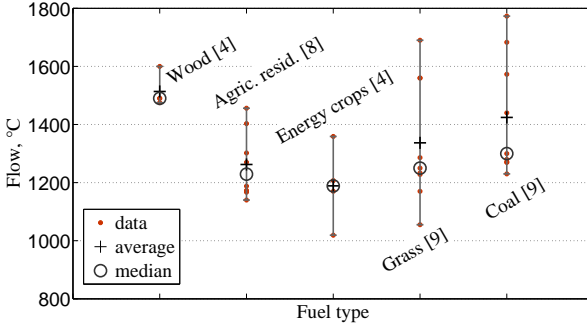
Figure 2.17: *Flow point of various ashes from eDaB*

Component	Melting point, °C
K_2O	740
P_2O_5	562
BaO	1973
SiO_2	1722
CaO	2613
MgO	2825
V_2O_3	1957

Table 2.4: *Melting points of ash components [120]*

Coal gasification and combustion has a long tradition and much ex-
perience can be taken from literature. There are some important key
numbers [87; 25], which can be used as indicators whether the ash tends
to sinter, form slags, or the alkalis tend to vaporise. One of the numbers
is the vitrification number. If the number is between 0.5 and 1, there
is a higher risk of the formation of low melting point compounds. The
elements are inserted as molar amounts. For grass it gives:

$$\frac{2(K + Na)}{3Si} = \frac{2(0.48 + 0.022)}{30.335} = 1.0 \qquad (2.10)$$

This value shows, that grass is at the upper boundary of the critical
range. Another key value is the alkalinity number. It places the amount
of alkaline elements in relation to the acidic mineral formers [25]. If this
value is larger than 0.8 there is a higher risk of sintering, due to the

excess of alkalis, which can form silicates if sand is used in the process. For grass it gives:

$$\frac{2Ca + 3Fe + Na + 2Mg + K}{2Si + Al + 3P + 2Ti} = 1.1 \qquad (2.11)$$

There are more of these numbers (see Strömberg [25]) but all of them must be treated with care, since the reactions are very complex and much dependent on process parameters. The numbers only give clues about problems that may turn up during the process.

2.7.4 Chemical analysis

Chemical properties can simply be seen as the elemental composition. Figure 2.18 shows the elements of the the periodic system reported in grass. The colours of the boxes give an overview, in which class the element is found with respect to its amount in the fuel. ζ gives the amount in %, g/kg or mg/kg, respectively. ϑ_B is the boiling temperature of the element.

The chemical elements affect processes in many different ways, energy production, ash composition, ash melting behaviour, deposition, fouling, corrosion and plant emissions. They can act catalytically, mechanically or chemically and obviously in a combination.

Among those, only a few elements are essential for the growth of the plants (table 2.5). These elements will mostly be found in rough amounts, though some plants manage to push the main part of these nutrients into the roots by the time they fade. Potassium seems to be existing mainly ($>90\,\%$) in water soluble forms (KNO_3, KCl) [24]. This is in agreement with the results for water leaching of the fuel. Here the authors report a highly reduced concentration of potassium after leaching (see section 2.8.3).

Figure 2.18: *Periodic table of elements in grass (molar mass Mills et al. [122]; boiling points Lide [120])*

Macro elements	uptake in form of	% of dry mass	possible compound in plant
Oxygen	O_2, H_2O	45	
Carbon	CO_2	45	
Hydrogen	H_2O	6	
Nitrogen	NO_3^-, (NH_4^+)	1.5	KNO_3, KCl
Potassium	K^+	1.0	
Calcium	Ca^{2+}	0.5	$Ca(NO_3)_2$, $CaCl_2$, $Ca_3(PO_4)_2$
Magnesium	Mg^{2+}	0.2	$Mg(NO_3)_2$, $MgCl_2$, $Mg_3(PO_4)_2$
Phosphorus	$H_2PO_4^-$, (HPO_4^{2-})	0.2	PO_4^{3-}
Sulphur	SO_4^{2-}	0.1	SO_4^{2-}
Micro elements	uptake in form of	% of dry mass	possible compund in plant
Chlorine	Cl^-	0.01	Cl^-
Iron	Fe^{2+}, (Fe^{3+})	0.01	Fe^{2+}, Fe^{3+}
Manganese	Mn^{2+}	0.005	Mn^{2+}, Mn^{3+}, Mn^{4+}
Borum	H_3BO_3	0.002	
Zinc	Zn^{2+}	0.002	
Copper	Cu^{2+}, (Cu^+)	0.0006	
Molybdene	MoO_4^{2-}	0.00001	
Nickel	Ni^{2+}	yet unknown	

Table 2.5: *Essential nutrients of higher plants [112; 77; 24]*

All other elements can fulfil useful tasks in plant cells and structure like Si but are not considered as essential since the plant can live without it. It must be noted, that the composition not only depends on the type and species of a plant but also on the age of the plant, the type of the soil and season of the year. The data provided does not distinguish between those effects but rather gives average data. The measurement methods for ultimate elemental analysis are complex and can be found elsewhere DIN/ ISO norms or [123].

Clean sampling   One of the main sources of errors in the data is the sampling of the material. Scientifically spoken the data is wrong when other materials like soil and sand are introduced into the sample when collecting the fuel. But the data might still represent the real situation much more precisely. This argument pictures the point of what the data should be used for. If in the real situation the collection of the fuel leads to the entrainment of other materials this is based on economical budget and the process must cope with it. It is then a bad sample but probably the more realistic value for commercial applications.

2.7.4.1 About the next chapters

In the next chapters more detailed information about the most relevant elements in grass is given. This includes general statements about the uptake and sources of the element as well as their part in gasification and gas turbine combustion.

Hot corrosion of gas turbine blades is a large area, which can not be covered here. Continuative literature is recommended for further review [124–128; 54; 55; 49; 87].

2.7.4.2 C Carbon

Carbon is the central element of carbohydrates, proteins, lipids, nucleic acids or any other organic structures of biomass [129]. Nonetheless carbon is hardly more than a trace element on earth compared to others. Its share is only around 0.04 %w of the earths crust. Still carbon is the main energy carrier in biomass.

The stable state is CO_2, whereas CO is one of the main combustible products in the product gas after gasification. Though carbon monoxide

is not counted as real greenhouse gas because of its short lifetime (1-3 months), it does indeed provoke the formation of other greenhouse gases. The net reaction is

$$CO + 2O_2 \rightleftharpoons CO_2 + O_3 \qquad (2.12)$$
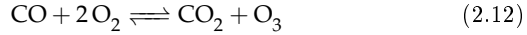
The interesting point is that ozone in the troposphere is counted as a greenhouse gas while being in the stratosphere it forms a shield and prevents the UV-B radiation from being transmitted to earth [130]. This means for one emitted CO two greenhouse gases are produced.

The carbon content of grass is similar compared to wood and coal see figure 2.19.
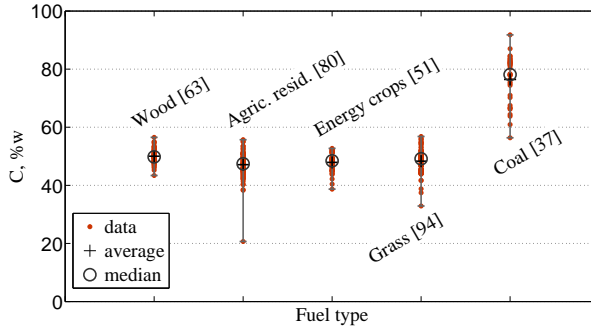
Figure 2.19: *Carbon content of various fuels from eDaB*

To be consequent it must be told that besides from being the most important element carbon can cause metal dusting or carborisation, which are two types of corrosion. This effect depends entirely on the way the process is run. It happens when materials are exposed to CO, hydrogen or hydrocarbons. This process already starts at $430\,^{\circ}C$ [131].

Carbon can agglomerate as coke or tar or leave the system as such, which decreases the efficiency. This loss is expressed in the carbon conversion value. Tar is generally a disturbing component that must be removed to prevent downstream components from damage. The type of gasifier and gasification temperature has a major influence on the tar formation and destruction.

2.7.4.3 H Hydrogen

Though the mass fraction of hydrogen is much smaller compared to carbon the molar fraction is about twice as much. The major part of the dry plant consists of starch, which can be written as $C_6H_{10}O_5$. This tells that the plant consists of approximately 50 %mol hydrogen and around 25 % each carbon and oxygen. All other elements are minor parts. This becomes very illustrative in figure 2.7.
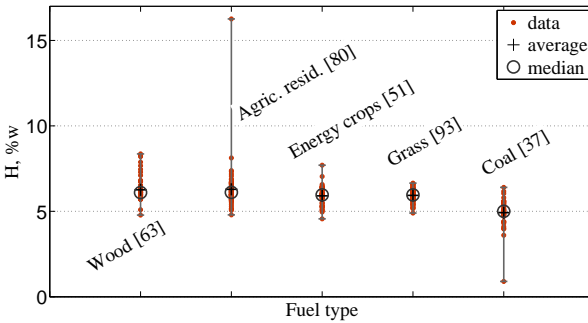
Figure 2.20: *Hydrogen content of various fuels from eDaB*

Hydrogen plays a major role in gas turbine combustion. It strongly influences the flame propagation in the combustion chamber. If to much hydrogen is in the mixture there can be a flash back or even an auto ignition within the mixing zone in front of the burner. But by adding only a minor part of hydrogen the flame stability can be enhanced [42].

2.7.4.4 O Oxygen

The oxygen content of biomass is very high compared to other fuels (figure 2.21). It reduces the amount of oxygen input needed for the process. But on the other hand is the reason why the energy density of biomass is comparably low. The oxygen has to be transported all the way along with the carbon and hydrogen.

Oxygen is a part in the celluloses structure, which itself is a major part of the cell structures.
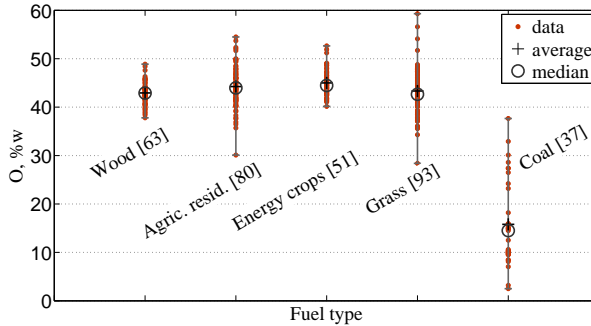
Figure 2.21: *Oxygen content of various fuels from eDaB*

Pyrolysis or torrefaction are the options to increase the energy density (see section 2.8.4) by removing oxygen in a medium temperature process.

2.7.4.5 N Nitrogen

As a component of proteins, nucleic acid, co-enzymes and chlorophyll, nitrogen is essential for all plants and needed in rough amounts. Plants normally incorporate nitrogen from soil and water, which is inorganically bound as nitrate ($R-NO_3$). Legumes can fix air nitrogen by means of bacteria. In the absence of nitrate plants are able to pick up nitrogen in the form of ammonia. This is important, since much of the applied fertilizer is distributed in this form.

Most of the nitrogen is found in pyrrolrings that form other compounds [132]. They are an important part of chlorophyll. Pyrrol and pyridine are also types of tar known from gasification experiments even after a scrubbing unit. Exchanging the nitrogen with sulphur pyrrol becomes thiophene.

Woody biomass normally contains half of the amount of nitrogen than coal, this is why it is sometimes used to decrease the NO_X emission of coal power plants by co-firing. Grass can contain as much nitrogen as coal and even more figure 2.22. The one extremely high value comes from a single analysis of Poa Pratensis. If removed, the natural range is 0.3 to 4.0 %w, which is about the same range as coal.
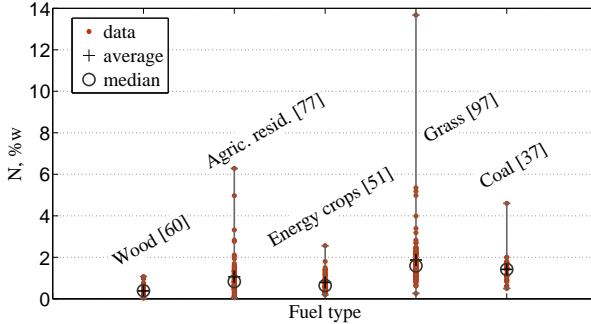
Figure 2.22: *Nitrogen content of various fuels from eDaB*

If fuel bound nitrogen is considered as the main factor of NO_X produc-
tion, using grass gives no advantage in NO_X emissions (combustion).
The major components formed during the process are NH_3 and HCN,
aside of which nitrogen containing tars can also be found. In fluidised
bed gasification between 50 and 100 % of fuel bound nitrogen conver-
sion into ammonia can be expected [133].

If ammonia is formed in the product gas or exhaust gas nitridation
can occur. This is a type of corrosion based on the absorption of am-
monia in alloys. It causes embrittlement of the material [131]. All
nitrogen compounds formed in gasification except N_2 are poisonous to
environment and must be scrubbed and catalysed back before dischar-
ged. Especially N_2O is a very effective greenhouse gas and was emitted
distinctly during the last decades. A very extensive work about nitro-
gen and its fate in gasification was done by de Jong [134] and can be
recommended for further studies.

During combustion the ammonia from fuel bound nitrogen reacts to
NO. Experiments using an ALSTOM gas turbine burner showed a
conversion of around 30 % [110], whereas simulations returned up to
60 %.

2.7.4.6 S, Sulphur

Sulphur is available for plants mainly in the form of sulphate SO_4^{2-}.
They are soluble in water and can be assimilated by plants. SO_2 can

also be assimilated by some plants via the leaves. Other available compounds must undertake various reaction steps from H_2S, SO_2, S, FeS to become eventually sulphates [132].

Sulphur is essential for plants since it it is part of many amino acids (e.g. cysteine and methionine) [135]. Grass contains more sulphur than woody biomass but less than coal (figure 2.23).
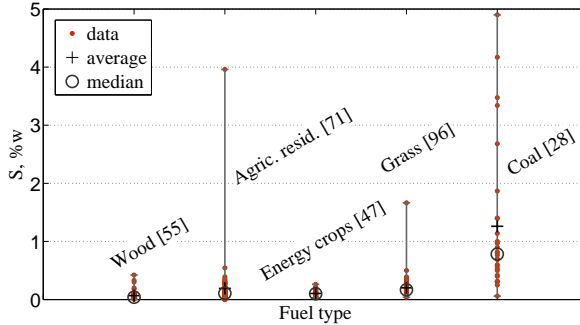
Figure 2.23: *Sulphur content of various fuels from eDaB*

Sulphur is a very reactive element at higher temperatures, which are given in gasification and combustion processes. It is one of the elements that can cause fouling and successively severe corrosion on downstream components [127; 125]. It is oxidised during combustion to SO_2 being the main component in the atmosphere to cause acidification. Though H_2S is known as corrosive element, it has been reported that alkali levels are usually limiting the corrosion of hot gas path materials [52]. H_2S is combusted quickly to SO_X in the combustion chamber and is for this reason not counted as a threat to the turbine blades. Since grass contains large amounts of alkalis and sulphur, the corrosion problem is suspected to become more severe. But grass also contains a large amount of calcium. Ca is able to bind sulphur to the ash. In coal gasification calcium is added for this reason. Nevertheless special care must be taken to prevent alkalis and sulphur species from travelling freely through the lining. Still much more care must be taken to avoid sulphur poisoning of catalysts if such are used in the process [136]. On the other hand there are catalysts that need a certain amount of sulphur

to work properly if there is not enough sulphur in the gas it must be added [137].

2.7.4.7 Al Aluminium

Aluminium is not known so far to be involved in any plant processes, though it was observed that it slightly enhances growth. Some plants still take up some aluminium if available in the soil [132; 112]. In higher amounts aluminium becomes very toxic affecting the growth of plants and forests. It also decreases the uptake of nutrients [138].
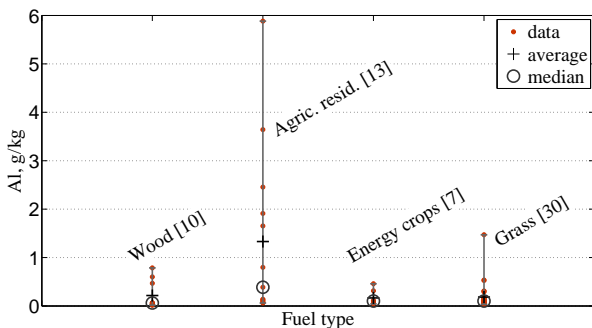
Figure 2.24: *Aluminium content of various fuels from eDaB*

Regarding gasification and gas turbine processes aluminium is reported to bind alkalis as alkali alumino silicates, which are minerals with a high melting point.

2.7.4.8 As Arsenic

Arsenic is mainly emitted by the copper producing industries, but also during lead and zinc production and in agriculture [139]. It can be taken up by plants very easily, so that arsenic enters the food cycle quite fast. Hence the content in plants is proportional to the content in the soil. In figure 2.25 various concentrations of arsenic in fuels are shown. Wood can display much higher contents. The reason is most likely CCA[11]

---

[11]Chrome-Copper-Arsenate

treatment of the material since these materials show higher contents of arsenic [140; 141].
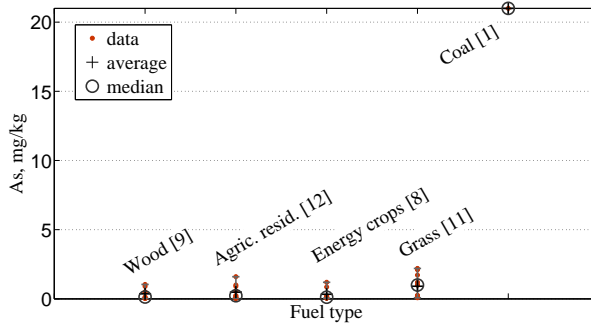
Figure 2.25: *Arsenic content of various fuels from eDaB*

Arsenic is considered to be totally mobilized at temperatures above 1500 °C [142] (equilibrium calculation). The retention of arsenic in the ash was measured to be around 50 % [143] whereas ash from coal shows clearly better absorbence than ash from wood or straw. Arsenic can be retained from leaving the system almost completely by recycling the fly ash as sorbent [144]. But as mentioned before the ash may not be used as fertilizer anymore after this step. The leaching of arsenic from wood is reported to take a long time [145]. Only after three days one can expect to have reduced the As level in the wood siginifcantly. The retention of arsenic on activated carbon was shown to be rather poor [146].

2.7.4.9 B Boron

Boron is taken up as boric acid H_3BO_3. Experiments, in which the absence of boron showed decrease of the cell dividing activity prove the need for this element. Boron also influences the usage of calcium [132] But the specific task of boron is not known so far. Figure 2.26 shows a few contents for boron published for fuels.

Boron is sometimes used in high temperature alloys for gas turbine blades and structural enhancements for plastics [147]. It is so far not mentioned as critical to process units. Leaching of coal fly ash for 24h
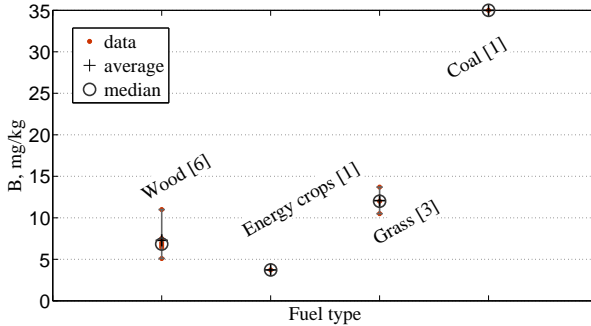
Figure 2.26: *Boron content of various fuels from eDaB*

with pure water leads to a reduction of around 40 % of the boron in the ash [148].

2.7.4.10 Ba Barium

Barium does not occur in pure form. Mostly it is found as barite $BaSO_4$. Most of the barium available in plants and animals was set free by human activities [139]. Naturally occurring barium is not very mobile and is not taken up by plants easily. It is not needed by plants for any known reason.

There are not many datasets available of barium in biomass. Some of those are printed in figure 2.27.

Though barium is more corrosive than phosphorus very similar to potassium [126], it is not mentioned by the gas turbine manufacturers. Presumably, the reason is that so far no barium concentrations worth mentioning has found its way into a gas turbine or it was not measured.

It still bears the danger of corrosion like all the other alkalis when they volatilise as chloride. Regarding grass, barium is only a tenth of sodium and a 100th of potassium in mass. Since this is well within the natural fluctuation of potassium contents in the fuel it is usually neglected. But in the gas phase those elements may be as well as important as potassium when mobilized to a higher degree.

2
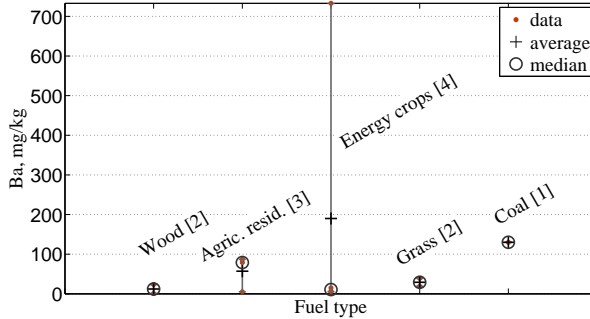
Figure 2.27: *Barium content of various fuels from eDaB*

2.7.4.11 Ca Calcium

Calcium is needed for the cell structure, cell division and thus like magnesium is essential for the growth and yield of grass [149]. It has a mechanically stabilising nature but also is a part of chlorophyll and enzymes and is needed for the metabolism [112]. It is not dangerous unless inhaled as dust. The main component of natural calcium is calcium carbonate $CaCO_3$, which is the main part of limestone. This is abundant in most places. If not (acid soils) it must be introduced artificially as fertilizer.
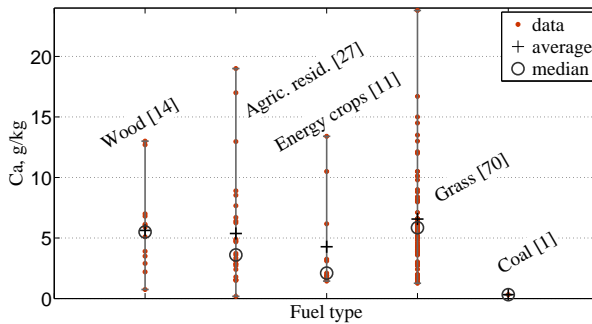
Figure 2.28: *Calcium content in various fuels from eDaB*

In gasification reactions calcium can form silicates, sulphates and phosphates [119]. Like K, Ca may catalyse char reactions and in contrast is not reduced in this function by silica as it was found for potassium [150]. It was also found that Ca does change its catalytic behaviour dependent on the state of the mineral.

Like potassium, sodium and vanadium, calcium causes deposition as gypsum [46; 49]. But unlike the first four calcium does not appear to be corrosive to gas turbine blades unless it is volatilised as chloride. Then Ca may be able to crack the protective oxide layer. There is a limit for gas turbines (table 1.2). It contributes to the ash melting behaviour by increasing the ash melting point [20].

2.7.4.12 Cd Cadmium

Cadmium is known to be carcinogen. Especially endangered are smokers who directly volatilize the cadmium in the plant (tobacco) and inhale it [151; 139].

Up to $26\,g/kg$ can be found in commercial fertilizer [152; 139]. It comes as a component of phosphate rocks e. g. in Morocco, which is used to produce the fertilizer[12]. Another source is surely the emission from anthropogenic processes [153]. Despite the fact that it does not seem to be needed by plants it can still be taken up by them in considerable amounts. It inhibits photosynthesis in most plants [154]. For this reason some studies propose to use certain plants to remove cadmium from soil and waters [155]. Soils must be considered as contaminated if too high amounts of cadmium are found.

About 75 % of industrial cadmium is used in Ni-Cd batteries. The battery companies emit large amounts of Cd [156]. Most of the remaining 25 % is used for pigments, coatings or plating, and as stabilizers for plastics. A very large amount of cadmium is naturally released into the environment. About half of this cadmium is released into rivers through weathering of rocks and some cadmium is released into air through forest fires and volcanoes. The rest of the cadmium emission is based on human activities, such as manufacturing [139].

In the process stream, the main part of cadmium is found in the fine particles likewise fly ash or cyclone ash [153]. This fractionation is also

---

[12]Communications of International Food Policy Research Institute
(http://www.ifpri.org)
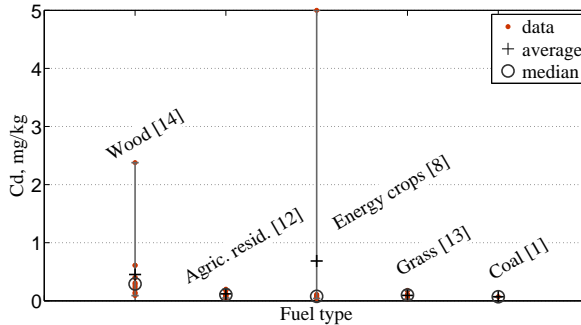
Figure 2.29: *Cadmium content in various fuels from eDaB*

depending on the size of the feed (dust, chips). Equilibrium calculations show that from roughly 400 °C, gaseous Cd is the main species [157; 144]. A maximum of 10 % can be retained using fly ash as sorbent.

Cadmium is rather an environmental threat than disturbing to gas turbines but it volatilises very early (<300 °C) in thermal processes [14]. So it has to be expected in the hot gas path.

2.7.4.13 Cl Chlorine

It is supposed that all chlorine exists in the biomass as inorganic components as diluted ions K^+, Cl^-. It is needed for osmotic processes and cell division activity. Absence of Cl in nature is rare and plants can take up more Cl^- than actually needed. This behaviour is pushed by chlorine fertilizer, from which potassium is distributed as KCl. The Use of K_2SO_4 in fact increases the sulphur level in the soil but analysis of the grown straw did not show a significant influence on the fuel [19]. Figure 2.30 depicts various chlorine contents in fuels.

It was found that chlorine tends to volatilize other elements like Si, K, Na and others. It is supposed that it can even stabilize the gas phase alkali compounds [158].

Since it is so reactive chlorine is one of the most unwanted elements in biomass gasification. It does not only volatilize other elements causing deposition and fouling but also causes high temperature corrosion itself. This can take place either as a direct corrosion or as induced
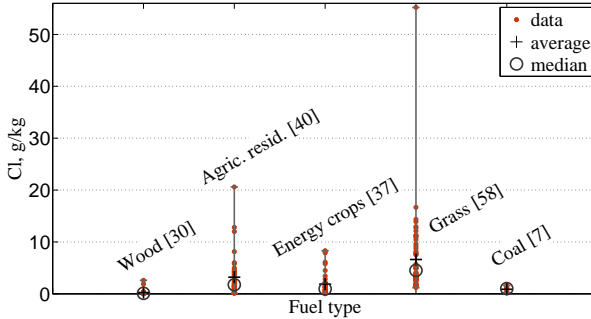
Figure 2.30: *Chloride content of various fuels from eDaB*

corrosion. Alkali sulphates were used to stress the surface, which was much more successful when the surface was prepared with chlorine before [159; 160]. Chlorine starts to vaporize at very low temperatures – below 200 °C [158]. It forms HCl and HCN during gasification. HCl is one of the main components to cause acidification in the atmosphere. In combustion systems dioxin is formed within a temperature window between 300 and 600 °C [161]. But the formation needs excess oxygen, which is not the case in gasification process. For this reason in the energy grass gasification the formation of dioxins are of minor concern.

Around 80-90 % of those Cl components were found to be water leachable after 1h treatment. This means natural or deliberate leaching will reduce the clorine content e. g. if the harvest is delayed over the winter period but at least over a raining period [162; 20; 163]. This is – as mentioned before – accompanied by a biomass loss; mechanically and by decomposition. Since grass shows a very fine structure and large surface the leaching will take much less time than for energy crops.

2.7.4.14 Co Cobalt

Cobalt is not one of the essential elements. It is taken up by plants in small amounts if available. Though accumulation can occur. Cobalt is not generally poisonous unless eaten or inhaled in large amounts. Figure 2.31 shows some measurements of the cobalt contents in fuels.
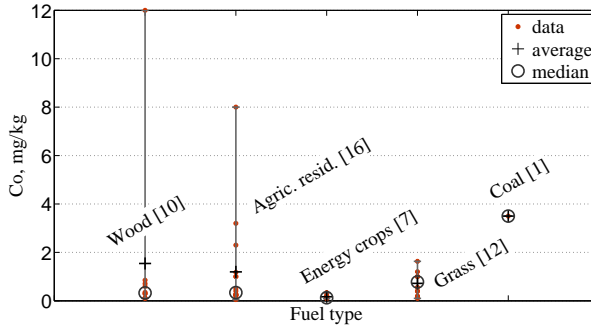
Figure 2.31: *Cobalt content of various fuels from eDaB*

Cobalt is mostly mined in combination with zinc. It is used especially for corrosion resistant alloys and not mentioned as corrosive itself. At temperatures below 1200 °C cobalt and its compounds are mostly crystals and thus in particulate form, which can be filtered. Above this temperature Co is also found in the gaseous phase (equilibrium approach [164]).

2.7.4.15 Cr Chromium

As far as it is known Chromium is not needed for plant organisms. It can occur in different oxidation states such as Cr(II) or Cr(III). Where Cr(III) is considered as not toxic, Cr(VI) is very poisonous and water soluble [139].

At standard reducing conditions $Cr_2O_3(cr)$[13] is the stable form of chromium up to 1800 K (equilibrium approach [164]). It is corrosive as CrF_2 and chromium potassium sulphate [126]. Due to its high boiling point retention in a particle filter even at higher temperatures – 600 °C– could be managed. Experiments with CCA treated wood showed that under slow pyrolysis conditions around 98 % of the cromium is left in the residue [141].

---

[13]crystalline
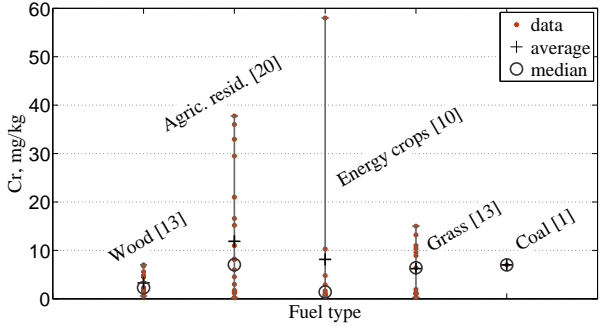
Figure 2.32: *Chromium content of various fuels from eDaB*

2.7.4.16 Cu Copper

Copper is used in the redox system of the plants. In absence of copper – being quite rare in nature – the leaves become dark green, deformed and show necrotic spots [112].

Copper is used in a very wide range of applications, which is connected to an increased occurrence of copper in the soil [139]. Copper is not poisonous unless absorbed in large amounts or inhaled as aerosol.
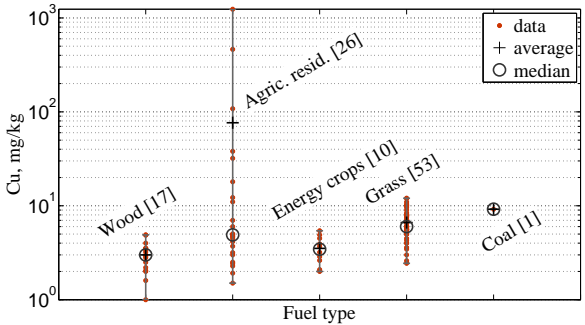
Figure 2.33: *Copper content of various fuels from eDaB*

Copper is commonly used as a material with good thermal conductivity. It is also used in alloys for gas turbine components. Together with

nickel it is also known as catalyst for carbon formation and methana-
tion [165]. Copper is volatilized by chlorine forming CuCl. This can
potentially cause corrosion on the downstream components if deposi-
ted or condensed at any metallic wall. Though copper is not included
directly in the analysis of gas turbine restrictions it is critical if it is
mobilised as particle like all other metals.

2.7.4.17 F Fluorine

For plants fluorine is not needed and if available in large amounts it
destroys the leaves and bork [132]. At normal conditions it is gaseous.
Since fluorine is extremely reactive it can not be found in its pure form
but always in mineral compounds like calcium fluorite (CaF_2). The
uptake of fluorine in the plants is entirely dependent on the type of
plant and type of the fluorine compound. A normal concentration in
the soil is around 300 mg/kg. Contaminated soil shows values around
3000 mg/kg [139].
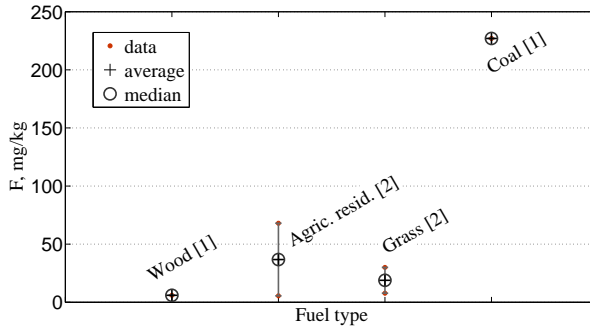
Figure 2.34: *Fluorine content of various fuels from eDaB*

As mentioned earlier fluorine normally occurs as minerals needing high
temperatures – mostly above 1000 °C– to decompose. Under pyrolytic
conditions (coal gasification) around 50 % of the fluorine is vaporized
at 900 °C. By adding more calcium to the fuel less gaseous fluorine
will be formed [166]. In grass similar contents of fluorine can be found
as in wood (figure 2.34), but more calcium is available (figure 2.28).
It was reported recently that fluorine tends to form solid CaF_2 under

gasification conditions which theoretically is stable up to temperatures of 1600 °C [167].

2.7.4.18 Fe Iron

Iron is also one of the essential elements. It is needed for the photosynthesis, respiration, redox processes and fixation of nitrogen. Lack of iron in the soil is one of the most frequently observed problems for plant growth. The result is displayed by pale and yellow leaves[14] [112]. Ferrous compounds are rather common in nature since iron is considered as the most abundant element on earth. Iron was reported to rapidly
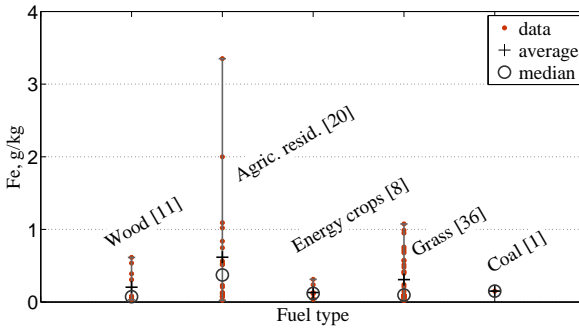
Figure 2.35: *Iron content of various fuels from eDaB*

form Fe_2O_3 during gasification and enhances char gasification [168].

In gas turbine technology iron is mostly used in combination with nickel as high temperature alloys. The element itself is not considered as hazardous to units. According to thermodynamic equilibrium studies iron is not expected to be volatilized at all at normal gasification conditions [169] – it is rather bound to ash. Still it is told that it can form iron carbonyls when the raw gas is cooled down. Iron carbonyl is formed in the presence of CO and is toxic [87]. Hydrogen sulphide H_2S and also ammonia can catalyse this reaction. Especially grass contains large amounts of sulphur and fuel bound nitrogen that will form H_2S and NH_3 during gasification.

---

[14]Absence of chlorophyll called chlorosis

2.7.4.19 Hg Mercury

In nature mercury occurs rather in ore in combination with sulphur e. g. HgS than purely. It also occurs organically bound or rarely as salt (Hg_2Cl_2). Normally mercury enters the environment by being washed out of rocks. But human activity has increased the amount being emitted mainly from fossil fuel and waste combustion, mining and agricultural processes [139]. But it can also enter through extraction by inappropriate deposition of waste in the environment. Once entered, it goes any available path through fish, vegetables, water and accumulates by being reintroduced through sewage an waste water. If emitted from industrial processes it is a severe environmental and physical threat.
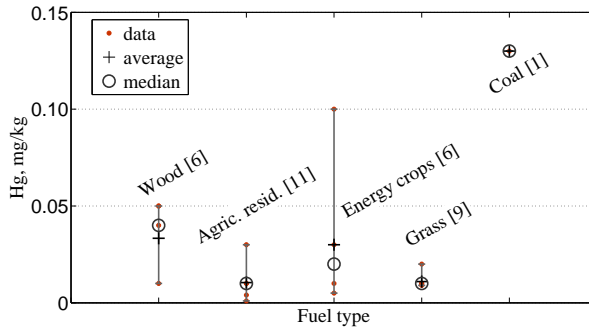
Figure 2.36: *Mercury content of various fuels from eDaB*

Figure 2.36 shows the contents of mercury in various types of fuels. The highest amounts were measured in energy crops (a switch grass sample). This might be caused by extensive fertilizing or other types of contamination, but is still not outside the expected range. As mentioned before the location of the harvested biomass is mainly responsible for the Hg content of the biomass. Thus the differences might be based on the location and not on the fuels itself.

Mercury is not considered to be corrosive to most materials. It is liquid under standard conditions and forms salt with chlorine HgCl. It is also very volatile (boiling point at $357\,°C$) and thus it can be expected that only a small part will be retained in the ash fraction [143]. Most of it will be found in the fine dust filter or else in the flue gas [170]. HgCl itself is corrosive and poisonous.

For gas turbines mercury is not mentioned to be hazardous according to GE [52]. Mercury can be removed by sulphided activated carbon at around 90 % efficiency [171]. Mercury is absorbed or transformed to HgS, which is a stable product and can be used for recycling or safe disposal.

2.7.4.20 K Potassium, Na Sodium

Since potassium and sodium behave much alike, these two elements will be discussed together. Mainly potassium but in some extend sodium as well plays an essential part in plant metabolism [149]. It takes part in osmotic processes. Also it is required for the transport of signals in the nerve tracts in humans and for controlling of the gas exchange of plants [135] and is essential for the photosynthesis process. It is also needed for the synthesis of proteins [132] but also for enzyme activation, osmoregulation, pH regulation and even the ripening process. Only the osmotic function can be replaced by sodium or even calcium and magnesium [138].

At the beginning the lack of potassium leads to increased sugar production [149] and eventually it ends in the termination of the growth while the leaves start to show necrotic spots [112]. When provided in huge amounts, some plants can built in far more K than needed, which is called K-culmination. Sodium seems to act as nutrient only in some special plants (C4 species, halophyte), but normally is not considered to be essential. Potassium has antagonistic effects on the uptake of Na, Mg and Ca [77]. Usually potassium is considered to exist in sufficient amounts in the soil, since it is very soluble it is easily washed out [62].

Young plants show a very high uptake of potassium while the matured plants tend to decrease the uptake, which leads to a dilution of the potassium in the total substance. El-Nashaar et al. [172] reported a decrease in potassium, chlorine and phosphorus content in matured plants. The potassium content in annual plants decreases significantly (around 40 %) during spring and summer [173]. This process is far less distinct in willow and poplar [20]. This is the reason why young plants – when they are rich in nutrients – make very good feed for cattle. For gasification older species with lower nutrients would be preferable.

The alkalis are suspected to get more volatilized with increasing chlorine content at high temperatures [174] and therefore get much more mobile.
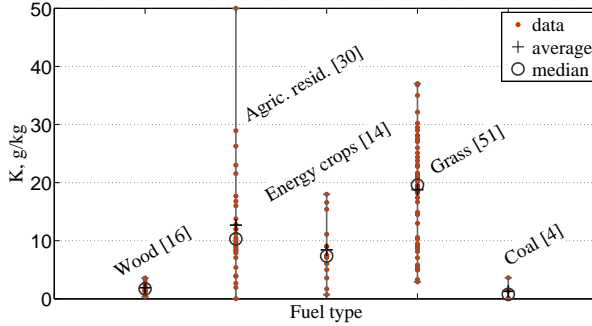
Figure 2.37: *Potassium content in various fuels from eDaB*
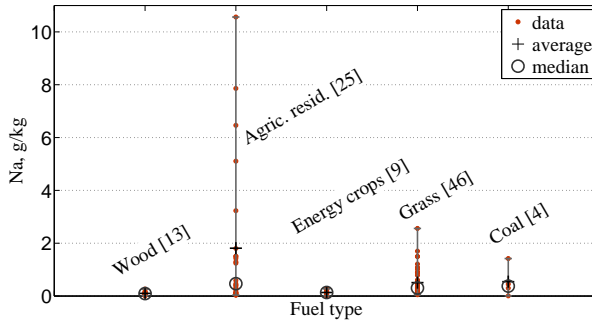
Figure 2.38: *Sodium content in various fuels from eDaB*

Thus the volatilization of potassium and respectively sodium is not only dependent on the potassium content itself but even more on the presence of Cl. Airborne alkalis condensate at around 800 °C [175] into particles forming aerosols and cause damage like corrosion, deposition and fouling on downstream components [49]. Aerosol particles are very hard to remove and are able to pass through most filters and even scrubbers. At usual gasification conditions alkali components like KCl can exist as particles but also in gaseous forms [176]. There is a good chance to retain most of the potassium in the cyclone ash or filter dust [177]. Sodium sulphates have been shown to posses a significantly greater potential of corrosion than potassium [55; 178].

As it can be seen from the plots there is much less sodium in grass than potassium. This often leads to the decision to neglect sodium because it is within the fluctuation range of potassium. But the mere elemental data does not predict the concentration in the gas phase, in contrast the transfer of sodium into the gas can be as well higher than for potassium Turn et al. [179] (for bagasse and banagrass) and Pintsch and Gudenau [180] for coal.

The main part of the nutrients will stay in coarse particles like bottom ash and cyclone ash [153]. Once bound to ash the alkalis can lower the ash melting point significantly [20]. This depends on the formation of alkali silicates (low melting point) or otherwise alkali alumina silicates (high melting point) [181; 182; 180; 183].

Na and K are also known to have catalytic effects on the combustion[184; 163], pyrolysis [163] and gasification [150]. It catalyses char gasification during the presence of CO_2 and H_2O [90]. This is the case under reducing conditions and especially pyrolysis. If high silica fuel is used, the catalytic effects are reduced when potassium forms silicates [150].

Once reached the gas turbine combustion chamber alkalis are known to cause severe damage to gas turbine blades at temperatures higher than $600\,°C$ [46]. To operate the gas turbine at lower temperatures would reduce the efficiency significantly. This is based on the fact that the efficiency of the cycle is proportional to the temperature difference between in- and outlet but also to the temperature level.

Salts of alkali metals usually are water soluble and can be leached applying passive (rainwater) or active (rinsing) leaching. This will reduce the gas cleaning task [173; 20]. Thus the time of harvest is a parameter with a high influence on the soluble elements.

The two Figures 2.39 and 2.40 depict the correlation of the content in biomass of potassium and chloride. The current data confirms the correlation, which Sander [19] published for straw in 1997. The graph also shows the line for KCl salt. The content in plants shows always more potassium, than chloride. This is most likely because potassium is mostly transferred as KCl but can only be taken up by the plants as K^+ and Cl^- (table 2.5). Chlorine is not easy to measure, so the line gives a clue about the maximum content of chloride in the plant depending on the potassium content. The mean value is less than half of this amount. No direct correlation of potassium fertilization and potassium content was found [19].
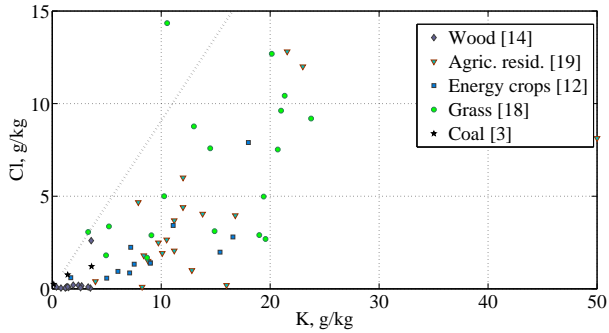
Figure 2.39: *Correlation of K to Cl of various fuels from eDaB*

Figure 2.40 illustrate the correlation of potassium content of the plant to the ash content. This information must be translated carefully since the amount of potassium going into the ash is dependent on the ashing process itself. The data is evaluated regardless of the process. Still the data suggests, that a minimum value for the ash can be assumed if the potassium content is known.
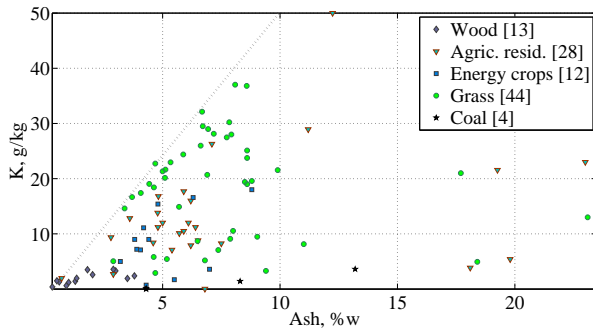
Figure 2.40: *Correlation of potassium to ash content for various fuels*

2.7.4.21 Mg Magnesium

Magnesium is also one of the most important elements in plant meta-bolism. It is part of the chlorophyll, takes part in photosynthesis and

also in the gas exchange processes. Too little Mg will result in chlo-
rosis [149] and decreases biomass yield. The data in figure 2.41 shows
some values for magnesium in solid fuels. The upper points among the
agricultural residues are from the same author, but from different re-
sidues from India. Since the author also reported residues with lower
values systematic errors in the measurements can be excluded.
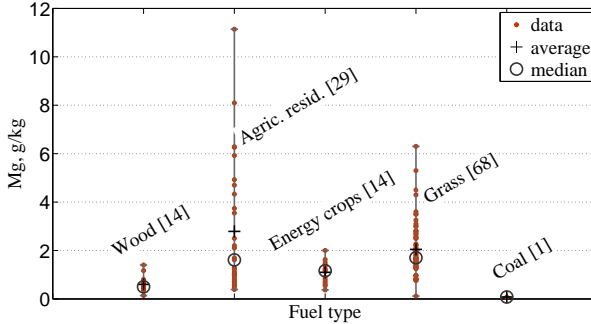
Figure 2.41: *Magnesium content of various fuels from eDaB*

Magnesium is known to damage downstream components by deposition
and corrosion if present as chloride. Only 40 *mg/kg* are allowed in the
gas turbine inlet in GE turbines [52]. But it is also used to prevent
vanadium corrosion by binding the vanadium [185]. Since vanadium
is also present in grass its not quite clear how helpful or damaging
magnesium is effectively. It is surely one of the elements that must be
observed more closely.

2.7.4.22 Mn Manganese

Manganese is an essential micro element for plants [112; 135]. It takes
part in photolysis (photo-hydrolysis) and metabolism, and is part of
chloroplasts and ATP[15]. Lack of Mn does not occur naturally, since it
is an abundant element on the earth.

Technically manganese is used in catalysts for combustion processes [186].
It is so far not mentioned to be hazardous to gas turbines or any other
unit.

---

[15] adenosine triphosphate
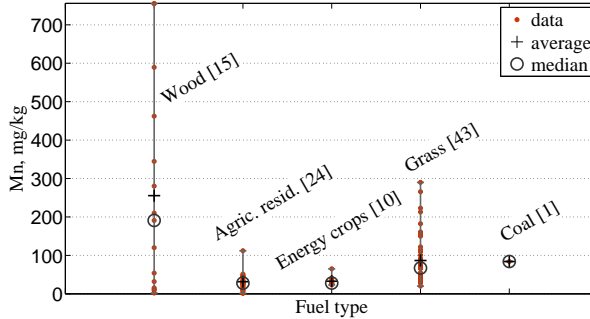
Figure 2.42: *Manganese content of various fuels from eDaB*

2.7.4.23 Mo Molybdenum

Molybdenum is one of the trace nutrition elements shown in table 2.5. It is essential for some enzymes. In the absence or lack of Mo, chlorosis occurs. If delivered in high amounts it is toxic. Figure 2.43 shows the elemental contents of some fuels. Grassland can easily accumulate Mo if available and therefore shows a wide range of this element.

Molybdenum is solved much better in alkaline soils and thus the availability to plants is dependent on the pH value of the soil [139].
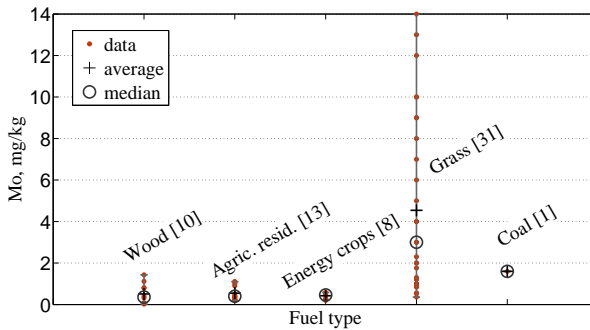
Figure 2.43: *Molybdenum content of various fuels from eDaB*

Molybdenum is used as a compound to manufacture alloys since it increases the durability of steel. Molybdenum is also a catalyst in the refining of petroleum. It is used in alloys e.g. Hastelloy (NiMo) to increase the corrosion resistance in reducing atmospheres [187]. The melting point is very high at around 2600 °C and the boiling point above 4800 °C [139]. So far it is not mentioned as hazardous to materials.

2.7.4.24 Ni Nickel

Nickel is essential for plants and higher organisms in small amounts. Some plants can accumulate nickel much more than needed. Nickel takes part in the metabolism of carbo-hydrates. It is used to make high temperature and low corrosion alloys.

It is mostly released by power and waste incineration plants in form of fine particles. They can stay in the atmosphere for a very long time and eventually get washed out by rain. They are finally immobilized by being adsorbed by soil or sediment.
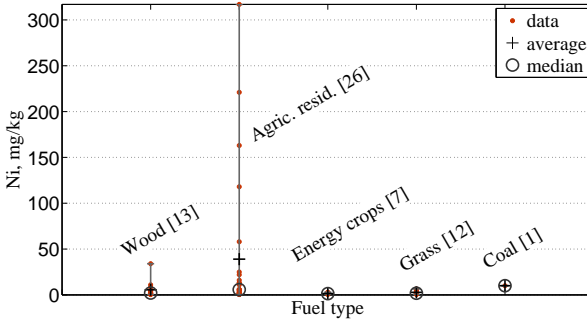
Figure 2.44: *Nickel content of various fuels from eDaB*

Metallic nickel can be released by sulphur components in cooling gasification product gas like hydrogen sulphide (H_2S). It then forms nickel carbonyl. Airborne nickel is afterwards most likely bound to fly ash [87].

Nickel is not one of the elements GE or others mentioned to be hazardous to gas turbines and is generally allowed as long as it stays below the particle limits. Though it might lead to metallic nickel deposition. General care should be taken in any case. Nickel is widely used as

catalyst for methanation, cracking and shift reactions by lowering the activation energy of the reactions. At lower temperatures it catalyses the reverse Boudouard reaction. It can thereby destroy the surface of the lining and provoke metal dusting. Sulphur interferes and poisons the catalyst by depositing and removing the nickel from the support by forming nickel carbonyl as mentioned. If any sulphur is present it inhibits metal dusting by employing the nickel for its own reactions [87].

The retention in the ash from gasification experiments is around 80 % [188]. It is equally distributed between bottom ash and cyclone dust. Cooling the product gas below 400 °C should increase the retention rate to 100 %.

2.7.4.25 P Phosphorus

Like nitrogen and potassium, phosphorus is absolutely essential for the formation of sugars, proteins and nucleic acids (DNA, RNA) [135]. In most soils phosphorus restricts the biomass growth if not added artificially [112]. But if not manufactured in high quality, it would lead to entrainment of heavy metals. The extensive use of phosphorus in fertilizing, results in eutrophication of lakes and rivers. This would also lead to an increased concentration in the surroundings and subsequently in the plants.

Most of the available forms can not be taken up by plants [132]. Since most natural phosphates are hardly soluble in water, only through complex decomposition mechanisms phosphorous becomes accessible to plants [132]. For this reason phosphates are artificially made and used as fertilizer.

Frandsen et al. [164] found that under normal gasification conditions (670-1250 °C) P_2O_5 is the main stable phosphorus compound (equilibrium approach). It is suspected to form particles in the PM1 category[16] [189]. Though the main part will be bound into the ash as an oxide.

Phosphorus is not listed in the gas turbine manufactures »black list« of contaminants. Still it is considered to be able to produce depositions and consequently corrosion [126] but it is far less hazardous than sulphur or alkali components. Phosphorus is used as a component for corrosion inhibiting films. Phosphorus is also mentioned to be poiso-

---

[16]particulate matter smaller than 1 μm
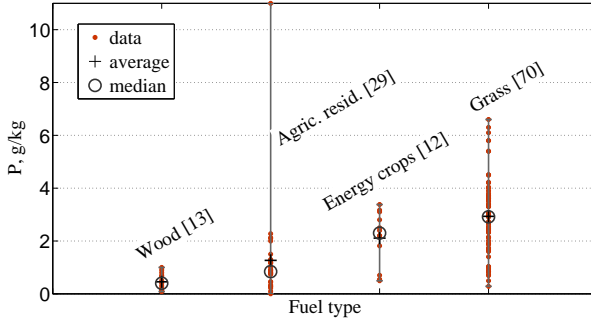
Figure 2.45: *Phosphorous content of various fuels from eDaB*

nous to Ni catalysts [190], which are used as bed material for catalytic gasification.

2.7.4.26 Pb Lead

Lead is poisonous to plants and humans. It inhibits the synthesis of chlorophyll and replaces calcium in bones and teeth and is deposited in the brain, where it causes development dysfunctions. It is lethal if consumed regularly even in small amounts [149].

It is released into the environment from lead processing industry and accumulated in the soils by atmospheric deposition and released waste water [191]. It was also mixed to the petrol to secure a larger runtime for car engines and was subsequently emitted into the environment. It is used extensively in batteries. Though it is not very common on earth the content in the soil is comparably high because of human interaction.

Figure 2.46 depicts some values for Pb in various fuels. There are two very high values for grass being around 14 mg/kg from two different authors. The other samples make an average of 1.35 mg/kg. The samples were taken from locations close to roads, which suggests the deposition from lead emission from cars.

Contents of about 20 mg/kg of lead is allowed in the gas turbine inlet [52]. Otherwise it will lead to substantial depositions and eventually corrosion on the blades [46]. Lead starts to volatilize at around 1100 °C– boiling temperature 1755 °C– where it forms $PbCl_2$ and PbO [164]
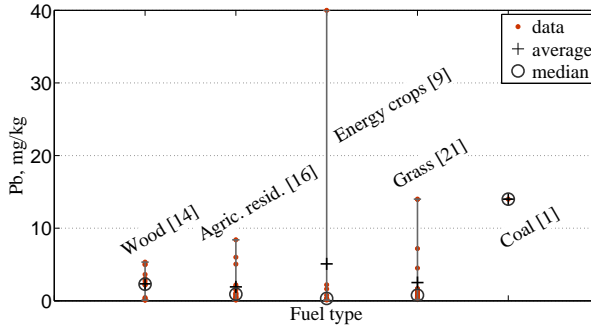
Figure 2.46: *Lead content of various fuels from eDaB*

(coal, equilibrium approach). Above 1300 °C it shifts to gaseous Pb. Lead but also zinc-sulphides solidifies below 800 °C; it deposits at the linings and can block the entire process [87].

The retention of lead in biomass gasification is as low as 10 % [188] for hot gas. Cooled down, the lead is expected to condensate and to be removed by downstream filters.

2.7.4.27 Sb Antimony

The availability of antimony in soils is increased by anthropogenic emissions mainly around ores. Nevertheless it is very mobile and once emitted it can travel the water paths a great distance. There is no functional coherence known so far between plants and antimony.

Antimony is one of the elements scarcely measured (see figure 2.47) when applying ultimate analysis to the fuels. Still it is very volatile and considered to be completely evaporated above 700 °C [188; 192]. This also leads to the conclusion, that cooling the raw gas will lead to condensation of antimony at the fly ash. It can be removed by filtering [192]. Predictions show that at higher temperatures the fraction in the gas phase is strongly pressure dependent [142]. Higher pressure leads to a significant reduction of antimony in the gas phase.
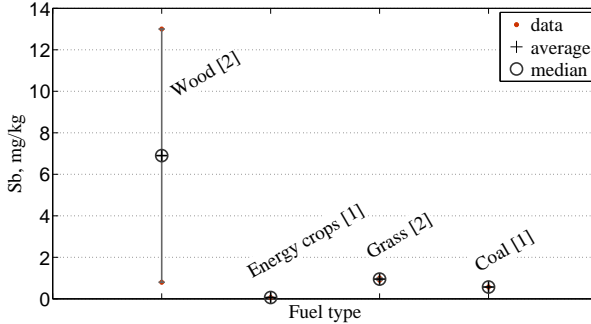
Figure 2.47: *Antimony content of various fuels from eDaB*

2.7.4.28 Se Selenium

Selenium can occur in various forms. Though it is not really known to be essential to plants it is for animals and humans. However the range from toxic amounts to deficits is very small [149]. It is brought into the environment among others mainly by phosphate fertilizer and waste disposal sites. Since it is immobile in its pure form it can accumulate at the site where it occurs. But it can travel via water ways to other areas where plants can take it up and thus it can intrude the food chain easily [139]. The immobility is dependent on the oxygen content of the soil. If it increases selenium will start to spread. Selenium is also very rarely measured for fuel analysis (figure 2.48). It was reported that recycled fly ash used as sorbent removes up to 80 % of the selenium [144].

2.7.4.29 Si Silicon

Silicon is mainly found in shoots of grasses [132]. In leaves and sheaths an average amount is found and the least amount was measured in stems of the plant [193]. Naturally annual grass shows little effort to produce many stems. The silicon content is therefore expectedly high. It is up to now not considered to be essential for grass species [112] but rather taken up because it is simply available. Nonetheless it can have positive effects in structure, against dehydration and strengthens resistance against pathogens. To humans silicon and its components
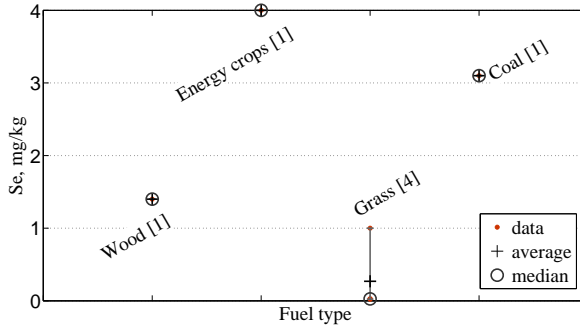
Figure 2.48: *Selenium content of various fuels from eDaB*

are not considered to be toxic. Though as it is the normal case, taken up as respirable particles it will cause damage.
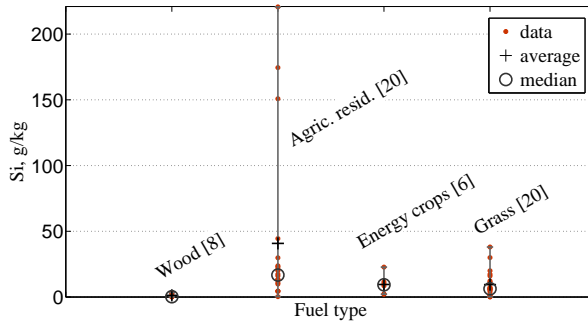
Figure 2.49: *Silicon content of various fuels from eDaB*

The bandwidth shown by the agricultural residues are quite wide. This is caused by two very high values from the same author. These two values are most likely to be understood as contaminated samples. The high values are mostly a result from a soil plant mixture [193]. Without these two numbers the average value is $24\,g/kg$.

Technically silicon is one of the main ash forming elements. It is found in any ash fraction downstream of the reactor. It hardly gets volatilized because of its high boiling temperature, though in some forms it can

become sticky [176], especially when low melting potassium silicates are formed during gasification.

Silica is often used as bed material in combustion and gasification because it is a cheap material. But when high alkali biomass is gasified, the probability to form low melting alkali silicates is very high.

2.7.4.30 Ti Titanium

For plants as well as for other organisms titanium does not play any specific role. It is not needed but is not toxic either. It is taken up as available. The titanium content in the fuel is not measured as a standard value (figure 2.50).
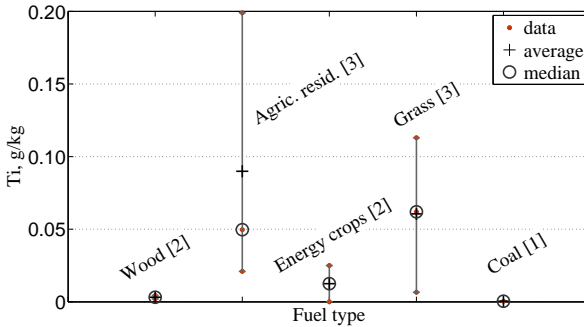
Figure 2.50: *Titanium content of various fuels from eDaB*

Titanium is found in the ash as TiO_2 but is generally a minor part of the ash. Under normal conditions titanium can not be volatilized and is a stable crystal up to 2000 °C. But it is reduced to crystalline TiO_2 above around 350 °C when fluorine is present [164] (coal gasification, equilibrium approach).

Titanium is technically used because of its nature to be very inert against temperature and chemicals. And at the same time being very light. Downstream components are not at risk because of titanium unless it comes as very fine particles and passes the filter barriers.

2.7.4.31 V Vanadium

Vanadium is not an essential nutrient for the plants, though it is said to have positive effects on the formation of chlorophyll [135]. Fossil fuels can contain high amounts of vanadium being emitted consequently by combustion. Figure 2.51 shows some measurements of vanadium done for different fuels.
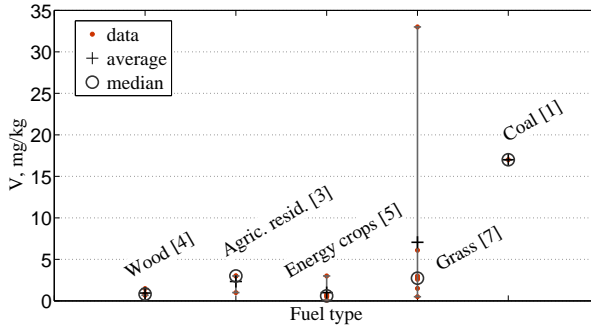
Figure 2.51: *Vanadium content of various fuels from eDaB*

Vanadium is used as part of alloys showing high resistance against corrosion and deformation. On the other side being an element of the fuel, vanadium is able to increase the corrosion rate together with sulphur species [194]. Vanadium pentoxide (V_2O_5), which is present in combustion systems can decrease the sulpidation inhibition of the alloys and subsequently salts like Na_2SO_4 can act more aggressively (see [57] for detailed information). It needs high amounts of vanadium to take place. Grass contains comparable amounts of vanadium to other bio-fuels. There is one extremely high data point from an intensive grass sample in Germany and no hint available if this value is possible or a measurement mistake.

Combustion measurements show that vanadium is retained in the ash at levels between 60 and 90 % [143]. In reducing environments (gasification, pyrolysis) vanadium forms V_2O_3, which is solid up to high temperatures (table 2.4). Care must be taken during start up and shut down of the gasifier when oxidising atmospheres is present [87]. Then V_2O_5 can be formed, which has a melting point of 681 °C [120].

2.7.4.32 Zn Zinc

Zinc is a micro element needed by all plants and other organisms [132]. It is only found in ore together with copper and lead [135]. Most of the zinc emitted is assumed to come from steelworks and electroplating industry. Accumulation from atmospheric deposition and waste water is therefore unavoidable [191]. This of course leads to accumulation in plants, which is the entrance to the food chain. Figure 2.52 shows the elemental zinc found in fuels. There is one extremely high value for salix from Sweden. It increases the average value for the wood group distinctly. Also for agricultural residues there is a data point for rice husk from India being very high. Without these data points the average data is rather 54 *mg/kg* for wood and 26 *mg/kg* for agricultural residues.
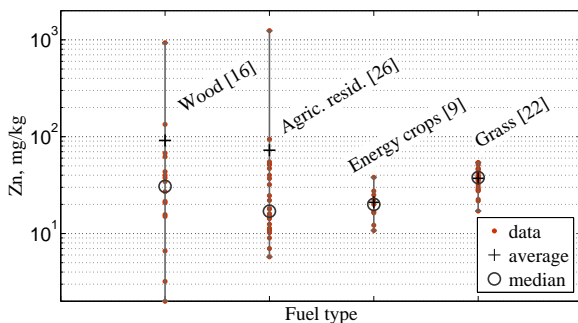
Figure 2.52: *Zinc content of various fuels from eDaB*

In combination with other materials zinc is used to produce sorbents for gas cleaning units mainly for desulphurisation [195; 196].

As Miller [143] states, zinc is not equally retained in the ash for different fuels. Coal combustion seems to bind zinc much better (80 -100 %) than biomass combustion (around 20 % at 900 °C). This is roughly confirmed by gasification tests carried out by Konttinen [188] whereas the equilibrium calculations stated no zinc in the ash. Cooling down the gas just before the filter increased the retention rate to nearly 100 %. Zinc appears to volatilize in measurable amounts above 850 °C using equilibrium calculations [164]. A newer publication [144] reports much earlier volitilization of $ZnCl_2$ above 400 °C.

2.8 Manipulation of the properties

Of course there are many ways to manipulate the properties of the fuel. But only those, which can be applied after the harvest shall be mentioned here.

2.8.1 Drying

Drying describes the reduction of water content in any material. Natural drying always takes an uncertain amount of time whereas forced drying needs large amounts of energy input. Applying the drying process to grass, natural drying is favourable, based on the low mass per area. Spreading the grass after cutting, on place, where it was cut, allows a maximum exposure of the surface for the mass transfer. Matured grass contains much less sugars than younger plants with many leafs, which leads to less degradation and heat development by respiration. The water content must be lower than 22 % to limit degradation and lower than 15 % to stop it. In this regard matured grass is also less sensitiv to degradation and therefore a higher water content may be alowed [102; 77]. Bruising the plants during cutting will quicken the drying process.

There are many ways to force drying but all include some kind of energy. The two most important parameters to enable a good mass transfer is to have a dry gas flow and a large surface. It does not necessarily need heat to dry grass properly but at least a fan to produce forced convection and possibly an air drier. Still, it must be noted that any energy applied to the grass is a reduction of the effective energy benefit unless it is a waste stream.

As it was mentioned before when the grass is dried too much it becomes brittle and mechanical treatment will result in loss of biomass.

2.8.2 Late harvest

With growing age the uptake of potassium decreases while the total mass still increases. This leads to a decreasing potassium content of the total plant [173]. A rather late harvest must be considered as beneficial. Some plants actively push nutrients back into the roots, which are usually not harvested.

2.8.3 Leaching

There are two types of leaching:

⬧ natural leaching [162; 20; 19]

⬧ forced leaching [197; 145; 198–200]

Where the first one is simply based on the rain falling on the already cropped biomass, the second one is active rinsing of the material after the harvest. A special type of natural leaching is to leave it on the field until spring. This of course also leads to a massive biomass loss [201] and is not honestly applicable to grass because the main parts, which decay are leaves and seed heads. The economic value also decreases if the amount of grass per area decreases.

Active leaching can be performed with simple water or other solutions. The process applies to water soluble elements like chlorine, potassium, sodium and magnesium, which show a high response to leaching [199]. It has been shown that leaching can reduce the content of soluble elements to less than 10 % of the natural value.

2.8.4 Torrefaction

Torrefaction or carbonisation is also referred to as mild pyrolysis. The process applies controlled heat to the material, where volatile matter is released. The product shows around 70 to 90 % of the original mass and is brittle and easy to grind. This brings much advantage to the conveyance of the fuel. Especially regarding the cofiring of biomass into a coal burner torrefied biomass shows advantages [202; 203]. Also the energy density of the product is increased compared to the original matter by 10-20 % at a efficiency of 95 % [202]. The torrefied materrial is much more brittle und thus can be grinded very well. Therefore it is suitable for entrained flow gasification [204] But it is an additional process, which is located upstream of the real gasifier and is also an additional effort with respect to energy and costs. Torrefaction is not a best option for any plant, but rather dependent on the type of gasifier used and the overall costs and efficiency.

There is a company in Australia [17], which operates on place torrefaction of hay and agricultural residues. The company is based on the idea that the transportation of char is much less costly compared to hay.

---

[17]www.BIGChar.com.au

2.8.5 Acid treatment

Acid treatment was mainly studied in relation with the CCA impregnated wood. The acid used was humic acid, which is a bio-organic solvent with a variety of small structures. The leaching of CCA showed significant effects after one day [145]. This is most likely not profitably for industrial applications. With respect to energy grass acid treatment will unlikely be necessary.

2.9 Intermediate conclusions

Many elements poisonous and hazardous to gasification systems, are essential for the growth of (energy) grass. Hence, reducing the elements in the soil will only result in less biomass yields. Matured plants show lower contents of critical elements like potassium, sodium and phosphorus.

Whether an element is desirable in the reaction is not only a matter of the element itself but rather what sort of compounds are formed and, which path the element finally takes to leave the system. Some elements would be considered hazardous but leave through the cyclone bound to the ash and are not getting in touch with the gas turbine or environment in the first place. Others would be considered as essential for the process but form aggressive components when getting in touch with other elements under certain conditions. And then there are some elements like Ca and Mg, which are used to bind certain other elements to ash and are thus useful but at the same time problematic if reaching the hot gas path.

For this reason it is obviously important to consider the gasification process as a part of the decision whether a certain element needs to be observed or can be considered rather harmless or even helpful.

From the elemental composition of grass it becomes clear that just the elements critical in gas turbine applications (K, Na, Ca, Mg, S) are found in rough amounts. Elements like vanadium and lead, which complete the list given in table 1.2 are also present in varying amounts. Especially for lead, the location of the grass plays a major role.

Additional elements can be located in grass fuel, which show similar or worse corrosion or deposition behaviour than the one given above. These elements are Ba, Sr, Li and P.

Where the technical specifications are only relevant for the raw gas cleaning, the exhaust gas processing has to handle the environmental aspect. This means the two restrictions can be handled separately.

Fixed bed gasification is not a good choice in this case because in order to reach a high conversion, the temperature must be as high as possible. Since the temperature in a fixed bed can not be controlled properly the gasifier must be operated at a sufficient low temperature to make sure no temperature peaks can cause slagging. This experience was made in an attempt to gasify grass in a fixed bed in 1998 [205]

Fluidised bed gasification is a proven technology and widely available. In two projects the gasification of grass in fluidised beds, proved to be feasible. Fluidised beds need solid input but processing the grass in a solid state, results in considerable losses depending on the distance, type of compression and water content. Concerning the ash melting, the fluidised bed is a good choice too since the temperature distribution is very uniform due to the good mixing behaviour. The process temperature can be set closer to the probable ash melting point.

Processing the fuel locally into a liquid pyrolysis oil or slurry would clearly show the smallest material losses and the best logistical features at the same time. During pyrolysis the inorganic compounds are not removed. There is no advantage from this point of view. An entrained gasification would be the best choice in this case. But the material and technological efforts here are much higher not including the preprocessing plants. The high temperature (1200-1600 °C) would also lead to a much higher mobilisation of inorganic compounds into the gas phase. This increases the gas cleaning effort to a uncertain degree.

Catalytic gasification is not an option as long as there are high amounts of elements, which can and will damage the catalyst. Pressurized gasification seems to be unfavourable based on the negative effects on the ash melting behaviour. Hydrothermal gasification could be an option but it would need a good preprocessing to make the grass pumpable. Further on, hydrothermal gasification is not a state of the art technology at the moment.

From this review only two ways seem feasible for the gasification of grass. This is based on sole material and process properties.

 ✧ compression of the grass and gasification via fluidized beds

✦ pyrolysis or torrefaction and gasification via entrained flow gasi-
fication

2.10 Recommended literature

Some special literature is recommended for extended studies.

✦ Bassam [61] *Energy plant species*

✦ Eltrop et al. [69] *Leitfaden Bioenergie: Planung, Betrieb und Wirtschaftlichkeit von Bioenergieanlagen*

✦ Hartmann et al. [20] *Naturbelassene biogene Festbrennstoffe umweltrelevante Eigenschaften und Einflussmöglichkeiten*

✦ Higman and van der Burgt [87] *Gasification*

✦ Miles et al. [206] *Alkali deposit found in biomass power plants*

✦ von Puttkamer [24] *Charakterisierung biogener Festbrennstoffe*

✦ von Sengbusch [132] *Botanik online – The Internet Hypertextbook*

✦ Strömberg [25] *Fuel Handbook*

✦ Zevenhoven and Kilpinen [185] *Control of Pollutants in Flue Gases and Fuel Gases*

✦ Hart and Cutler [124] *Deposition and Corrosion in Gas Turbines*

Chapter **3**

Sampling raw gas from gasification processes

In chapter 3 the sampling system is presented. It was used for all tests. The sampling system is characterised by slip-stream measurements and step response analysis. Experience made with the sampling system can be found in section 3.6.

3.1 Basic expressions and definitions

3.1.1 Tar, definitions and usage

Tars are generally summarized as all aromatic and poly-aromatic hydrocarbons present in the gas, Moersch et al. [207]. The author states: »*hydrocarbons ... that condense at ambient temperature are considered tar. According to this definition benzene, in the concentrations in which it is typically present in the producer gas, does not belong to the tar.*« van Paasen et al. [208] reports a similar definition for tar. Tar is a: »*generic (unspecific) term for entity of all organic compounds present in the producer gas excluding gaseous hydrocarbons (C1 through C6). Benzene is not included in tar.*«

One way of determining tar is the gravimetric measurement. The tar is scrubbed from the raw gas by a solvent. The solvent later undergoes

a distillation under reduced pressure, in a way that all volatile compo-
nents like water, solvent and benzene will evaporate. The rest can be
determined by weighing. The residue consists only of heavy tars, the
light tars will evaporate during the distillation. The complementary
way to measure the light tars is a analysis GC/MS device [209]. Online
tar measurements have been proposed by Moersch et al. [207] using
FID[1] sensors or with mass spectrometer as suggested by Carpenter
et al. [210]; Neubauer [211]. Tar will not be a major issue in this work
but for the general characterisation of the process, tar measurements
were conducted.

3.1.2 Permanent gases

The expression permanent gases will be applied to all gases, that do
not condensate under moderate pressure ($<5\,bar$) and -10 °C. These
conditions govern the sampling system as described in section 3. The
influence of absorption-desorption processes between the gas and the
solvent is not considered. Permanent gases discussed in this thesis are:
CO, H_2, CO_2, N_2, CH_4, C_2H_Y, C_3H_6, He, H_2S, COS, NH_3 and O_2.

3.1.3 Particles and aerosols

According to Hinds [212], particles are solid or liquid materials showing
sizes smaller than $1\,mm$. Fines are a subgroup of particles within the
designated range of 10 to $1000\,nm$. An aerosol is defined as a suspension
of solid or liquid particles in a gas. The Suspension is not considered
an aerosol if the particles can not stay in suspension (floating) for at
least several seconds. The aerosol produced by condensed components
in combustion or gasification products is called fume.

3.2 Standard methods, advantages and drawbacks

Gas from gasification units is more difficult to handle than gas from
other gas streams like combustion flue gas or atmospheric gas. This
is based on the composition of the raw gas, which includes permanent
gases but also particles of various sizes and condensible matter.

Generally two different types of measurements must be distinguished:

---

[1]Flame Ionization Detector

1 Direct measurements: the sensor measures non-destructive within the main gas stream or a by pass. Direct measurements are very difficult to apply because the optical access to the components is very limited in fume. Optical systems like LIF[2], FTIR[3] or NDIR[4] could in principal be used without a sampling system but normally fail because the access to the raw gas stream is difficult. The elements to be analysed, must be visible to the optics, which is not the case if the elements are hidden within tars or particles. Many optical systems are described in [213; 214].

2 Indirect measurements: a sampling system is applied to prepare the sample stream for the sensor. Preprocessing of the gas by a sampling train mostly results in at least three distinguished samples: the permanent gas stream, a liquid sample containing the condensible matter and a solid sample containing the dust. The analysis of the three different samples demands a higher effort. Another option is to dilute the gas until the condensables fall beyond their dew point. This leads to a lower concentration of all compounds. The solid particle stream must be collected in a filter.

Preprocessing is the commonly applied method to get access to the gas data. The sampling train must be capable of delivering the components in such a way that they are detectable by the measurement device. Permanent gases like CO, H_2, CO_2, N_2 or C_XH_Y can be extracted quite easily by scrubbing and dedusting. The much more complicated exercise is the proper sampling of the contaminants like the mentioned elements in table 1.2. Those can be present as fume, which is difficult to sample.

The fines passing the particle filter need to be collected directly at the outlet. It is well known that large particles are subject to sedimentation phenomena, whereas small particles are subject to diffusion phenomena. But all types of aerosol particles can hardly be recovered once attached to the wall of the lining. The adhesion forces are higher than the forces applied through the gas velocity [212].

At this time, systems with good particle sequestration efficiencies are filters and impactors [212]. The current standard to measure elements

---

[2] Laser Induced Fluorescence
[3] Fourier Transform Infra Red
[4] Non Dispersive Infra Red

in particles like Pb, Ba, Sr or V is given in standards such as VDI [215]. The proposed sampling equipment is purified silica wool with a fibre not larger than $0.4\,\mu$m diameter in a filter cartridge. This approach does not allow a continuous monitoring of contaminants.

A few sampling systems were reviewed by Stahlberg et al. [216]. The state of the art procedure at the moment is described in the tar protocol [208]. The main scrubbing part consists of three to six bottles, the first of which is operated at $20\,°$C and the last ones between -15 and -20 $°$C. The gas is cooled down to at least -15 $°$C to ensure efficient condensation of water and tars. Fast cooling of the raw gas would result in formation of aerosols, which can escape the impinger bottles.

The major draw backs of the protocol is the limited capacity of the stationary solvent, which accumulates tars, water and to a certain degree particles. Due to the low temperature there is a maximum allowable water concentration which will lead to the formation of ice.

Another possible method is the »*Petersen column*« [208]. This scrubber is a semi continuous device, in which two scrubber stages (isopropanol) are installed. It can be operated in flow through mode. Additionally, an aerosol filter (G3 glass frit) is positioned between the two stages. This filter can not be exchanged during the operation.

For all sampling systems the extraction of the condensables works reliably (table 3.1) but the collection of fines involves particle filters, which can not be operated continuously. Thus, using the available systems, the synchronous analysis of permanent gases and contaminants can not be achieved. For this reason a different approach was chosen in this work.

Sampling type	Continuous	Condensables	Ultra fines	Remark
Tar protocol	✗	✓	✗	complex
Peterson column	✓	✓✓	✗	simple
Quartz wool filter	✗	heated	✓	react with alkalis
Porous fritt filter	✗	heated	✗	react with alkalis

Table 3.1: *Properties of the common sampling systems*

3.3 Sampling approach in this work

A dedicated sampling system that can handle the requirements was invented at PSI[5][6] and further optimised and characterised in this work. A flow chart is presented in figure 3.1. The system is a continuous and pressurized scrubber. The raw gas is sampled and instantly quenched by a fresh solvent at room temperature to avoid the formation of aerosols. The two phase flow is compressed and cooled down to -10 °C to ensure a high condensation rate for water and tars. A 10 m long tubing at this temperature ensures an excellent mass transfer due to a higher area of the gas liquid interface. It also results in a longer residence time of the solvent and gas compared to impinger bottles (see section 3.5). After this tubing the gas is separated from the solvent and both streams are guided out of the cooling box. The system delivers two streams, which can be analysed separately: a dry gas stream containing the permanent gases, and a solvent stream containing the water, tars and particles. The gas stream is analysed by a micro GC but can as well be analysed by an FTIR , MS, etc. The solvent stream can be analysed e. g. by means of an ICP-OES or GC/MS dependent on the information that needs to be found.
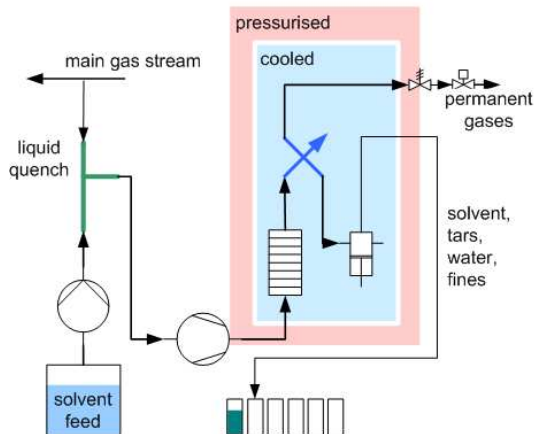
Figure 3.1: *Flow chart of the dedicated sampling system*

---

[5] Paul Scherrer Institut
[6] based on the idea and efforts of Jörg Schneebeli

The solvent used in the described system is Arcosolv PM®[7]. It shows good solvent properties for tars and at the same time mixes well with water. The solvent stream was set around 1.5 *ml/min*. The mean gas flow was around 1 *l/min*. The sample gas flow depends on the compression and the gas composition. It was therefore constantly monitored. The contaminants in one litre of dry sampling gas will be found in 1.5 *ml* of solvent.

3.4 Evaluation of the particle slip-stream

In order to proof the performance of the sampling system experiments were conducted to verify different scrubbers for particle slip-streams. Three general types of scrubbers were evaluated.

◇ four laboratory impinger bottles in series connection

◇ a continuous atmospheric scrubber

◇ a continuous pressurised atmospheric scrubber

The aerosol was produced by vapourising KCl in a TG[8] at 900 °C using a condensation interface as described in Ludwig et al. [217]. The particle size distribution peaked around 200 *nm* as described in Kowalski [218]. The sensor used was a surface ionisation detector (SID) being described in literature several times [219; 214; 220] (see section 5.4.2). This sensor is qualified to analyse airborn alkali components (K, Na, Cs). The strategy was a measurement of the alkali particles before entering the scrubber and directly after the scrubber. The inlet signal was set to 100 %. The ratio of outlet to inlet signal is described as slip-stream (bar 1-3 figure 3.2). These particles will be lost if this type of sampling is applied. Additionally, a slip-stream measurement during the gasification of a single grass pellet (see section 5) was conducted using an improved version of the first SID (bar 4 figure 3.2).

Impinger bottles were never thought to operate as particle retention system. But as an example the retention of the particles in the series of 4 impinger bottles is expressed in bar 1 showing 60 % slip. A continuously operated scrubber at atmospheric conditions still shows a slip-stream of 20 %, wheras the pressurised scrubber already reduced the particle slip to 1 %. Bar 4 in the graph shows the slip for the alkalis

---

[7] Propylene Glycol (Mono) Methyl Ether
[8] Thermo gravimeter
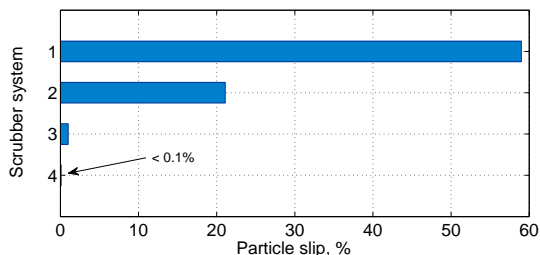
Figure 3.2: *Slip-stream of particles through different sampling systems.*
(1) four impinger bottles at 0 °C,
(2) atmospheric scrubber at -25 °C,
(3) pressurised scrubber at 20 °C,
(4) PSI pressurised scrubber at -10 °C

emitted during the gasification and subsequent combustion of a real grass pellet. With the improved design of the SID the slip-stream was just detectable (see figure 5.5) and smaller than 0.1 %.

The reason why the scrubber shows an excellent particle sequestration is the fact that the sampling stream is compressed after it was quenched. This leads to a saturation of the gas phase with the solvent, which condenses at the particles during the compression and subsequent cooling. This behaviour is very similar to a condensation particle counter (CPC). Here particles are guided through an n-Butanol saturated atmosphere and subsequent cooling leads to condensation and an increase in particle size.

From figure 3.2 it can be derived that only the PSI invented pressurised scrubber led to a satisfying result. For all sampling jobs in this thesis this sampling system is chosen.

3.5 Signal change due to the sampling system

By its nature, the chosen sampling system leads to an increased delay between the actual process and the measurement data. Additionally the signal may be blurred due to backmixing of components. In order to evaluate this behaviour step response measurements were carried out for both the GC and the ICP-OES.

Figure 3.3 illustrates the step response for the gas measurements. The step was produced by the addition of H_2S to the gas stream. Sulphur was selected because both used measurement devices (micro GC, ICP-OES) can detect sulphur adequately. From the graph it can be read out, that for the gas measurements the delay to detect 90 % change in concentration is below 5 min. This value is valid for both: step up and step down. Since the experiments are set to last for 5 h and are conducted in steady state mode this response is sufficient.
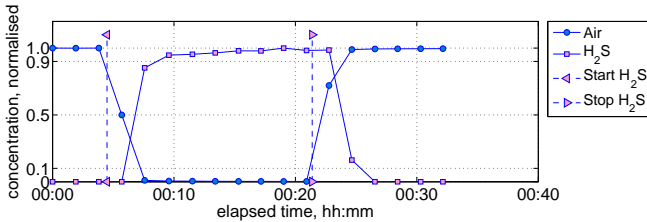
Figure 3.3: *Step response of the sampling system including lines to the micro GC*

Figure 3.4 illustrates two step responses for the ICP-OES installation. The first step was done by adding constant amount of Ca to the solvent the second step was the addition of H_2S to the gas phase. Two things can be observed here. The delay for the ICP measurements is longer and depends on the direction of the step. A 90 % increase in concentration can be detected much faster (10 min), than a decrease (34 min). This includes the dead time of 9 min. This behaviour can not be explained solely by the method of the sampling system. The step down should proceed exactly like the step up. The fact that the step up was performed from a clean system to a Ca doped system indicates, that this effect is maybe due to adsorption- desorption precesses in the lining or in the vaporiser of the ICP-OES.

The second step response corresponding to the sulphur addition to the gas stream, shows a response of 9 min to reach 90 % for the step up; but 11 min for the step down. From this result, it can be concluded, that the gas travels much faster through the lining than the solvent. The measurement dynamic for changes in the gas phase concentration is much better. For a steady state 5h run the dynamic is fast enough to detect significant fluctuations with both described systems.
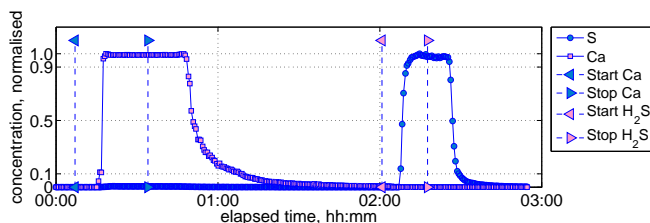
Figure 3.4: *Step response of the sampling system including lines to the ICP-OES*

There is an further characteristic of the sampling system: being able to measure substantial amounts of sulphur in the ICP-OES analyser means, that there are significant amounts of sulphur being absorbed in the solvent (figure 3.4). The micro GC measurements during the gasification experiments revealed that after about $20\,min$, H_2S and COS broke through; about 10-40 ml/m^3 could be measured. This means sulphur is not separated properly but distributed in both solvent and gas phase. Sulphur also adsorbs at metallic surfaces and thus without a specially equipped reactor and lining (e.g. sulfinert$^{®}$ coated) the diagnostic of sulphur components is always imprecise. For further measurements sulphur will be excluded from the analysis.

3.6 Challenges with the sampling system

The sampling system had to be optimised during the first tests to achieve stable operation. The changes were mainly related to the compressor and phase separation part. The major trouble – only during the gasification of grass – was the formation of ammonium hydrogen carbonate (NH_4CO_3H), which fell out as a powder. Figure 3.5 shows two infra red (IR) spectra: one ammonia hydrogen carbonate for lab us and one for the sample. The spectra are in agreement with the SDBS[9] [221]. The marked peaks correspond to the double bond stretching of C=O (around $1630\,cm^{-1}$) within the carbonate and nitrogen bond stretching $N-H$ (around $3120\,cm^{-1}$) within the ammonia structure. The two distinct signals at 830 and $700\,cm^{-1}$ correspond to the bending vibration of NOC and OCO. The difference of the transmittance amplitude can be due to unevenly pressed samples or inhomogeneous sample.

---

[9]Spectral database for organic compounds
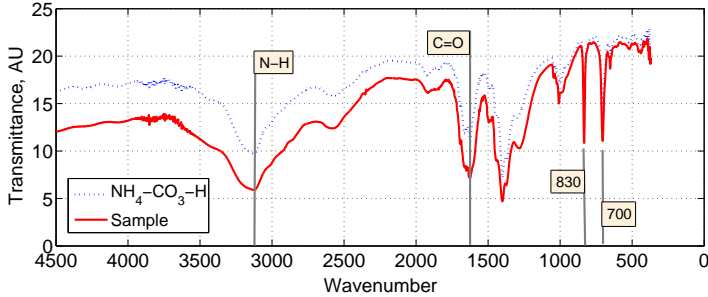
Figure 3.5: *IR spectra of the sample and ammonia hydrogen carbonate*

Ammonium hydrogen carbonate is formed under low temperature pressure when ammonia, CO_2 and water is present [222] (equation (3.1)).

$$NH_4CO_3H \rightleftharpoons NH_3 + CO_2 + H_2O \qquad (3.1)$$

The mere existence is not a problem in general but the large amount of carbonate leads to clogging of the capillary tubing. Especially the tubing to the ICP-OES device was affected. Because this did not happen during the gasification of wood it indicates there large amount of ammonia in the grass gas. The measurement of ammonia was not a topic in general, but there were some measurements yielding concentrations over $2000\,ml/m^3$ dry. This corresponds to roughly $15\,\%$ of the grass bound nitrogen. The ammonia concentration in fluidised bed gasification of wood is usually $<900\,ml/m^3$ [223]. Turn et al. [169] reported as much as $1710\,ml/m^3$ for the gasification of banagrass [10]. But values as high as $3\,\%$ were reported by Zhou et al. [224] for Leucaena. Figure 3.5 also shows a part that is clogged by the carbonate. The sampling system could always be reactivated by reducing the pressure and increasing the temperature. The maintenance could always be done within less than an hour.

ICP-OES devices are normally used with aqueous solutions. Running the ICP on a solvent loaded with tar turned out to be very challenging and not yet state of the art. The calculated detection limits are not trustworthy anymore.

For the important elements the detection limits were determined manually by comparing spectra, baseline and background noise. Table 3.2

---

[10] Pennisetum purpureum

lists the elements with a major difference. These differences lead to substantial misinterpretation for measurements close to the detection limits. Sodium and calcium can be detected in much lower concentrations than expected, whereas potassium is much less sensitive for the used solvent.

	DL Software	DL by hand
Na	69	5.6
K	21	92.9
Ca	38	0.3

Table 3.2: *Difference of detection limits as determined by software or by hand*

Chapter 4

Fluidised bed experiments

In the first part of chapter 4, a short introduction is given to gasification in general and specifically grass gasification.

From section 4.4 page 99, the construction and setup of the bubbling fluidised bed will be presented, including the theoretical background of fluidisation. Methods and measurement techniques as well as heat loss calculations of the reactor will be given from section 4.5.5 page 111.

Section 4.6 page 118 treats the general procedures used for the experiments and the characterisation of the fuel used.

In section 4.9 page 123 all the results concerning the fluidised bed experiments are presented and discussed. This includes the permanent gas data, process stability, contaminant readings and the axial profile experiment.

The monitoring of the contaminants were conducted as a cooperation with the working group of Christian Ludwig (Chemical Processes and Materials at PSI). The development of the method to run the ICP-OES on solvent instead of aqueous solutions was decisively realised by the group members and further tested and optimised in the presented experiments.

4.1 Brief review of gasification processes

Gasification is as old as fire itself. Burning a solid fuel is always a combination of gasification and combustion. Industrial gasification technologies started at the beginning of the 19th century, at which time the gas was used mainly for illumination and cooking [87]. At the beginning of the 20th century a considerable knowledge about gasification was established and first books written [225–228]. The gasifiers were fixed bed reactors of various types. One is illustrated in figure 4.1. Since then gasification became very sophisticated based on its potential to transform solid fuels into all kinds of gaseous fuels or chemicals. There is much interesting literature on the history of gasification and its technology progress.

Very early publications about gasification or partial combustion as it was called too are » *Gas Producers and Producer gas power plants* « by Wood [225] or » *Modern power gas producer – practice and application* « by Horace [228] and a few more [226; 227]. Amazingly, they already managed to built plants with sizes as large as 30 *MW*, processing coal at rates of 10 *t/h* at the turn of the 19th century. The reason to pass from combustion onto gasification was: » *The chief reason why the preliminary gasification of coal is advantageous is that the direct combustion of raw coal can only be effected by the employment of a very considerable excess of air.* « Horace [228]. Another reason was the idea to use the gas in » *gas-engine cylinders* «, flexible process heat or lighting. The solid and gas analysis were already surprising sophisticated, still not as convenient as today. Some years later the liquefaction of coal became an interesting application due to an increased need of liquid fuels for various applications like aero planes, ships and cars, or stationary power engines (Fischer [229]).

Later publications added better understanding of the kinetics of the reactions, pre-treatments, post-treatments and a variety of additional applications and products ([230; 223; 231; 127; 87]). It is recommended to review the cited literature if deeper insight is needed by the reader.

Gasification takes place in several steps, which can overlap depending on a variety of parameters like fuel size or moisture. The first step is the drying of the fuel followed by pyrolysis and gasification by which the volatile matter is driven out of the fuel due to the high temperature. The remaining char is gasified by H_2O (equation 4.3) or if oxygen is
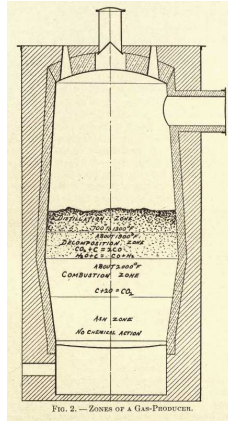
Figure 4.1: *Historical Siemens gas producer 1906 Wyer [226]*

present combusted (equation 4.1 and 4.4). The char gasification process takes much longer and is the limiting step. This step is additionally dependent on the type of the char. Char produced by grass gasification shows a very open structure and thus good access to the reacting gases. For wood or coal the char is much more compact and the residence time can be expected to be longer.

Equations (4.1) to (4.7) are the major gasification and combustion reactions as given in [232; 223; 87]. Equation (4.6) is the methanation reaction. It is of minor influence since the equilibrium favours H_2 and CO at gasification conditions. The first three reactions ((4.1)–(4.3)) correspond to the solid-gas reactions, whereas the later four ((4.4)–(4.7)) are homogeneous gas phase reactions. Following equilibrium calculations (stoichiometric input), H_2 and CO are promoted at higher temperatures the other species at lower temperatures. The carbon conversion is better at higher temperatures.

$$C + \tfrac{1}{2}O_2 \rightleftharpoons CO \qquad (\Delta H_R^0 = -111\, MJ/kmol) \qquad (4.1)$$

$$C + CO_2 \rightleftharpoons 2\,CO \qquad (\Delta H_R^0 = +173\, MJ/kmol) \qquad (4.2)$$

$$C + H_2O \rightleftharpoons CO + H_2 \qquad (\Delta H_R^0 = +131\, MJ/kmol) \qquad (4.3)$$

$$CO + \tfrac{1}{2}O_2 \rightleftharpoons CO_2 \qquad (\,\Delta H_R^0 = -283\,MJ/kmol\,) \quad (4.4)$$

$$CO + H_2O \rightleftharpoons H_2 + CO_2 \quad (\,\Delta H_R^0 = -41\,MJ/kmol\,) \quad (4.5)$$

$$CH_4 + H_2O \rightleftharpoons 3\,H_2 + CO \quad (\,\Delta H_R^0 = +206\,MJ/kmol\,) \quad (4.6)$$

$$H_2 + \tfrac{1}{2}O \rightleftharpoons H_2O \qquad (\,\Delta H_R^0 = -242\,MJ/kmol\,) \quad (4.7)$$
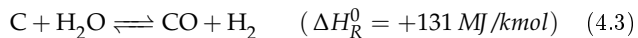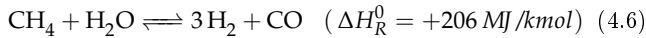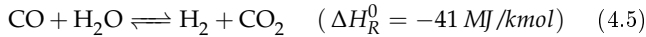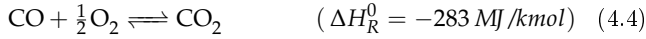
If the gasification is autothermal, the heat for the endothermic reactions ($\Delta H > 0$) is taken from partial combustion equation (4.1) or total combustion (4.4) and (4.7). For allothermal gasification the required heat must be introduced from outside.

The basic gasification types are depicted in table 4.1. From the left fixed bed i. e. downdraft, fixed bed updraft, fluidised bed and entrained flow. The fluidised bed can be designed as bubbling fluidised bed without recirculation of bed and fines or as depicted as circulating fluidised bed.

Furthermore, there are a variety of modified gasifiers like the Battelle/FERCO process [233], Blauer Turm [234] or annular reactors [183; 27]. The goal is usually to better control the various types and completeness of the reactions in the reactor; mainly the gasification and char conversion. The main motivation is the heat control between those two processes. While the char gasification is endothermic (equation (4.3)), the entire process should be autothermic. The named processes aim to either separate the processes and transfer the heat from the char through combustion back or bring them closer together so the exothermic reactions can feed the endothermic char gasification without producing local cold spots.

The main advantages of the basic types are noted in the table 4.1 below the pictures. Concerning the gasification of grass the ash melting being critical property, excludes the fixed bed gasification due to both experience (see below) and theory. During fixed bed gasification local hot spots can not be avoided based on the nature of the process. The tendency of the fixed bed to form channels and can lead to temperatures as hot as 1000 °C. This would certainly lead to bed agglomeration and eventual termination of the process. Leaving aside special designs, this leaves the two remaining options. Entrained flow gasification is fed by a slurry or powder. This makes fuel preparation a crucial point. For fluidised bed gasification the fuel can be heterogeneous instead. The high temperatures of the entrained flow reactor would inevitably lead to a high volatilisation of inorganic components, which later on

need to be removed by possibly additional gas cleaning units. The SFG gasifier e. g. uses water quenching to cool the gas and scrub it partially. The contaminant load in the water would further lead to an increased waste water treatment. From this point of view, the fluidised bed technology with a dry hot gas particulate removal seems more suitable. The complexity of a fluidised bed is smaller, which is an important point when it comes to the economic value of the fuel. Lower costs for the plant maybe essential for a realisation of a demonstration unit (see also [235]).

Table 4.1: *Comparison of basic gasifier types (pictures taken from [216])*

Type	Downdraft	Updraft	Fluidised bed	Entrained flow
Temperature, °C	600–1000	600–1000	700–900	1200–1600
Size, MW	< 10	< 10	< 200	< 1000
Tar load [223], g/m^3	0.1-6	10-150	1.30	< 0.1
Fuel flexibility	medium	medium	high	low
Complexity	low	low	medium	high

4.2 Basic expressions and definitions

4.2.1 Air to fuel ratio Lambda λ

Lambda (λ) is the Greek symbol usually chosen for the air to fuel ratio. It is defined as 1 when the molar amount of air, which is added to the fuel exactly matches the amount needed to get a complete combustion of the elements C, H and S to CO_2, H_2O and SO_2 (Baehr [236]). The reaction scheme is given in formula (4.8), by which the meaning of *lambda* becomes quite clear.

$$C_mH_nO_pS_q + \lambda(m + \frac{n}{4} - \frac{p}{2} + q)O_2 => mCO_2 + \frac{n}{2}H_2O + qSO_2 \quad (4.8)$$
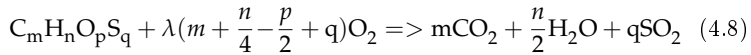
By this definition λ is

$$\lambda = \frac{\text{Oxygen added}}{\text{Oxygen necessary to reach complete combustion}} \quad (4.9)$$

If the fuel contains oxygen like bio-fuels do, it is subtracted in the denominator as can be seen from equation (4.8). This definition refers to dry fuel since water takes no part in the combustion other than reducing the temperature.

4.2.2 Carbon conversion Ψ_C

The carbon conversion tells about the ability of the process and the applied settings to convert the solid carbon into gaseous carbon. This equally applies to combustion and gasification, since solid carbon is not meant to be a product of both processes. It is thus

$$\Psi_C = \frac{\text{Carbon converted}}{\text{Carbon provided in the fuel}} \quad (4.10)$$

A high carbon conversion is always desirable, but it does not give any information about the energetic efficiency.

4.2.3 Cold gas efficiency η_C and hot gas efficiency η_H

The cold gas efficiency η_C and hot gas efficiency η_H describe the energetic efficiency of the conversion process. The difference between these two efficiencies is the sensible heat and heat of condensation of the hot gas, which can be useful if the gas has not to be cooled down, or the

heat included the heat of condensation can be used in another part of the plant. This is the case for IGCC power plants, where the heat can be used in the bottoming cycle. The efficiencies are defined according to Basu [127]

$$\eta_C = \frac{\dot{V}_{gas} LHV_{gas}}{\dot{M}_{fuel} HHV_{fuel}} \tag{4.11}$$

$$\eta_H = \frac{\dot{V}_{gas} HHV_{gas} + \dot{Q}_{sensible\ heat}}{\dot{M}_{fuel} HHV_{fuel}} \tag{4.12}$$

4.3 What literature tells about grass gasification

In table 4.2 projects are listed, which seriously tried to gasify grass or grass-like biomass. The first experiments were conducted in 1993 in a 100 kW HTW[1] gasifier. It is a fluidised bed invented by Fritz Winkler in 1921 [127]. In the tests rye grass was successfully gasified at moderate temperatures (620-640 °C) in order not to risk ash melting. In 1995 Alfalfa was tested for its gasification suitability in the IGT Renugas process (bubbling fluidised bed). Tests were successfully conducted up to 800 °C with additions of dolomite to influence the ash melting behaviour. A trial which employed the fixed bed was not successful due to problems with the fuel. The higher density of the finer particles of grass compared to wood in the bed resulted in a higher pressure drop and bad gasification behaviour [237]. It was stated that the fuel fell apart in a way such that a good air fuel contact could not be ensured anymore. The experimental reactor [27] produced very low heating values and thus is considered not competitive. The fluidised bed experiments reported by Öhman et al. [119] were conducted in order to analyse the deposition layers on the bed material not to analyse the gas composition. The supercritical gasification is not available in large scales at the moment.

In all projects permanent gas data was collected but apart from [169] no analysis for inorganic compounds other than sulphur compounds was accomplished. Turn et al. [169] reported measurements for alkalis using a batch filter setup for 3 h experiments. The bed material used was likely of olivine type and alkali adsorbing as it can be seen from the experiments. Banagrass belongs to the fuel type of energy crops

---

[1]High Temperature Winkler

and shows lower alkali contents than native grass. Due to the analysis above, the fluidised bed technology seems the best suitable approach.

Ref.	Gasifier	Fuel	ϑ, °C	Size, MW	Success
[3]	Fluidised bed	Rye grass	640	0.1	Yes
[4]	Fluidised bed	Alfalfa	*800	1.7	Yes
[5; 237]	Fixed bed	Native grass	–	0.2	No
[169]	Fluidised bed	Banagrass	**800	–	Yes
[119]	Fluidised bed	Alfalfa	600	0.05	Yes
[238]	Supercritical	Clover grass	900	Lab scale	So far
[27]	Fluidised bed	Blue grass	650	0.02	No

Table 4.2: *Review of projects with the topic grass gasification (*with additives to avoid ash melting, **with reactive bed material)*

4.4 Brief introduction of fluidised beds

The fluidised bed as a reactor was introduced in section 4.1 for gasification applications. Fluidised beds can be used for almost any gas-solid interactions. Besides gasification, this may be combustion boilers, catalytic reformers, absorption- desorption processes or the production of chemicals.

The main advantages of a fluidised bed as described above are the uniform bed temperature due to the good mixing possibilities and the option to use the bed material in order to influence the reactor behaviour. Here adsorbing, reactive or even catalytic bed materials have been employed.

4.4.1 Fluidisation

A fluidised bed is established when the velocity through the reactor is just high enough to lift the material which is in the reactor. The floating of the material marks the transition from a fixed bed to a fluidised bed. This point is called minimum fluidisation with the characteristic minimum fluidisation velocity u_{mf}. Increasing the velocity leads to an expansion of the material until the grains are entrained. Before this point the bed is called bubbling. If the material is deliberately entrained and recirculated into the bed it is called circulating fluidised bed. Then the velocity in the reactor is higher than the terminal velocity u_t.

From a certain point the flow rather resembles a pneumatic transport of particles, then the process is called transport reactor. A bubbling fluidised bed consists of two phases a bubble phase which is considered particle free and a dense bed, where a mixture of gas and particles is found. From this view it becomes clear that heterogeneous reactions like char gasification will take place only in the dense phase, whereas homogeneous reactions can take place in both phases. Further reading of fluidised beds may be found in Yang [239], more specialised literature on fluidised bed gasification can be found in Basu [127]; Higman and van der Burgt [87].

4.4.2 Bed materials

The bed material can be of various types. The reacting particles may form the bed themselves or additional bed material can be used which may be catalytically active or inert. There are several important pro-perties of the bed material which should be considered:

✧ reactivity (influence on the reaction mechanisms)

✧ density and size of the particles (responsible for the fluidisation characteristic)

✧ specific heat (responsible for the temperature texture in the bed)

✧ Moh's hardness (responsible for abrasion of the reactor or the bed itself)

As long as there is not a need for a reactive bed material the inert material should be preferred. Reactive bed material has to be repla-ced, which increases the maintenance effort. Furthermore, reactive bed material changes its properties after taking part in the reaction, e. g. if $CaCO_3$ forms $CaSO_4$ Moh's hardness will be reduced to only 2. This would lead to an increased grinding activity of the bed and the dust would be carried away with the gas. Whereas $MgCO_3$ can form $MgSiO_3$ which has an increased Moh's hardness of 7.

Table 4.3 lists basic information about three different bed materials which are commonly used in gasification applications. The solid density of the materials can differ due to the changing porosity. Porous alu-mina can have density of only $1300\,kg/m^3$. This type is mostly used for catalyst applications. It has to be noted, that real inert bed material is almost impossible for a gasification environment. It has been reported

Mineral	Silica	Dolomite	Alumina
Chemical composition	SiO_2	$CaMg[CO_3]_2$	Al_2O_3
Influence (reactivity)	alkali silicates	ash melting point, sulphur retention	alkali-alumino-silicates
Solid density, kg/m^3	2650	2860	3970
Specific heat, $kJ/(kg\,K)$	0.962	1.01	1.1
Moh's hardness	6.5	3.5	9
Heat expansion, %	1.3	1.7	1.2
Geldart classification	B	B	B
$d_p(50)$ μm	200	200	270

Table 4.3: *Bedmaterials and properties (specific heat and heat expansion from [240], Moh's hardness and density from [120])*

that silica bed material combines with alkalis which leads to a sticky surface, whereas alumina can form alkali-alumina-silicates [180; 119]. However, the latter reaction is not expected to have any grave influence on both gasification and fluidisation.

4.5 Experimental setup of the bench-scale gasifier

4.5.1 Construction of the bubbling fluidised bed

The bubbling fluidised bed test rig is depicted below (image 4.2). It is a semi continuous system since it possesses a fuel feeder and a storage large enough to run a test of several hours but is not equipped with an ash removal system. This means the ash stays in the bed for the entire time of the experiment or is entrained if the particles become small enough.

The fuel enters the system from the silo ①, which contains most of the grass. It is released from the silo into a dosing container ③ by a rotary feeder ②. About 90 *ml/min* of nitrogen is given into both the silo and dosing feeder to prevent the product gas from flowing upstream into the fuel container and thus causing a back-burning. From the feed container the fuel is transported into the reactor ⑤ close above the frit by a feed auger ④. The auger runs within a water cooled double jacked (figure 4.7) to prevent early heating of the fuel, which would result in slow pyrolysis. Within the fluidised bed the fuel reacts with
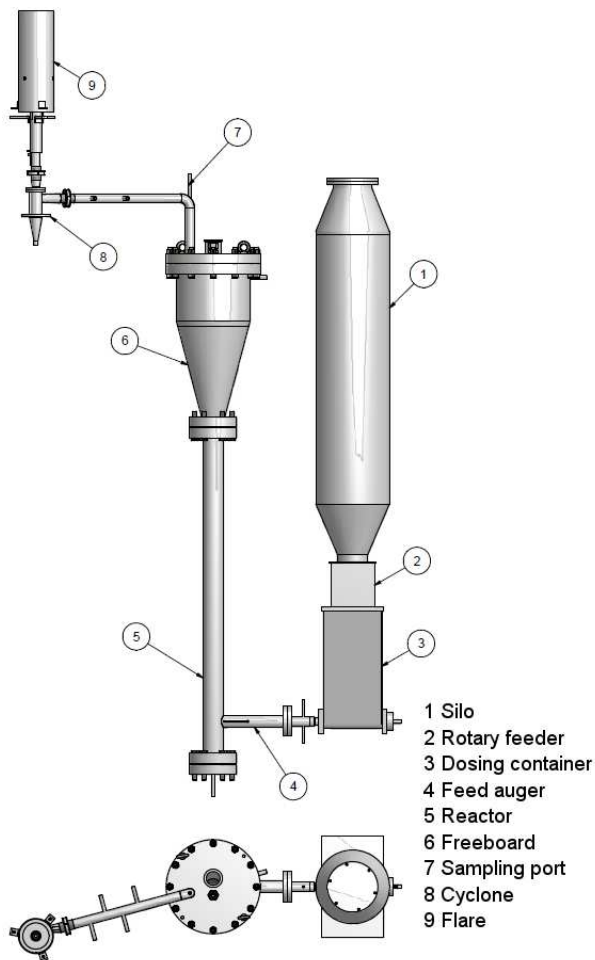
Figure 4.2: *General design of the bubbling fluidised bed test rig.*

air to mainly H_2, CO, CO_2, CH_4 and steam. The ash stays in the bed, whereas the product gas leaves the system through the freeboard ⑥. Several sampling lines are available directly after the gas exit e. g. ⑥. The product gas flows through a cyclone ⑧ and then into a flare ⑨. To secure no reactive product gas is emitted the flare is equipped with a

pilot burner running on methane. The hardware will be described in the order of downstream components as far as possible.

Feature	Value
Reactor height	$1\,m$
Freeboard height	$0.5\,m$
Solid feed	$0.3\text{-}3\,kg/h$
Gasification agent	air
Temperature	$600\text{-}900\,^\circ C$
Pressure	atmospheric
Reactor diameter	$52\,mm$
Bed material	$SiO_2/\ CaMg(CO_3)_2/\ Al_2O_3$
Size	$2\text{-}10\,kW$
Fuel	chaffed wood/ chaffed grass
Bed material size range	$100\text{-}300\ \mu m$
Reactor material	high temperature alloy (Inconel$^\circledR$)

Table 4.4: *General properties of the bubbling fluidised bed*

4.5.1.1 Silo

The silo is a $25\,l$ container with a conical exit onto a rotary feeder. Here the biomass is placed before running a test. The bulk density of chaffed grass is $377\,g/l$; thus the container may keep around $9.4\,kg$ of fuel. For shredded wood the capacity is slightly higher because the bulk density is $400\,g/l$.

Based on the conical shape of the exit, bridging will inevitably occur unless special care is taken. Extra devices normally result in extra sealings which should be avoided as long as possible. The solution is a simple approach best explained by means of the picture given below. It is a system, which is not dependent on extra machines or controlling devices but self-sustaining and reliable.

It is made of a hollow steel sphere, into which a steel tube is soldered. Several steel wires are soldered into the tube to form a figure similar to a dead tree. The sphere is placed directly onto the rotary feeder. Since the radius of the sphere is much bigger than the hight of the blades of the feeder, the force applied by the passing blade will lift the sphere. The weight of the structure will pull it back down again. If the system runs properly, there will be always material within the cabins and the sphere will float on top not stressing the blade or vice
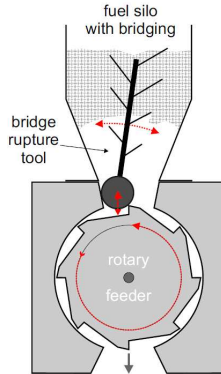
Figure 4.3: *Device to avoid bridging of the fuel in the exit of the silo.*

versa. If the cabins stay empty in the case of bridging the movement of the structure will rupture all bridges. The system proved to be very reliable.

4.5.1.2 Feed auger

To generate a continuous gas stream a controlled fuel stream has to be ensured. This is done by a feed auger, which takes the fuel from a small container and feeds it by a screw into the reactor. The mass flow is proportional to the fuel column above the screw if a constant rotation of the auger is applied. This means the level in the container must be controlled. This is managed by a level sensor which controls the switch of the rotary feeder. Fuel from the silo is then released into the container of the feed auger. The auger is controlled by a special system bought with the feeder. The speed can be adjusted from zero to 2000 rounds per minute referred to the engine. There is a gear box, which transforms the speed to 100 rounds per minute at the screw. The controller gives out an alarm signal if the auger is blocked and the current of the motor rises above the given limit.

Two augers were manufactured from a $18\,mm$ standard hammer drill and a wood snake-drill. The shafts were changed to match the dosing feeder (figure 4.4).

Feeding augers are always one of the major failing points in thermal process engineering. The dimension and geometry of the screws must be

Figure 4.4: *Feeding augers of different sizes.*

optimized for each task they have to do. Transporting fuel showing fines and bigger clusters at the same time is one of the most difficult tasks. First of all the screw must not block itself by forming plugs, which is the case, when the downstream part of the screw transports faster, than the upstream part. Second the auger must not push the fuel to the inner wall of the outside tubing, which is the case if the transporting shoulder of the auger is tilted too little. Then the fuel is ground between the auger and the wall of the tube and compacted and the screw will be blocked by the densified fines. Instead the shoulder must show a geometry such that the fuel is moved back into the auger. And third the auger must be much more smooth then the wall, otherwise it will not transport the fuel properly. The drills were manually adopted to all of these criteria. Additionally at the tip of the screw the shoulder was sharpened to avoid the clogging of the exit. This blade was added to cut the coke away from the wall which is formed during the transition from the cooled feeding tube into the hot reactor. This also means, the auger must reach slightly into the reactor to achieve this goal. To avoid the heating of the auger – this would result in an uncontrolled pyrolysis of the fuel in the transport tubing – The shaft was drilled open. This results in less heat transfer through the material figure 4.5.

Figure 4.5: *Tip of the auger showing a drill hole for less heat transport into the fuel pipe.*

The feed augers were calibrated in place using the original setup of silo and rotary feeder. The calibration curves are plotted below. For the tests the stone auger was used since its feeding characteristic was more

suitable. It has to be noted, that the auger transport rather by volume than by mass. Usually it is more important to feed a constant heat rate (LHV per time). To achieve this the feed rate needs to be corrected for the water content of the fuel. For each experiment the fuel was weighed before the test and after the test. So the overall amount of fuel could be properly determined.
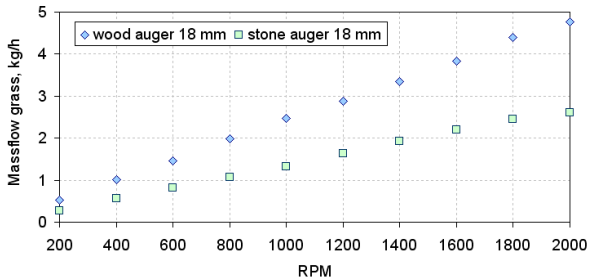
Figure 4.6: *Calibration of the feeding screws.*

The auger and fuel within is cooled by a double jacket . For construction reasons the cooling fluid must enter and leave the jacket at the same end (①, ② in figure 4.7). Therefore a double helix was chosen to separate the inbound and outbound stream and distribute the cooling effect circumferentially along the tubing.

The dosing feeder is not mounted fixed to an external frame but connected to the bottom of the reactor by a metal wire. This is necessary because the thermal expansion of the reactor between 20 and 800 °C leads to a lowering of the feeding entrance of about 18 *mm*. As illustrated in figure 4.8, the wire runs from the reactor to the bottom of the test rig over a pulley up to the top of the test rig over a second pulley and down to the dosing feeder. This way, the dosing feeder moves exactly the same distance as the bottom of the reactor does. This is very important since the auger would clamp otherwise. A thermocouple ensures that any increase in temperature is detected in case there is a back-burning.

1 Cooling water inlet
2 Cooling water outlet
3 High temperature seal
4 Low temperature seal to feeder
5 Reactor flange
6 Cooling helix.
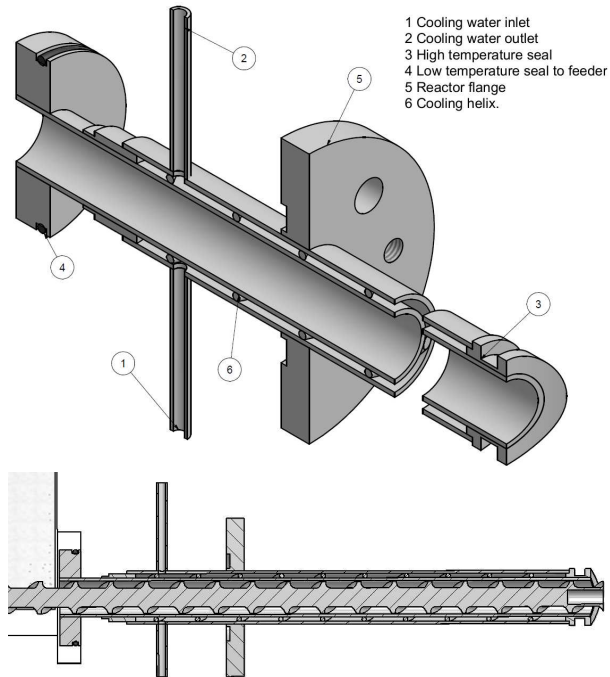
Figure 4.7: *Double jacket for the cooling of the feeding screw.*

4.5.1.3 Reactor

The reactor – which is also depicted in figure 4.2 – is made of Inconell® 600, which is a high temperature alloy. It contains around 72 % nickel and minor amounts of chromium and iron. The inner diameter of the reactor is 52 mm. The maximum diameter at the outlet of the cone is 220 mm. The gasification agent enters through the bottom of the reactor after it is preheated. It then passes through a frit made of sintered Hastallloy® having a mean pores size of 40 μm.

4.5.1.4 Cyclone

A cyclone was used to remove particulate matter of the gas before the gas is burned in the flare. According to Perry [242], the calculated cut off diameter is 102 μm, the number of rotations within the cyclone is
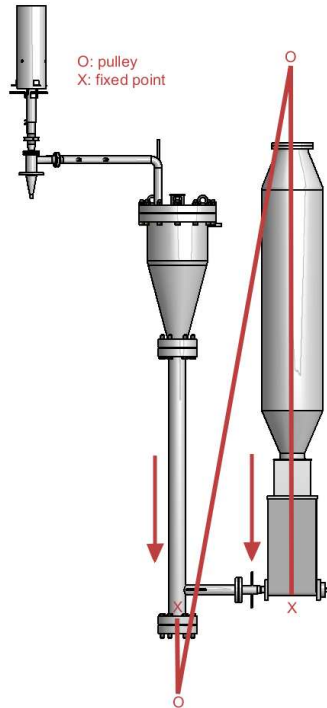
Figure 4.8: *Mounting of the feeder system.*

Property	Dimension	Value
Material number	–	2.4816
Density	kg/m^3	8430
Thermal expansion	$\mu m/(mK)$	14.6 (21 - 427 °C)
Specific heat	$kJ/(kg\,K)$	0.444
Melting point	°C	1354 - 1413

Table 4.5: *Physical properties of Inconell® 600 [241]*

2.4. The cyclone container shows an exit tube, from which the fines can be removed by a screw. It is also heated to prevent the tars from condensing within the cyclone, which would eventually block the system.

4.5.1.5 Flare

A simple flare was used to combust the product gas before leaving through the duct. It is possible to adjust primary and secondary air separately. A methane pilot burner secures that the flare re-lights whenever blown off by a pressure wave. This happens when coke and tars are deposited at the wall of the downstream pipes and are suddenly blown away when the velocity in the pipe has increased sufficiently. The pilot burner proved to be very reliable during the tests.

4.5.2 Sampling

The gas was sampled by using the pressurised sampling system presented in section 3.2. The gas stream is divided into two streams: the clean permanent gas stream and a solvent stream, containing the tars, water and particles which pass the filter. The gas stream was measured with a Varian micro GC (gas chromatograph)[2] and the wet stream using a SPECTRO ICP-OES[3].

Directly after the gas exit several sampling ports are positioned (figure 4.9) ③ and ⑤. One of them is an isokinetic sampling port ③. The figure shows the lid of the reactor ①. The gas exits in the tubing ② passes the knee and runs straight into the cyclone ④. In order to achieve isokinetic sampling, the sampling flow must be adopted to the output flow of the reactor. The velocities at the cross section where the sampling line opens must be constant. Isokinetic sampling becomes an important topic when sampling gas which contains particles. Hyperkinetik sampling e. g. would result in a higher particle loading in the sampling line than in the main line. The variation of the flow velocity may be 5 % less or 15 % more than the isokinetik velocity [243]. From latter standard it can be derived, that isokinetic sampling is best positioned in a vertical duct. Using one central sampling tube is enough for ducts with sizes up to 350 mm in diameter.

The sampling gas runs through a heated porous metal filter (5 μm) before entering the sampling system. If isokinetic sampling is established, the material in the filter can be considered to be equivalent to the one in the main gas stream.

---

[2] www.varianinc.com

[3] www.spectro.com
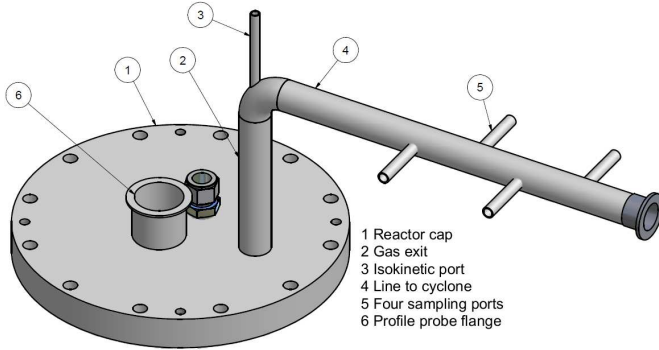
Figure 4.9: *Sampling ports at the gas exit of the plant*

A second sampling port was installed to record the axial concentration profiles along the reactor height. The probe was a lance of about $1.7\,m$ length and $8\,mm$ in diameter. It is inserted from the top of the reactor through a centred inlet ⑥ figure 4.9. By using a gland the probe becomes movable in axial direction. Since only the small particles and permanent gases were recorded, a porous metal filter was installed directly at the tip of the tubing. An additional thermocouple was inserted at the tip to monitor the temperature alongside the gas profile.

4.5.3 Controlling system

The system is controlled by a PC based system consisting of a PC and a SPS[4] controlling box. The PC is equipped with National Instruments (NI) LabView. The controlling box contains inlets for pressure, temperature and logic signals and outlets for mass flow controllers (MFCs), heaters and switches. The overall scheme of the controlling structure can be seen in the flow chart figure 4.10.

4.5.4 Safety concept

The safety is ensured by limiting certain sensor values and setting an alarm if those limits are exceeded. In case one or more of the limits are exceeded the gasification agent stops flowing, the feed auger stops

---

[4]Speicher Programmierbare Steuerung

running and the nitrogen flow starts streaming somewhat higher than the minimum fluidisation velocity. This ensures that the bed material and the ash will not agglomerate in the case of cooling. If there is an electrical blackout the same will happen because, the nitrogen valve is normally open and the gasification agent MFC is normally closed.

If the pressure in the reactor is to high safety valves [244] will go off and release product gas from the reactor into the exhaust pipe. If the pressure in front of the reactor is too high, the plant will shut down automatically.
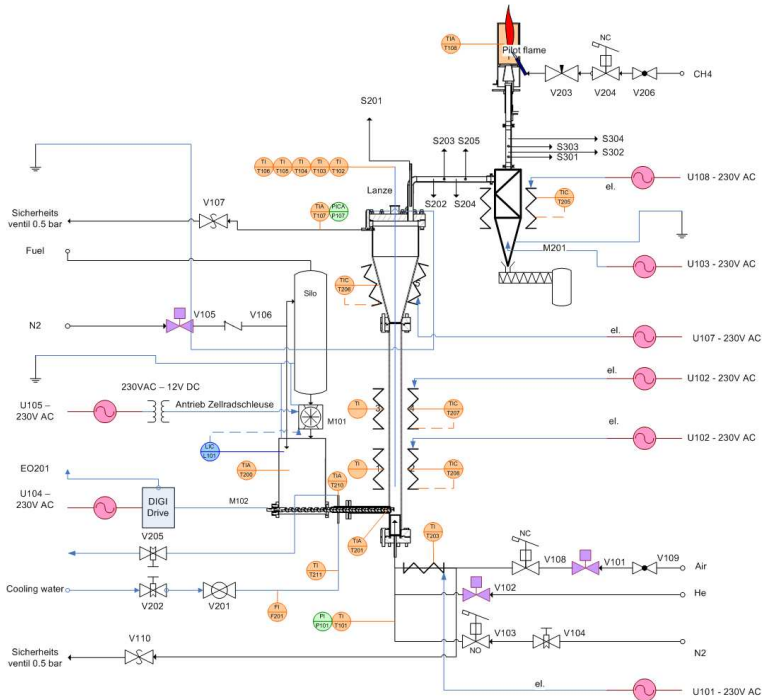
Figure 4.10: *Flow chart of the bubbling fluidised bed*

4.5.5 Instrumentation and measurement methods

Several measurement techniques were applied. Most of them are online and continuously. Some had to be offline since the samples could not be

taken out of the process during the run time. These are bed material, ash and filter ash.

4.5.5.1 Fluidisation and Inertisation

Three gas mass flow controllers (MFC) from Bronkhorst are used: the first one controlling the airflow (gasification agent), the second one controlling the nitrogen purge and the third one controlling the He spike flow. The last one is used as standard addition in order to obtained the total gas flow at the exit (see equation (4.13)). Calibrations were done by means of a Ritter gas meter, which as an accuracy of 0.2 %rel.

4.5.5.2 Temperature

The temperature sensors are type K thermocouples which are standard for these kind of operations. The accuracy can be expected to be around 0.5 %rel. But care must be taken when the sensor exceeds 600 °C. The material recrystallises and may well show an additional shift of 5 °C at 400 °C when standard calibration curve is applied [245]. All together an uncertainty of around 10 °C must be accepted when working with type K thermocouples above 600 °C. More accurate but as well more expensive options are Type N thermocouples or resistance thermometer (PT) up to 850 °C.

Measurement response by radiation could be observed during the heating up of the reactor, but were not evident during the operation of the gasifier due to the good mixing behaviour of the fluid bed.

4.5.5.3 Pressure

The pressure is measured by means of relative pressure sensors with a range of 0-2.5 bar. The pressure is recorded as difference compared to the ambience. The accuracy for this sensor is 1 %rel [246].

4.5.5.4 Cooling water

The cooling water flow is measured by a Gems water turbine [247] operating inline. The signal is an impulse for each round which is transformed into an analog 0-20 mA signal. The accuracy of 3 % within the

normal range plus the uncertainty of 0.5 % concerning the repeatability. The standard flow was around 2.5 l/min.

4.5.5.5 Gas analysis

For the measurements of the permanent gases a Varian micro GC was used [248]. It is equipped with two lines each with two columns (Mol-seive 5 Å and PoraPLOT U) and a TCD[5] sensor. The measurements are done redundant on both lines. The columns are calibrated with mixtures showing an uncertainty of 2 %rel and a standard deviation of 0.2 % at a single point. Besides the main components (N_2, CO_2, CO, H_2, CH_4) the colums can detect O_2 mainly to detect leakages in the sampling line, C_2H_X since the contribution to the heating value can be substantial, C_3H_6 which can be present in minor amounts, the sulphur components H_2S and COS and finally He for the He-spike method. The concentrations are not normalised to 100 %. This is simply due to the fact, that each components has its own calibration with its own un-certainties and errors. By normalising, all concentrations are changed, wheras maybe only one concentration is wrong or else there may be a component which can not be detected.

To check the ammonia concentration a Draeger tubes were used in one experiment.

4.5.5.6 Tar and water analysis of the gas

The tar is determined gravimetrically for selected experiments by wei-ghing the residue after vaporising the solvent. Since this leads to the loss of the lighter tars, GC/MS measurements of tars are done for se-lected samples in one experiment.

For the water content and tar analysis several samples were taken du-ring the experiments and analysed using Karl-Fischer titration.

4.5.5.7 Product gas flow

The product gas flow could be quantified by using the He-spike me-thod. The helium is introduced into the lining of the gasification agent before it enters the reactor at a constant flow $\dot{V}_{He}$. By measuring the

---

[5] TCD: Thermal Conductivity Detector

concentration of helium x_{He} in the gas phase the gas flow $\dot{V}_{gas}$ can be calculated with the following formula.

$$\dot{V}_{gas} = \frac{\dot{V}_{He}}{x_{He}} - \dot{V}_{He} \qquad (4.13)$$

This method was successfully applied in an additional project during this thesis, in which the slip stream of methane from a PSA separation plant was evaluated see appendix γ .

4.5.5.8 Analysis of inorganic components in the gas

The ICP-OES measurements were conducted in a collaboration with the work group of Christian Ludwig at PSI. The device is a SPECTRO ICP-OES located in a truck and thus being able to be placed very close to the test rig. The ICP-OES is operated with a argon plasma torch into which the sample is injected continuously by an ultra sonic vaporiser. The device detects the elemental composition of the sample with a CCD detector simultaneously.

4.5.5.9 Analysis of solids

The fuel was analysed externally for elemental composition. The water content was determined by gravimetric drying and the ash content by incineration following [249].

The remaining bed and hot gas filter fines are taken once after each experiment and weighed to determine the particle load of the gas. The fines of the filter are then incinerated and analysed with ICP-OES for the selected inorganic constituents.

An additional portion is analysed for total organic carbon (toc) to get the amount of unreacted carbon.

4.5.6 Heat losses of the reactor

Bench-scale reactors for thermal processes are very sensitive to heat losses, because of their large surface to volume ratio. There can be several sources, e. g. convection, conduction, radiation or mass bound energy losses. In figure 4.11 the major sources for heat losses are illustrated. The following calculations are made for a typical experiment, where the process temperature was 750 °C.
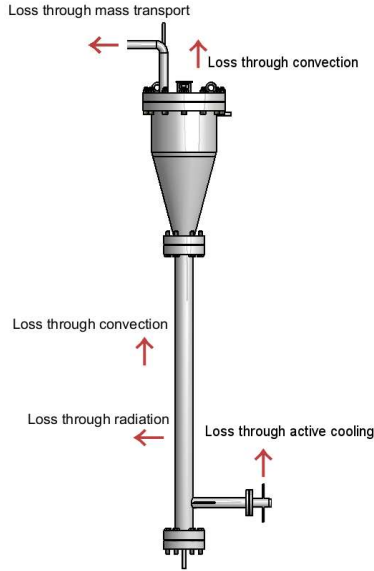
Figure 4.11: *Major heat losses of the bench-scale fluidised bed*

The cooling water is typically 2.5 *l/min* with an increase of the water temperature from 29 to 30 °C . With a given specific heat of 4.177 *kJ/(kg K)* [250] the removed heat is

$$\dot{Q}_{cooling} = \dot{M}_{cooling} c_p \Delta T = 173 \ W \qquad (4.14)$$

where

$\dot{Q}_{cooling}$	is the energy flow transported by the cooling
$\dot{M}_{cooling}$	is the mass flow of the water
c_p	is the specific heat of water
ΔT	is the temperature difference between inlet and outlet

The reactor shield was measured to be 80 °C. This temperature leads to convective losses and losses through radiation. The radiation can be expected to be very low at this temperature [250].

$$\dot{Q}_{radiation} = A_1 F_1 2\epsilon\sigma(T_2^4 - T_1^4) = 0.42 \ W \qquad (4.15)$$

where

$\dot{Q}_{radiation}$	is the energy flow transported by radiation
A_1	is the surface of the shield

$F_1 = 1$ is the fraction of the surface visible to the environment

ϵ is the emission factor (0.118 for stainless steel [250])

σ is the Stefan-Boltzmann constant

$T_1 =$ 25 °C

The convection can only be estimated because there are many distur-
bing items around the reactor, which hinder a proper free convection.
This will be neglected here. The responsible equations were taken from
Bejan and Kraus [251]. The Nusselt correlation of Le Fèvre for vertical
cylinders yields a value of:

$$\dot{Q}_{convection} = \frac{4}{3}\left[\frac{7GrPr^2}{5(20+21Pr)}\right]^{0.25} + \frac{4(272+315Pr)L}{35(64+63Pr)D} = 266\ W \quad (4.16)$$

Where

$\dot{Q}_{convection}$ is the energy flow transported by free convection

Gr   is the Grashof number

Pr   is the Prandtl number

L   is the length of the body

D   is the diameter of the body

Additionally there is also a heat loss from the top of the freeboard.
With appropriate equations for natural convection [251] this will be
around 11 W (equation (4.17)).

$$Nu = \frac{5}{3}0.394Gr^{0.2}Pr^{0.25} = 11\ W \quad\quad\quad (4.17)$$

It has to be noted that the natural convection up the shield will affect
the natural convection from the top lid. Since there is no need here to
be more accurate than the given numbers this effect shall be neglected
here.

Altogether, there is a heat loss of around 451 W, which is very large
compared to the size of the reactor (2-5 kW). For this reason the reac-
tor must be stabilised by electric heaters during the experiments. For
larger reactors this problem diminishes due to its much better surface
to volume ratio and thus power to heat loss ratio.

Finally there is a substantial heat leaving the reactor bound to the gas
flow. The product gas possesses a temperature close to the reactor
temperature. If we consider cooling the gas down from 750 °C to 20 °C
(using average data of $c_p = 1.4\ kJ/(kg\ K)$, $\rho_{gas} = 0.7\ kg/m^3$), the sensible
heat coming with the stream is around 0.7 kJ/l) of gas. For the pre-
sented experiments this is roughly 190 W. For the corresponding input
power of around 2.9 kW this is 6.6 % of the energy. It shows another

major advantage of integrating the gasifier into a combined cycle. This sensible heat can be recuperated for the bottoming cycle.

4.5.7 General experience

The fluidised bed   installation ran very well during all experiments. The de-bridging device in the silo showed an excellent performance. No bridging occurred during close to $100\,h$ of accumulated operation.

The feed auger   proved very reliable. No clogging or blocking occurred. After each test the auger was removed; there were hardly any significant depositions visible. Only a thin black layer at the tip of the auger was evident figure 4.12.
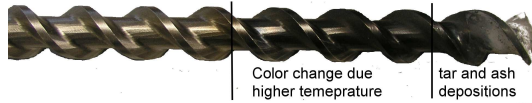
Figure 4.12: *Auger after the experiments*

The fluidisation   could be accomplished throughout all experiments without inducing any defluidisation or slagging of the ash.

The He-spiking   of the gasification air to determine the gas flow, was successfully conducted throughout all experiments.

During all tests   it could be observed, that the char is separated from the bed and floats on top of it. This could be detected by promptly terminating the fluidisation and remove layer by layer of the bed starting from the top.

The tar content   of the gas was not measured for each experiment. But its was low enough that no depositions in the downstream lining could be observed in any of the tests at all.

Commissioning of the gasifier   The gasifier was first tested with crushed wood pellets. The bed material used was silica sand. One of

the experiments is presented in appendix α .1. The result was stable gasification during $5\,h$ of operation. The gas composition was good, the lower heating value was 6.8 MJ/kg for an air to fuel ratio of 0.22.   1

4.6 Experimental procedures

Graph 4.16 displays three different fluidisation characteristics at three different temperatures for the same bed material. It shows the pressure drop over the bed versus the velocity of the fluidisation agent (air). The first increase of the pressure drop is due to the rising velocity through the immobile bed of particles. The minimum fluidisation velocity is reached when the particles break loose and start to float. Then the pressure drop rises much slower with increasing velocity. At the same time the bed expands much alike a rotameter.

If the fluidisation is accomplished from low to high velocities there will be a hysteresis at the relaxation point u_{mf}. The initial fluidisation velocity seems higher than expected. This effect is based on the fact, that the initial force to unclench the particles of the fixed bed is higher than the effective force needed to start the fluidisation. The relaxation point is not visible if the measurement is conducted from higher to lower velocities.

All experiments were conducted using the same procedure:

- ✧ Cleaning of the reactor
- ✧ Filling in $500\,g$ of the selected bed material
- ✧ Filling in an appropriate amount of fuel in the silo for a 5h run
- ✧ Heating up the reactor to the process settings with electrical heaters
- ✧ Starting the fluidisation
- ✧ Starting the fuel feed

When the reactor reached its temperature set point, the fuel auto ignited rapidly. The first flame in the flare could be observed already $1\,min$ after starting the fuel auger. The experiment was terminated after around $5\,h$ by stopping the fuel feeder. The gasification agent (air) was stopped and a nitrogen purge flow was started in order to cool down the remaining bed more efficiently and keep the remaining materials from reacting.

4.7 Experimental matrix

Table 4.6 lists the parameters varied in the experiments. The axial profile measurement was conducted for λ=0.3 at 750 °C with alumina. The characters denote the experiments conducted and will be used as reference in the discussion below.

λ	Dolimite	700 °C SiO$_2$	Al$_2$O$_3$	750 °C Al$_2$O$_3$
0.17	a	b		
0.20		c	d	g
0.25			e	h
0.30			f	i[6]
0.35				j

Table 4.6: *Experimental matrix for the gasification experiments, (6) axial profile measurement for this point*

Additional experiments were carried out to test the fluidisation characteristic of the bed material (section 4.9.1) and the ash melting behaviour of the grass together with the chosen bed materials (section 4.8.2)

4.8 Fuel characterisation

The fuel was characterised by several methods:

- ✧ Water content: Mettler/Toledo infra red dryer once for each experiment [252]
- ✧ Major elemental analysis: once for each type of fuel (ETHZ)
- ✧ Minor elemental analysis: once for grass (external laboratory)
- ✧ Ash content: once applying DIN 1978 No 51719 [249]

Table 4.7 gives the average dry major elemental composition of the grass used in the experiments. The second line illustrates values derived from the fuel analysis in section 2. The data is quite comparable to the average expected composition.

In table 4.8 the average measured composition of some important minor elements is given. These values too are very comparative to the expected average composition. The data was not acquired for wood. Lead

	C	H	O	N	S	Ash
grass avg. %w dry	43.11	5.66	41.05	1.30	0.12	8.76
grass avg. eDaB %w dry	44.88	5.51	40.00	1.64	0.19	7.78
wood avg. %w dry	47.31	6.23	44.44	0.18	0.01	*1.83
wood avg. eDaB %w dry	49.24	6.14	42.26	0.41	0.07	1.83

Table 4.7: *Major elemental analysis (*assumed from eDaB)*

could not be verified in the grass (the detection limit of the method was 4.6 *mg/kg*).

	P	Cl	Ca	K	Mg	Na	Si
g/kg dry	2.15	4.45	7.0	17.3	1.58	0.11	13.9
eDaB *g/kg* dry	2.17	6.62	6.6	18.8	2.04	0.51	9.4
	Ba	Sr	Li	V	Pb	Mo	
mg/kg dry	16	17	↘	2	↘	4.8	
eDaB *mg/kg* dry	29	21	–	7	3	4.5	

Table 4.8: *Minor elemental analysis for grass (↘: below detection limit)*

The energy content was not measured but calculated from the elemental data as proposed by Channiwala and Parikh [107] (equation (4.19)). The elemental data is inserted as %w. The HHV can be expected to be accurate within an uncertainty of 3 %rel. The lower heating value was calculated using the correlation proposed by Oasmaa et al. [100] (equation (4.19)).

$$HHV \quad = \quad 349.1\ C + 1178.3\ H - 103.4\ O + \cdots \qquad (4.18)$$
$$100.5\ S - 15.1\ N - 21.1\ Ash$$
$$LHV \quad = \quad HHV - 0.21813\ H \qquad (4.19)$$

Where

The heating values are given in *MJ/kg*
The elemental data is given in %w

HHV, *MJ/kg*	17.28
LHV, *MJ/kg*	16.05

Table 4.9: *Caclulated energy content of grass*

The water content of the fuel varied for each experiment. The grass showed a significant hygroscopic behaviour, which can be derived from

figure 4.13. The diagram shows the water content of grass dependent on the date, when the sample was taken. The grass pellets took up around 3 % of moisture in first half of the year being within the bag. This is an important hint for the storage facilities of a larger plant, where the fuel must be kept up to a year. The grass bags stayed closed until used. The grass was chaffed and stored in a sealed bin until the experiment was conducted.
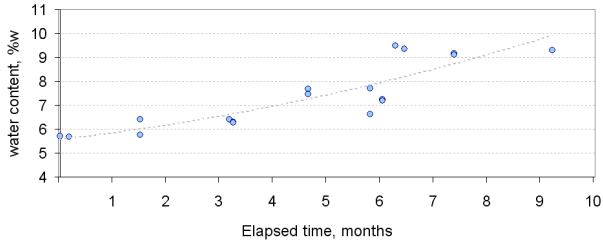
Figure 4.13: *Change of water content of grass samples during time*

4.8.1 Fuel preparation

The grass and wood pellets were delivered by Mühle Scherz AG, CH as 16 mm respectively 6 mm pellets. Since the size of the plant limits the size of the auger the pellets had to be crushed in advance. This was done by a cutting mill SM2000 [253]. The matrix was 10 mm square through which the fuel was shredded. The resulting particles showed every size from fines to 4 mm. The density of the original pellets were determined to be 1.3 kg/l for grass and 1.2 kg/l for wood.

Figure 4.14: *Fuel pellets as received, left picture: grass 16 mm/ right picture: wood 6 mm*

The fuel was then put into the silo which stayed closed until the experiments started. Wood was only used as reference fuel to test the fluidised bed. No profound analysis of the gas phase was conducted for the wood experiments.

4.8.2 Ash melting: preliminary microscopic observations

To test the ash melting behaviour of grass in combination with different bed materials, samples of grass were mixed with each bed material. The mixture was softly freed from volatiles at 400 °C during one hour. Then the mixture was heated up to the final temperature of 700, 750 or 800 °C for another hour. The result was analysed under the microscope for appearance and mechanical strength.

For all bed materials the resulting ash was weak at 700 °C and showed a rising brittleness with increasing temperature. Figure 4.15 shows an example of photographs taken from the microscope of the ashes. The reference sample consisted of ash of pure grass. It showed a significant brittleness from around 800 °C. Additionally small molten beads could be recognized, which is first signal that agglomeration can occur. This behaviour was comparable with the addition of silica. For the alumina bed the ash was significantly weaker and the molten beads much less obvious, though a few could still be observed. These tests showed that the gasification of native grass without additives to bind the alkalis becomes critical above 750 °C.
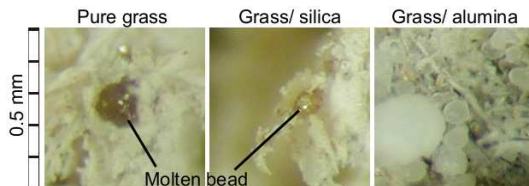
Figure 4.15: *Ash melting observations by means of a microscope at 800°C.*

4.9 Results and discussion

4.9.1 Fluidisation

The fluidisation of the bed and the fuel was done by the gasification air directly. The fluidisation diagram (figure 4.16) was taken at three different temperatures within the reactor. The data points near zero are distorted because the MFC[7] used for the fluidisation was very inaccurate in this area.
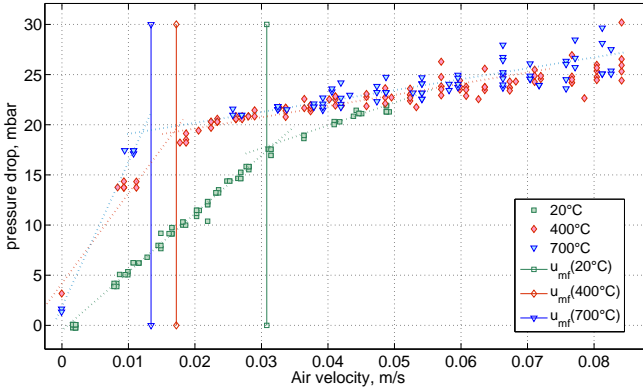
Figure 4.16: *Fluidisation diagram of Al_2O_3 with a mean size of 270 µm*

The minimum fluidisation velocity can be calculated with the Ergun formula (4.20) ([254]).

$$\frac{\Delta p}{H} = 150\frac{(1-\epsilon_{mf})^2}{\epsilon_{mf}^3}\frac{\eta_g u_{mf}}{(\Phi d_p)^2} + 1.75\frac{(1-\epsilon_{mf})}{\epsilon_{mf}^3}\frac{\rho_g u_{mf}^2}{\Phi d_p} \qquad (4.20)$$

where

$\frac{\Delta p}{H}$	is the pressure drop over the height of the bed
a_p	is the specific surface area
ϵ	is the void fraction at the fluidisation point
η_g	is the gas phase viscosity
u_{mf}	is the minimum fluidisation velocity
ρ_g	is the density of the gas phase

[7] Mass Flow Controller

The pressure drop on the other hand can be replaced by a balance of forces around a particle which gives the pressure drop that can just lift the particle (equation (4.21)). The force of the particle trying to fall and the force of the flow trying to lift the particle are balanced.

$$\frac{\Delta p}{H} = (1 - \epsilon_{mf})(\rho_s - \rho_g)g \qquad (4.21)$$

For real systems the specific surface area and the void fraction are very difficult to determine. For this reason the equation was reformulated in order to reduce the unknown to possibly constant numbers. The result is given in formula (4.22). Re_{mf} is the Reynolds number at the fluidisation point and Ar is the Archimedes number given in formula (4.23). C_1 and C_2 are constants which can be taken from literature e. g. Yang [239] and Basu [127]. The calculated fluidisation velocities (from equation (4.24)) are plotted in the diagram as solid vertical lines. They match the experimental values very nicely. The constants used for the calculations are $C_1 = 33.7$ and $C_2 = 0.04$. The standard deviation is reported to be above 30 % [255].

$$Re_{mf} \quad = \quad \frac{u_{mf}d_p\rho_g}{\eta} = \sqrt{C_1^2 + C_2 Ar} - C_1 \qquad (4.22)$$

$$Ar \quad = \quad \frac{\rho_g(\rho_p - \rho_g)g d_p^3}{\eta^2} \qquad (4.23)$$

$$u_{mf} = \frac{\eta}{d_p\rho_g}\left(\sqrt{C_1^2 + C_2\ Ar} - C_1\right) \qquad (4.24)$$

u_{mf} decreases with rising temperature as shown in figure 4.16. The controlling mechanisms are the temperature dependency of the density and the viscosity. For small particles as it is the case for these experiments the first part of equation (4.20) becomes relevant above the second part. From this part it can be seen, that the fluidisation velocity is inversely proportional to the viscosity. Between 100 and 700 °C the viscosity approx. doubles and hence the fluidisation velocity drops. The diagram also shows very nicely that the dependency on the temperature gets weaker with increasing temperature.

The bed expansion above the fluidisation point is dependent on the velocity and the minimum fluidisation velocity of the system [127][recited].

$$\frac{H - H_{mf}}{H_{mf}} = \frac{u - u_{mf}}{u_{mf}} \qquad (4.25)$$

If the velocity is chosen to high, the bed will entrain. For this reason a freeboard with an extended diameter is used to decrease the superficial velocity before the gas exit. The volatilisation of the fuel during the gasification leads to an increase of the volume flow. The bed expansion must therefore be expected to be non linear.

4.9.2 General stability of the process

4

4.9.2.1 Dolomite bed

Dolomite ($CaMg[CO_3]_2$) has a Moh's hardness between 3.5–4. Compared to other bed materials like sand (hardness 7) or alumina (hardness 9), dolomite appears rather week. In fluidised bed gasification the turbulences in the reactor especially at higher temperatures are very strong. The experiment with dolomite resulted in a continuous removal of bed material out of the reactor by entrainment. Usually the pressure drop during the run time increases slightly because the ash accumulates in the fluidised bed as it can be seen from figure 4.20. Figure 4.17 shows the pressure drop over the bed during the run time of the experiment. It decreases substantially, which can only happen if the flow decreases, the temperature decreases, the particles get smaller or less particles are in the reactor. Since the temperature effectively increased and the flow was hold constant only smaller or less particles can be responsible. It was stated in literature that under certain conditions dolomite becomes friable [256]. For this reason dolomite was excluded from further tests. It though might still be interesting as additive to bind alkalis.

4.9.2.2 Silica and alumina bed tests

The main experiments were carried out with silica and alumina bed material. Simultaneous runs of the complete diagnostic was done for selected tests only. For the main fraction of the experiments besides temperature and pressure only micro GC measurements were taken. The loaded solvent was fractionated and analysed afterwards.

From the gasification of agricultural residues, alkali metals especially potassium and sodium have been known a long time to form sticky melts together with SiO_2 bed material [257–259]. If these melts form eutectic mixtures, which have the characteristic to solidify at low temperatures, the bed material and fly ash is glued together and the flui-
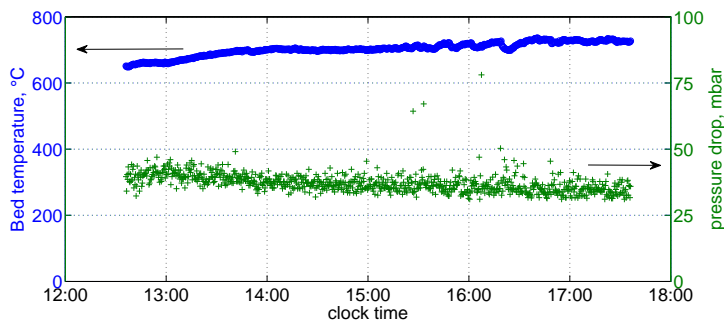
Figure 4.17: *Pressure and temperature for the dolomite experiment.*

disation is terminated. For this reason SiO_2 is used as bed material only up to $700\,°C$. For tests at $750\,°C$, Al_2O_3 was used. The ash can still agglomerate since grass itself contains significant amounts of silica and alkalis. But alkali alumino silicates, which can be formed on the bed material are known to possess very high melting points [260; 258], which lessens the problem. As long as the amount of bed material is much more compared to the ash in the reactor agglomeration should be of minor concern at temperatures up to $800\,°C$.

Figure 4.18 shows an typical example of gas phase, temperature and pressure readings. The graphs show a section of a run at $750\,°C$ with alumina bed material. The first graph shows the permanent gas data. The permanent gas data stops due to the blocking of the sampling system, which was explained in detail in section 4.5.7.

Figure 4.19 shows an equivalent example of a run with silica at $700\,°C$. The sampling system was maintained during the time, which shows the shaded overlay. The gas phase concentrations after the maintenance was entirely the same. Only C_2H_2 shows a decreasing trend, which is stopped after three hours. The important conclusion is that the process is stable during the $5\,h$ run for both bed materials. The main experiments and analysis were conducted for the alumina bed, since it proved to be the better option.
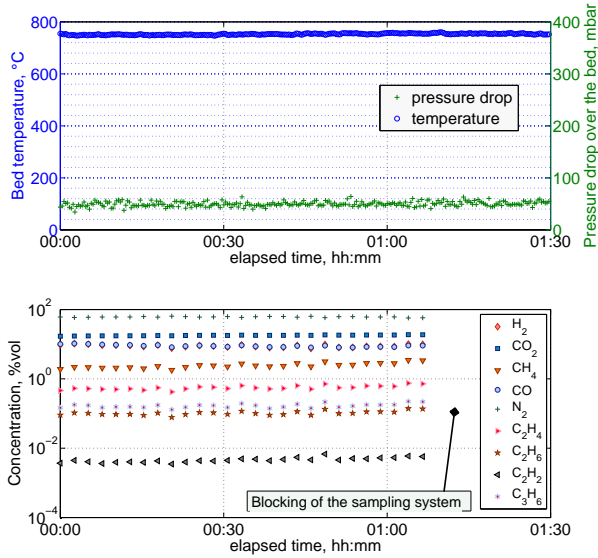
Figure 4.18: *Example of a gasification run for grass in a Al_2O_3 bed at $750\,^{\circ}C$.*
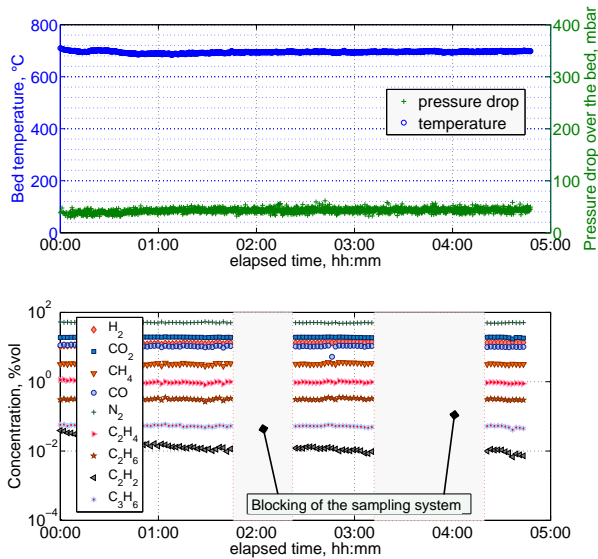
Figure 4.19: *Example of a gasification run for grass in a SiO_2 bed at $700\,^{\circ}C$.*

4.9.2.3 Extended test (10 h)

Additionally to the standard tests a long run lasting 10 h of gasification was conducted. The temperature and pressure signal is depicted in figure 4.20. The temperature drops slightly during this run. This is due to the electrical heaters, which were subsequently reduced as the reactor wall temperature increased. There was no evidence, that the process became unstable during this run. It thus can be derived, that a continuous operation at the given settings is feasible without risking ash melting problems.
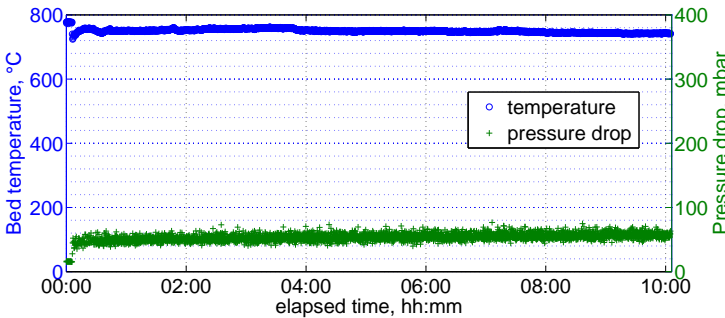
Figure 4.20: *Temperature and pressure during the 10h experiment with grass, alumina bed, 750°C.*

The gas composition was checked only at the end of the run and is listed in table 4.10.

H_2	N_2	CH_4	CO	CO_2	C_2H_4	C_2H_6	C_3H_6
10.01	56.89	3.47	8.46	18.58	0.78	0.16	0.23

Table 4.10: *Permanent gas concentration at the end of the 10h run*

4.9.3 Axial profile measurements

There was an attempt to analyse the alkali release along the height of the reactor during the gasification. Based on the experiments with the single pellet gasifier (see section 5), there is a strong evidence, that the major alkali release is subject to the char gasification, which takes place

at the top of the fluidised bed. The probe was a lance inserted from the top of the gasifier being mobile in axial direction. Any vertical position could be accessed and the gas composition measured. There was a 5 μm filter at the tip of the probe in order not to remove any bed material and keep the fines out. The attempt failed, due to problems with the filter of the probe. During the measurement the filter got more and more plugged and the sampling gas stream decreased steadily. Though it was possible to obtain enough gas to feed the micro GC, it was not enough to obtain a proper sample to analyse the in the ICP-OES for contaminants.

The permanent gas data is presented in figure 4.22 (dashed lines). Using such a probe in a fluidised bed results in data that is most likely to be assigned to the dense phase [261]. This is the reason why the concentration above the bed (above 0.9 m) abruptly changes. The difference of compositions between the bubble and dense phase has also been a result from a mathematical approach by Bilodeau et al. [262]. The last data set at the exit of the gasifier and the one at the entrance were not measured with the probe and can be considered as real gas phase concentrations. At the entrance the volatiles react with the oxygen mainly in the first 30 cm (heater section). Then most of the oxygen is consumed. From there the change of the gas phase concentration in the bed is a complex combination of gas diffusion between the bubble phase and the dense phase, char gasification and homogeneous gas phase reactions.

In the first 60 cm a decreasing CO_2 flow combined with an increasing CO and H_2 flow is observed. This component change can be explained by the Boudouard- and water-gas-reaction, which produce CO and H_2 through the reaction of CO_2 and H_2O with solid carbon. Both reactions are endothermal.

The concentration change in the upper part of segment II is possibly due to the temperature decrease but also to diffusion between the bubble and dense phase.

From the remaining bed after the experiments, it could be concluded that the char is to a great extend floating on top of the bed. The main endothermic char gasification thus takes place in the unheated section.

The local mechanisms in a fluidised bed gasification including diffusion as well as homogeneous and heterogeneous reactions are not understood today. One point surely is that such profiles for gasification reactors
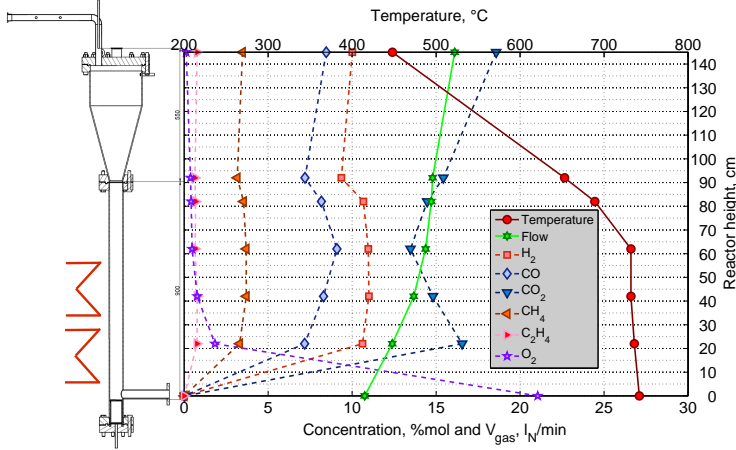
Figure 4.21: *Permanent gas concentration and temperature profiles in the fluidised bed*

are very rare in the literature for the reason that they are very difficult to accomplish. But exactly such measurements are the keys to a better understanding.

Through the He spike method, an estimation of the local product gas flow can be made. It is plotted in figure 4.22 as stars. Helium diffuses very fast and the difference between the bubble and the dense phase can be assumed small. This is confirmed by the profile. It indicates that the difference of the concentrations between the two phases is small. The major increase of the flow takes place in the first part of the bed. This corresponds to the volatile part of the fuel. The remaining increase is likely due to the char gasification.

The last plot in figure 4.22 is the temperature profile. It shows that the temperature in the bed is very constant. It decreases in the upper bed and the freeboard because the reactor is not sufficiently insulated and there is no stabilising heater in this part. In addition the endothermic char reactions in segment II are partly responsible for this cooling.
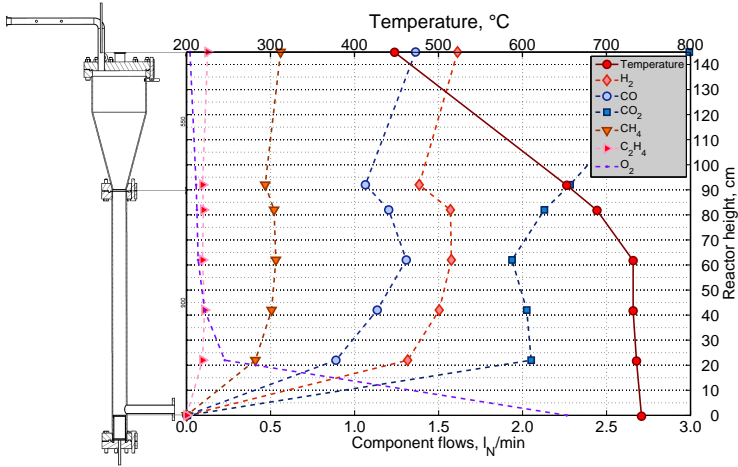
Figure 4.22: *Permanent gas flow and temperature profiles in the fluidised bed*

4.9.4 Monitoring the permanent gas data

It is hardly possible to change an isolated parameter without changing at least some more by doing so. For a constant fluidisation both air and fuel feed must be changed to get a variation of λ. Though the final space velocity will stay constant, the smaller portion of fuel will lead to a different bed expansion behaviour and thus different mixing of the bed. The comparison of datasets from different fluidised bed experiments should be compared with care.

Graph 4.23 shows the change of the concentration of the main species. The concentration of CO, H_2 and CH_4 increases, whereas the concentration of CO_2 stays nearly constant with decreasing air to fuel ratio. This is an expected behaviour since the decrease of O_2 leads to less combustion products (CO_2, H_2O) and shifts the equilibrium to CO and H_2. This also leads to a higher char fraction since both O_2 and H_2O are less present. One experiment (encircled) shows unusual high amounts of hydrogen and CO at $\lambda = 0.26$. This indicates an increased water gas reaction (equation (4.3)). The concentration is stable for the run of the experiment and no inconsistency could be found in the micro GC dataset. The obvious difference of the fuel is 1.5 % less

moisture, which can not account for this significant difference. It is neither explained by the uncertainty of the measurements. There is an unvalidated uncertainty concerning the gasification air. It was taken out of the technical pressure grid and the moisture may fluctuate due to outside moisture or technical failures of the condenser. Air at $8\,bar$ can contain as much as $0.5\,\%$mol of water. This corresponds to about $60\,mg/kg_{fuel}$. This amount can hardly account for the difference. There is not enough data available so far to give a propper explanation for this behaviour. In contrast these values are barely out of the usual range (see table 4.12).
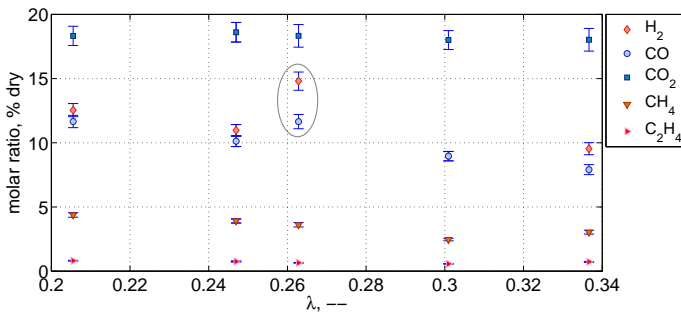
Figure 4.23: *Change of gas composition versus the air to fuel ratio for alumina bed experiments at* $750\,^{\circ}\mathrm{C}$

Graph 4.24 illustrates the same correlation for the tests at $700\,^{\circ}\mathrm{C}$ in the alumina bed. The major differences are an increased hydrogen concentration and a decreased CO concentration. This tendency corresponds to the temperature change and thus is an expected behaviour.

The gas production rate is depicted in figure 4.25. The increasing gas production is primarily a consequence of the nitrogen flow introduced as part of the higher air flow. To some extend the combustion of hydro carbons also lead to an increase of the flow.

4.9.5 The carbon balance

In order to evaluate the measured flows of various kinds, the carbon balance was made for one experiment. Carbon was chosen because it was the element to be measured with a sufficient accuracy ($<5\,\%$) in all
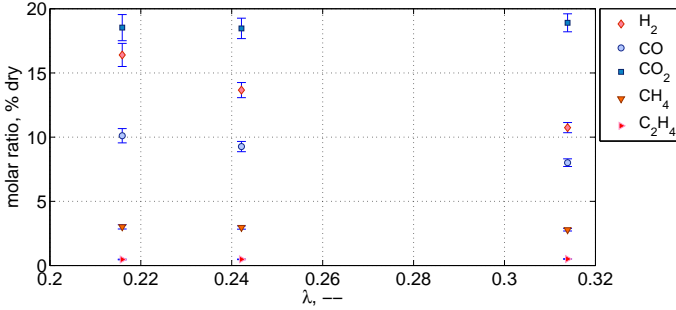
Figure 4.24: *Change of gas composition versus the air to fuel ratio for alumina bed experiments at 700 °C*
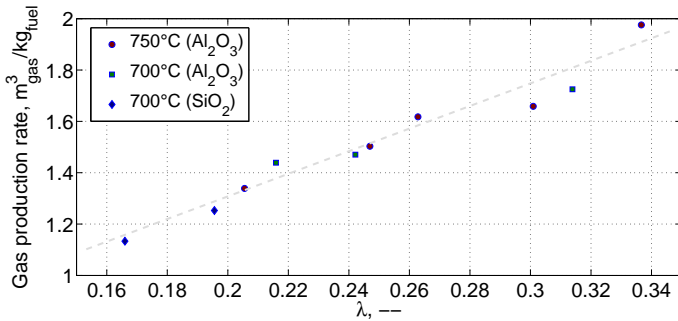
Figure 4.25: *Change of gas production rate versus λ for the alumina and silica bed*

relevant streams. The balance could be closed to 96 % as it is depicted in the Sankey chart 4.26. The result leads to a second conclusion. As it was said before isokinetic sampling was used to get access to the fines of the product gas flow. The carbon content of the fines was usually between 40 and 50 %w. The closure of the balance proves that isokinetic sampling was conducted sucessfully. The amount of carbon which was not found was 4.5 % of the carbon inlet flow. This number is well within the uncertainty of the sampling and measurements.
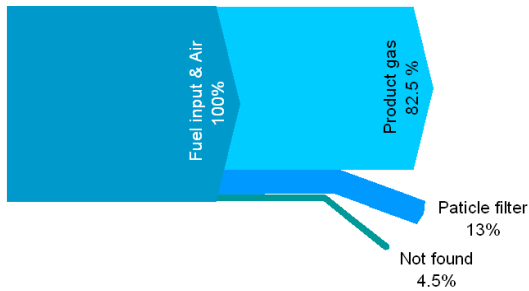
Figure 4.26: *Exemplary Sankey chart for the carbon flows for experiment i*

4.9.6 The heating value

It is very important to measure the concentrations of the higher hydro-carbons because they contribute a substantial part to the heating value and subsequent validation of the gas. Table 4.11 lists the contribution in percent of the combustible gases for a typical gas composition. It is fairly impressive that C_2H_4 holds a portion of almost 10 % and C_3H_6 still a contribution of 4.7 %.

Component	concentration, %vol	contribution, %
H_2	11.0	25.62
CH_4	3.9	30.29
CO	10.1	27.66
C_2H_4	0.8	9.60
C_2H_6	0.2	2.10
C_3H_6	0.2	4.70

Table 4.11: *Contribution of the combustible components to the heating value*

The lower heating values for the different tests with alumina are plotted in figure 4.27. For lower temperatures the values decrease because of a worse carbon conversion. There is a minor fluctuation of the values because the heating value is not only dependent on the air to fuel ratio and temperature but as well on the fluidisation properties. These settings are somewhat different for each of the data sets. The dots, which are framed by a box e.g. are taken for the same fluidisation settings and same fuel moisture. The encircled data point was taken for lower moisture and higher fluidisation. The data point marked by an ellipse was measured for lower moisture but same fluidisation settings

than the first three. The heating values are well within the expected range and are large enough that the gas can be used even in a mono-fuel application.
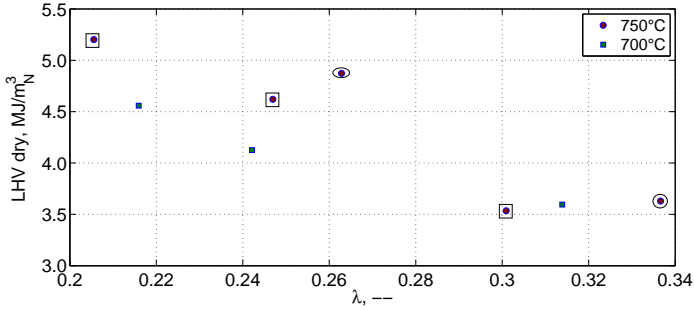
Figure 4.27: *Lower heating value for the dry gas at different temperatures for alumina*

The lower heating value can be increased if steam is added to the gasification air. This way less air is used and more char is converted by the water gas instead of the oxidation reaction. Steam can be extracted from the HTSG in the IGCC process, there is no need to install an extra steam generator. The temperature can be increased if the ash melting problem is controlled for better char conversion.

The LHV of grass is generally lower than for wood. This is mainly due to the higher carbon content in the dry biomass. A smaller portion accounts for the process temperature, which is usually higher for wood, than for grass (see table 4.2).

4.9.7 Tar content and composition

The data plotted in figure 4.28 illustrates the non volatile content of the solvent, which is usually reported as gravimetric tar. The amount was determined by vaporising the solvent and weighing the remaining substance. By this way, it can not be distinguished between non volatile tars and fines that are in the solvent as well. The lighter tars can not be measured by this procedure and must be analysed by a GC/MS. For the single value at $\lambda = 0.31$, which is significantly higher, a higher fluidisation was used. This decreases the residence time of the gas in

the reactor. In addition the fuel showed a smaller moisture content (approx. 1.5 % less). This finding is in agreement with van Paasen and Kiel [209] where a lower fuel moisture resulted in a higher tar content. Steam produced from the moisture can crack tars.

The lower contents for lower air to fuel ratios may be due to the higher char inventory. Those could be observed for the mentioned settings. If the tars combine with the char they will be subject to steam gasification as the char itself and are subsequently decomposed.
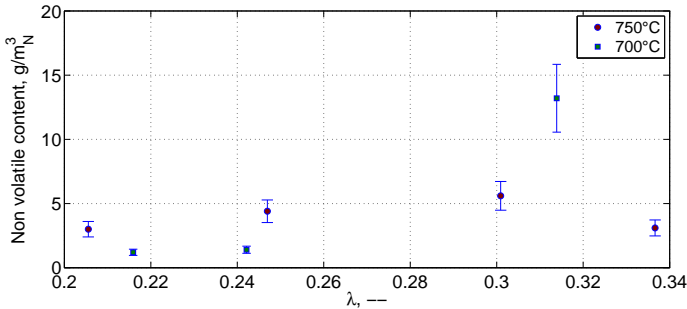
Figure 4.28: *Non volatile content for different temperatures and air to fuel ratios in the alumina bed*

For certain experiments (h-j table 4.6) the tar composition was measured by means of a GC/MS. The tars analysed were chosen from the chromatogram as depicted in the appendix figures α .3ff. The selection of the compounds was based on their significant presence in the chromatogram. The light tars did not change significantly over the air to fuel ratio as can be seen from figure 4.29.

Usually the tar concentrations in fluidised beds at the given temperatures are expected to be higher [209] (10-20 g/m^3). It is obviously a characteristic of the fuel type grass that generally lower tar concentrations can be expected. Even more since most of the common tars are not converted at 750 °C according to van Paasen and Kiel [209]. This conclusion is in agreement with von Scala [93] who stated, that more char is produced if more potassium is present at the expense of tars. This condition is certainly true for grass.
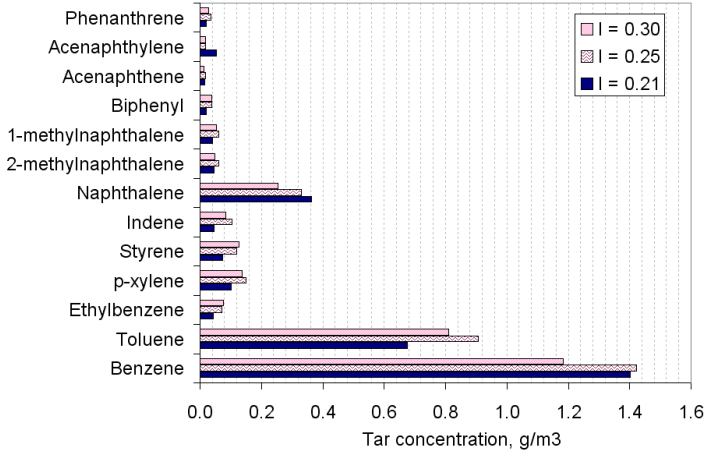
Figure 4.29: *Tar from GC/MS analysis for experiments h-j*

4.9.8 Water content

The water content as depicted in figure 4.30 increased with increasing λ. For higher air to fuel ratios more steam is formed as a combustion product. This also corresponds to a lower hydrogen content and less char inventory, which consumes less steam for the char reactions. No data was acquired for the experiments at 700 °C.
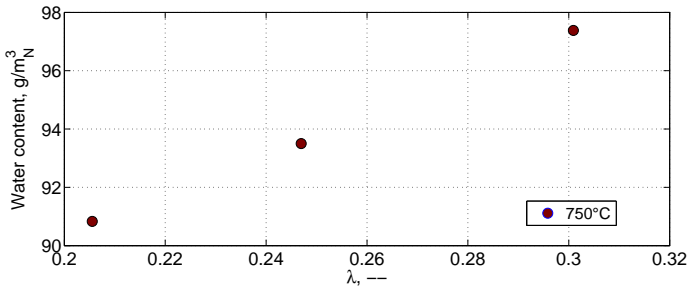
Figure 4.30: *Water content for different air to fuel ratios in the alumina bed*

4.9.9 Comparing the gas compositions to literature

Table 4.12 compares a typical gas phase composition to other gasifiers with similar fuels or larger sizes. It is instantly clear, that the product gas composition is quite comparable including the tar load. The particle load seems high compared to the Värnamo plant. Circulating fluidised beds can reintroduce a part of the fines through a cyclone. This is not possible for bubbling fluidised beds. Here a weaker fluidisation instead would lead to a smaller particle load. The lower heating value of the gas is already good but can surely be improved by optimising the process parameters. The carbon conversion for $\lambda = 0.25$ is around 90 %.

	this study	HNEI	HTW	Värnamo	Arbre
H_2, %vol	11	11	10	11	13
CO, %vol	10	13	13	16	17
CH_4, %vol	3.7	3.9	3	6	4
CO_2, %vol	18	16	19	16	15
N_2, %vol	55	54	55	48	52
NH_3, %vol	< 0.2	< 0.17	–	< 0.16	–
LHV, MJ/m^3 dry	4.6	–	3.9	5.5	5
Gravimetric tar*, g/m^3 dry	< 4	< 19	< 4	< 5	< 1.5
Fines, g/m^3 dry	80	–	–	< 10	–
Size, MW	0.01	0.01	0.1	18	25
Fuel	grass	banagrass	rye grass	wood, straw	wood
Temperature, °C	750	800	630	850	850
Bed material	alumina	*	NA	magnesite	
Reference	this study	Turn et al. [169]	Gudenau et al. [3]	Stahl [41]	Waldheim [263]

Table 4.12: *Comparison of the product gas compositions to literature data*
*(*not published from the composition it could be a type of augite).*

4.9.10 Monitoring of the contaminants

In the following chart (4.31) the beginning of the monitoring is depicted for run j (see table 4.6). There are two phenomena, which occurred that can both be seen in the graph. The first one is a phenomenon reasoned by the hot gas filter. The increasing filter cake of the hot gas filter leads to a better retention of the contaminants. In this measurement only K, P, Mg were detectable. The detection limits are given in the slim graph on the right hand side. The potassium concentration was detectable only during the first $20\,min$; then the concentration went below the detection limit.
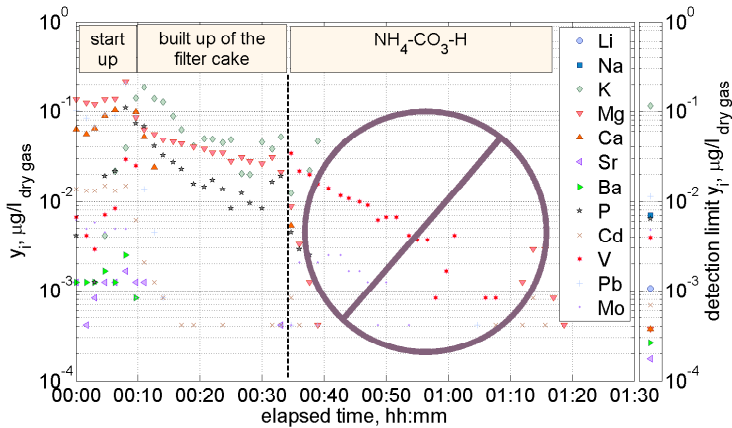
Figure 4.31: *ICP-OES monitoring of the product gas at 750°C in an alumina bed*

The second phenomenon is due to the formation of NH_4CO_3H. This leads to plugging of the lining and distorted the measurement data. Due to these difficulties back up samples were taken and evaluated offline.

The offline data is presented in table 4.13. The values are all significant but close to the detection limit. The data for potassium could not be evaluated since it was below the detection limit. Though the signal in figure 4.31 is evidence, that there is potassium at least during the built up of the filter cake. Afterwards it disappears below the detection limit. The data for the other elements mentioned earlier were all below

the detection limit and were not verified in the presented experiment at all. Though for some other experiments the existence could be shown.

Lambda ⟶ dry gas ⟶	0.30 $\mu g/m^3$	0.25 $\mu g/m^3$	0.21 $\mu g/m^3$	Turn et al. [179] $\mu g/m^3$
Na	44	30	26	10'000
K	↘	↘	↘	64'000
Mg	11	6	3	–
Ca	↘	16	11	2'900
P	5	6	8	19'000

Table 4.13: *Contaminant readings for the gasification of grass in an alumina bed at 750°C (↘: below detection limit)*

The contaminant concentrations reported by Turn et al. [179] were measured using a sampling port inside the reactor at 725 °C, which is why the concentrations are much higher. Additionally within the reactor, no substantial filter cake can exist. It has been stated: temperatures above 650 °C the vapour pressure of the alkalis is high enough that an unacceptable high fraction can pass to the gas turbine [32].

Since the acquired data is so close to the detection limit, it is not possible to derive any trend concerning the parameter settings. A partial exception is magnesium. There is a trend of the values rising with the air to fuel ratio. This could be a hint, that during the combustion of char the volatilisation behaviour differers from that of char gasification with steam. But more profound data is needed to evaluate this assumption. This effect would suggest, that the addition of steam could be a parameter to influence the volatilisation behaviour of some contaminants.

Table 4.14 compares the gas turbine requirements (see table 1.2) with the detection limits of the system. The data was calculated by using the gas to solvent ratio of the sampling system and assuming an air to fuel ratio for the gas turbine according to section 1.4. It becomes obvious that for that case of the cofiring configuration the detection limits are well below the concentrations of proof. This is not the case for the alkalis sodium and potassium in the mono-fuel configuration. Here the detection limits are not low enough to proof the given restrictions. All the other elements though can be verified with the system. It is believed though that with a carefully adopted calibration for each element
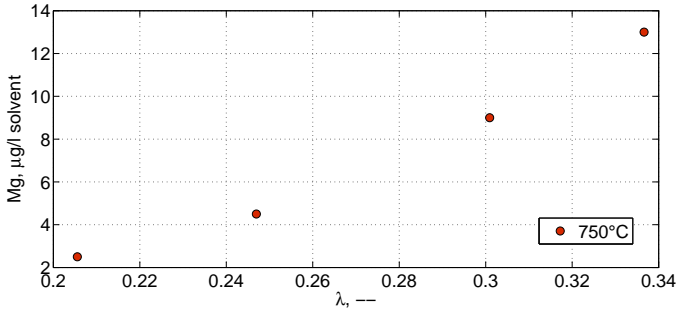
Figure 4.32: *Magnesium content for different air to fuel ratios at 750 °C, alumina bed*

the detection limits can be tuned and using a longer sampling interval the raw counts of the ICP-OES will further enhance the detectability of potassium. From experience it can be told, that the potassium concentrations in the raw gas is usually in the same range as sodium [180; 169]. It may be repeated here, that the given limits are the most restrictive ones found in the literature review.

	concentration of proof cofiring *µg/l* solvent	concentration of proof mono-fuel *µg/l* solvent	detection limit sampling train *µg/l* solvent
K	181	20	92.9
Na			5
Pb	603	28	9.19
V	301	14	3.2
Ca	1205	56	0.2
Mg	1205	56	0.3

Table 4.14: *Comparison of gas turbine limits and detection limits for the cofiring configuration*

The presented results show that, the gas after a hot gas filter at 400 °C is clearly clean enough (in terms of gas turbine contaminants) to supply a gas turbine in a cofiring mode, whereas the applied sampling train does not allow a verification for potassium in the mono-fuel mode. The sodium concentration alone is already to high to pass the specifications. The result also proves, that hot gas filtration at 400 °C does not by

all means hold back all the inorganic compounds though latter are expected to be present as condensed matter. Secondary measures must be involved to reduce the sodium and potassium levels to a sufficient degree for the mono-fuel configuration.

4.9.11 Verification of the hot gas filter

The elemental analysis of the fines in the hot gas filter is given in figure 4.33. The filter fines were ashed at $400\,^{\circ}\mathrm{C}$ for $9\,h$. Though the standard procedure allows $815\,^{\circ}\mathrm{C}$ for at least $60\,min$, the lower temperature was chosen to prevent the volatilisation of inorganic elements like, alkalis or cadmium, which are known to evaporate long before $815\,^{\circ}\mathrm{C}$. To compensate for the lower char reactivity at the chosen temperature, the duration was increased to $9\,h$. The ash was then cooled down to $150\,^{\circ}\mathrm{C}$ in the furnace and down to ambient conditions in an exsiccator. The samples were then enclosed to prevent the uptake of moisture and delivered for ICP-OES analysis. The fines consisted of 40-60 % carbon (rest ash) with increasing carbon content for smaller values of λ.
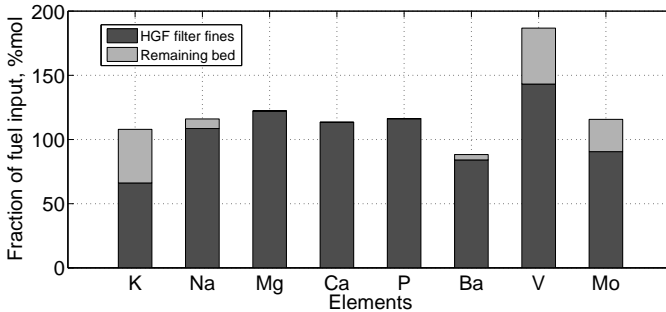
Figure 4.33: *Elemental distribution in the hot gas filter fines and bed after the test*

The graph illustrates nicely that all verified elements were found to a high fraction in the fines for the given process settings. Only for potassium a large part was found attached to the bed material. The uncertainty for this kind of analysis is around 10 %rel by experience. Since both the fuel content and the HGF content were determined by ICP-OES analysis this uncertainty becomes 20 %rel. The used alumina

NWa 155 from Sasol shows minor impurities of SiO_2, Fe_2O_3 and Na_2O. Sodium is reported to be below 0.005 % [264]. But especially the sodium impurities of the bed could have led to the excess of the output. Lead was neither verified in the grass sample nor in the gas or hot gas filter ash. The analysis for vanadium yields a much higher value for the output than for the input stream. One reason for the higher output concentration of the elements could be the analysis method for the elemental composition of grass. Applying the standard DIN method results in the release of a part of those elements into the gas phase being lost for the mass balance.

This result confirms, that only a very small portion of the contaminants could have passed the hot gas filter and reached the solvent.

XPS measurements[8] – which give information about the composition of the surface atoms of a solid material – confirmed, that about 2.4 %at of the surface consisted of potassium (see table 4.15). The amounts of aluminium and oxygen fit the main fraction, which is alumina Al_2O_3. The major part consited of carbon. The measurement does not tell if it is sticking soot or maybe a carbonate. The potassium could be attached as alkali alumino silicate such as $KAlSiO_4$ (kalsilite), $KAlSi_2O_6$ (leucite) or alkali silicates such as K_2SiO_3 or $K_2Si_2O_5$ [181; 265; 258; 119], which would be feasible based on the given data.

Atom	surface concentration %at
Al	21.4 %
O	29.5 %
K	2.4 %
Si	4.2 %
Ca	1.2 %
C	40.2 %

Table 4.15: *XPS analysis of the surface of the bed material after the experiment.*

4.9.12 Note about sulphur and ammonia

As it was stated before, the sampling train does not allow a proper validation of the sulphur components as well as the ammonia concentration. It became very clear during the experiments, that both are

[8]X-ray Photoelectron Spectroscopy

present in comparably large amounts. Sulphur scrubbers are state of the art technology and are installed in IGCC power plants from the beginning to remove H_2S and COS [32]. Ammonia is also an issue in coal gasification. The Claus kiln is therefore equipped with a catalyst to convert the nitrogen species NH_3 and HCN to N_2 [32].

A novel single pellet gasifier M_iV

Chapter 5 presents the design and experimental results for a novel single pellet gasifier. Unlike common options, the design of the reactor offers the opportunity to expose a single solid fuel pellet to conditions very similar to real gasification, combustion or pyrolysis processes. The characterisation and optimisation of the alkali sensor applied in the experiments is the scope of the PhD thesis of Marco Wellinger from Chemical Processes and Materials group at PSI. The experiments presented in section 5.6 were conducted in close collaboration with Marco Wellinger.

5.1 Motivation for this approach

Bench-scale gasifiers ($2\text{-}10\,kW_{th}$) are the first step to demonstration plants. In terms of controllability (flows, temperature) and detailed analysis these gasifiers are already too large. To understand certain influences, such as moisture of the fuel, alkali content or gasification agent, smaller devices are required ($<100\,W_{th}$). With the result of small reactors the behaviour of gasification reactors can be predicted, if similar conditions can be created. The main drawback of these small reactors is the problem to reproduce the exact conditions of the represented process.

Thermogravimetric analysis (TGA) e. g., has been widely used to gain insight into the volatilisation of all sorts of biomass and materials. The

parameters, which has been varied mostly are heating rate, terminal temperature and feed gas. It has also been used to predict volatilisation characteristics in biomass gasification processes [266–268; 163; 269; 270]. The major drawbacks of TGAs are the limited heating rate of the system and the small amount of the sample. In biomass gasification the fuel enters the reactor within seconds, where it experiences a temperature increase from ambient temperature to between 700 and 1000 °C. New TGA devices can be operated at heating rates up to $200\,K/min$, which is still hardly comparable to the real system. A literature review reveals that the influence of the heating rate on the product is remarkable [89; 270]. This has also been proven for the volatilisation of alkalis by Keown et al. [271]. Starting from 600 °C to 900 °C, the volatilisation of K, Na, Ca and Mg starts to increase strongly for fast heating rates, whereas for slow heating rates it stays nearly constant.

TGA normally uses very small amounts of material (10-40 mg approx. 200 μm fines). Recent results about the elemental distribution for different particle sizes [203] rise doubts, whether the chosen sample and subsequently the kinetic results are representative. Where entrained gasifiers effectively use fines, fluidised bed and fixed bed usually use larger particles of sizes between 1 and 10 cm. The different behaviour of a standard TGA and a macro TGA (larger samples) is confirmed by Haselbacher [269]. The kinetic behaviour of a larger particle is quite different from a small sample due to diffusion limitation. This is obviously a critical point for fuel particles, which follow the shrinking core mechanism [272; 273]. This mechanism describes the ongoing reaction within a particle. The reaction takes place along the interface of the shrinking core leaving the remaining ash shell at constant size.

A few attempts were made to introduce a fuel particle into an already hot furnace [274–276]. The amount still did not exceed 40 mg of material. The introduction of the small amount of fuel positioned in a sample holder led to substantial thermal delays.

Putting the described experience together, the result of a TGA will differ from common tests if larger particles would be used and real heating rates would be achieved. In this thesis a novel single pellet gasifier referred as M_iV[1] was developed, which aims to eliminate both of the two drawbacks. Since large particles (entire pellets[2] 500 mg)

---

[1]German: Mini Vergaser (English: Mini Gasifier)
[2]Pellet size: 5x20 mm, density: 1.3 kg/l

can be used and a real heating rate is realised by letting the particle drop through a lock within a second. Furthermore, no thermal delay is introduced by means of additional sample holders. The gasification agent circulates completely around the single pellet and does not flow by above the fuel like in common furnaces. Also from this point of view, the reactor resembles a fluidised bed better.

The reactor will be utilised to analyse the alkali emission during the gasification of grass more profoundly than it is possible with the presented fluidised bed gasifier. The properties which will be tested are the water and alkali content of the grass. The absolute alkali content can be reduced by leaching the fuel in advance. It was shown that leaching leads to less emission of alkalis during the gasification process [179]. It has not been evaluated so far, how much of the remaining alkalis would pass a particle filter and subsequently enter the gas turbine.

5.2 Realisation of the M_iV

The design of the reactor is illustrated in figure 5.1. The internal height is $100\,mm$, and the internal diameter $16\,mm$. The reactor consists of three parts: a lower part ⑥, where the pellet is gasified, a middle part ⑦, where the gas exits the reactor and a top part ④, from where the pellet is introduced. Into the first part the grate ① is inserted. This part is entirely within the furnace. The gasification agent enters the reactor through the line ⑧ below the grate. The middle part is connected to the lower part by a conical flange, which – under moderate conditions – is gas tight itself and does not need an additional sealing. Nevertheless, there is a sealing nut provided in case such is needed at higher pressures. From the upper reactor the gas can exit through line ②. This point is not in the furnace anymore (see also figure 5.2). In this part the inlet ③ for the thermocouple is positioned. It reaches down through the reactor to position ⑨. The third part is the pellet lock hopper ④. The real locking valve is not depicted in the CAD drawing but is illustrated in figure 5.2. This part houses the pellet as well as the reactor locking bead ⑤ and is separated from the reactor and on the other hand the atmosphere through valves. The reactor can be equipped with additional liners to study the influence of the reactor material.

The reactor is made of Inconel® matching the material from the fluidised bed. Using glass as reactor material was avoided, since in house ex-
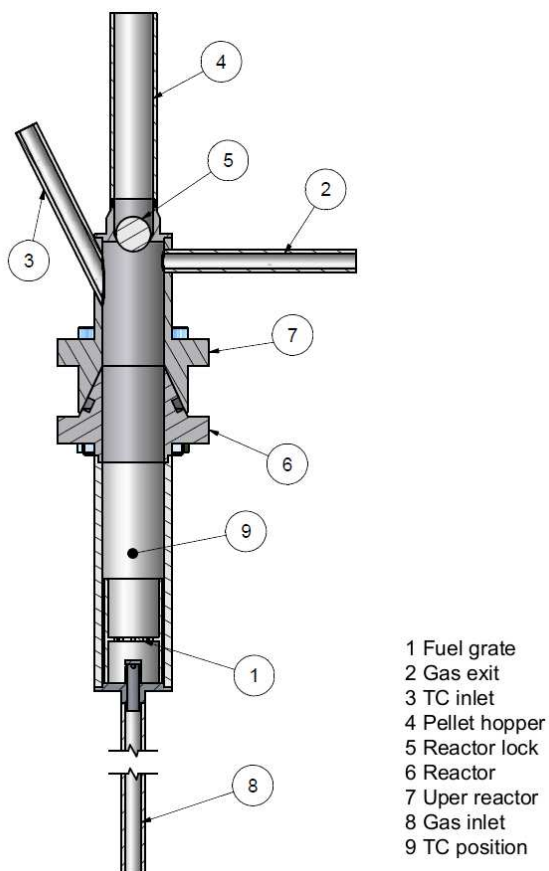
Figure 5.1: *Design of the $M_i V$ 1:2*

perience showed, that at high temperatures ($>600\,°C$), the glass tends
to adsorb alkalis. The reactor locking bead is a standard bearing ball.
It is magnetic and thus can be removed from its locking position with
a magnetic rod. By this option several pellets (1-3) can be inserted in
one run, without opening the reactor. Due to the design and small size
of the reactor, it is also able to run at higher pressures.

5.3 Controlling and safety aspects

The furnace was heated by electrical heaters by means of an in house built 48V transformer. The transformer was controlled by the very same LabView software as the sampling system. It incorporates alarm functions similar to the one in the fluidised bed. Additionally, there is a pressure relief valve that opens above 0.5 *bar* to avoid high pressures. This is necessary, since the reactor is provided with compressed air by means of a mass flow controller. Blocking of the lining would lead to full grid pressure in the reactor.

5.4 Measurement techniques

The measurement devices for this reactor must be in any case fast enough to follow the signal. The proposed sampling frequency must be at least 1 *s*. Gas chromatography and ICP-OES measurements are too slow. Only mass spectrometer and surface ionisation measurements were available and fast enough to keep up with the signal.

5.4.1 Mass spectrometer (MS)

A Thermo Onix mass spectrometer from ProLab [277] was used to monitor the concentration change of the permanent gases (CO_2, H_2, CH_4, O_2 and N_2). To analyse CO properly a different system is required, since m/z 28 and 29 also respond to nitrogen. There was a signal during the gasification at m/z 30, where the ^{30}CO isotope can be found, though the signal was very weak. With the MS measurement it is possible to distinguish between gasification and combustion, which both take place during the processing of a pellet.

5.4.2 Surface Ionisation Detector (SID)

Surface ionisation technology for analysis goes back to the beginning of the seventies. The principle of the sensors are based on the high probability of some alkali metals to get ionised during the desorption process from the ionising filament [278]. The sensor is especially sensitive to potassium, sodium and caesium at the same time and thus measures the sum of those [220]. Barium is an element, which also

can be ionised by the filament but the ionisation probability is much reduced compared to the first three elements [279]. Furthermore Ba was not found in the fluidised bed gasification analysis, and hence is neglected. Such sensors have been built several times in the past and tested successfully [280; 279; 219]. The SID is an in-line sensor giving the option to connect a second analyser directly after the SID. For instance the SID can be coupled with a MS. This would additionally yield the information, what kind of alkali component is passing by.

The normal signal of the SID is given in nA and corresponds to the alkali concentration. The integral of the signal then corresponds to the sum of all ionised alkalis. The signal depends on the effective volume flow carrying the alkalis. For this reason the volume flow was kept constant for all runs. The signal also depends slightly on the bulk gas composition. In order to reduce this influence and account for the high sensitivity of the sensor the gas from the reactor was diluted with nitrogen. The fraction of sample gas was chosen to be around 8 % of the total gas stream flowing through the SID (see also section 5.5).

5.5 Experimental setup and procedures

The M_iV reactor is positioned inside a cylindrical furnace (see figure 5.2), which can be electrically heated to the desired temperature. The gasification agent (reactor gas) enters from the bottom through a distributor that at the same time serves as grate for the pellet. The pellet is given into a lock hopper above the reactor. When the temperature and all sensors are stable, the pellet is released through the ball valve into the reactor. The pellet drops through the tubing from ambient conditions into the hot reactor and thereby experiences similar conditions as if it would be transported into a gasifier. After the pellet has dropped a metal bead is released to lock the pellet entrance and reduce the dead volume of the reactor to a minimum. The product gas leaves the reactor at the top through a heated line in order to prevent the condensation of tars. Additionally, the product gas is quenched and thereby diluted by a nitrogen flow at Q1 after leaving the reactor. This is a common procedure to limit the particle growth [217]. The flow introduced in Q2 was smaller than the flow of the sampling system, and can be adjusted that around 8 % sample gas from the reactor was used for the analysis. (A photograph is given in appendix β figure β .1.) The gas enters the
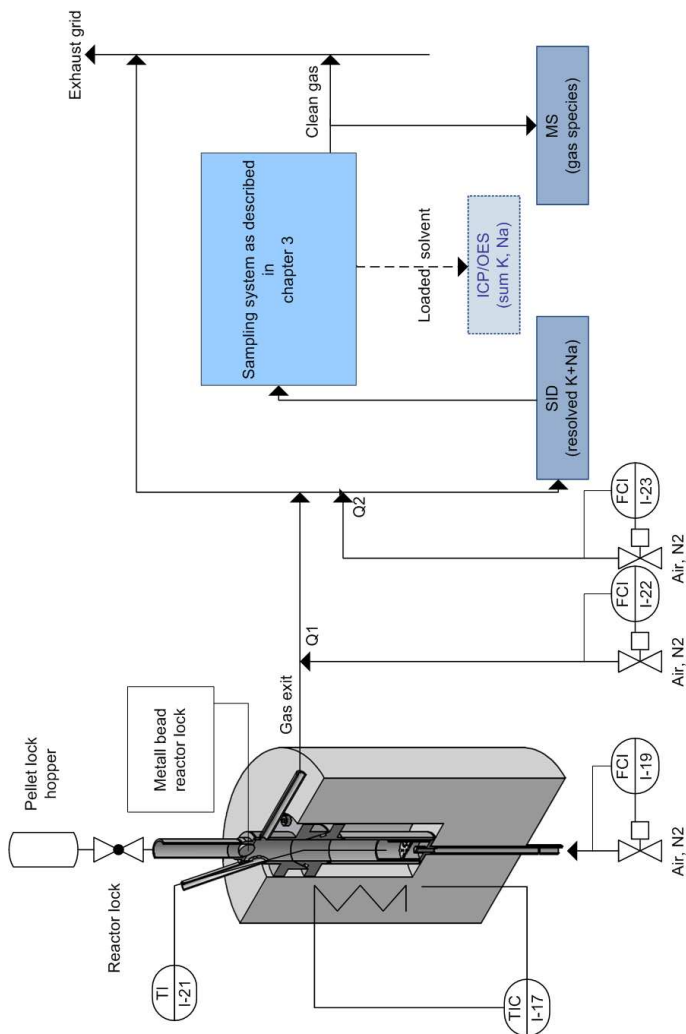
Figure 5.2: *Flow chart of the experimental setup*

heated SID, which measures the alkali content in the gas. After leaving
the SID, the gas is instantly quenched by a solvent as described in sec-
tion 3.2. The two phase flow is pressurised and cooled to enforce the
condensation and separation of tars and separation of particles. The

cleaned gas is directed to a MS to measure the concentrations of the mentioned gases. In addition, the temperature in the centre of the reactor and close vicinity of the pellet is recorded at all times. Similar to the fluidised bed experiments the loaded solvent could be analysed by means of ICP-OES measurements. Due to the small amount of solvent and the low concentration of alkalis, these measurements could not be accomplished satisfyingly. Still, this analysis should be done in future experiments to quantify the alkali emissions. After the experiments the grate was removed, the ash recovered and the reactor cleaned.

Fuel preparation: The elemental data of the fuel was presented in section 4.8. The data is very similar to the values presented in literature. Compared to wood, especially the potassium and silicon but also magnesium, sulphur and nitrogen concentrations are higher in the grass (see section 2.7.4). The grass was pelletised by the fuel supplier and crushed at PSI to produce a suitable pellet for the M_iV setup.

In order to influence the volatilisation behaviour of the alkalis certain properties can be manipulated. Among those properties are the water content and the water soluble minerals. These properties were altered accordingly to the following experimental matrix (table 5.1).

Fuel	Reactor gas	Fuel preprocessing	ξ_{H_2O}, %
grass	air	none	8.8
		Mocca Express (105 °C, 4min)	7.8
		doped (KNO_3, $NaNO_3$)	8.1
		dried (24 h, 105 °C)	2.1
	N_2, air	none	8.8

Table 5.1: *Experimental matrix; ξ_{H_2O}: Water content*

Leaching of alkalis: There are many extraction methods to remove alkalis from the fuel. Leaching was done before by rinsing, spraying or mechanically enhanced extraction [281–283]. At first leaching as proposed by Dayton et al. [283] was tried, but it became clear that soaking the grass for 24 h in water resulted in anaerobic decomposition of the grass. For this reason a different method was tried with excellent results.

A hot water extraction was performed by means of a standard well known mocca express machine as depicted in figure 5.3. A scheme of the working principle is illustrated alongside the picture. Though being a method not commonly used in scientific research, it is a very serious and efficient extraction method in process engineering. The extraction takes place at around $105\,°C$ when the boiling water is pressed through the grass by vapour. This temperature is not decomposing the grass it rather increases the extraction efficiency. The process takes about $4\,min$ only. The amount of grass that can be processed in the 3 cup version was $11.5\,g$ using $144\,ml$ of demin water. The extracted liquid
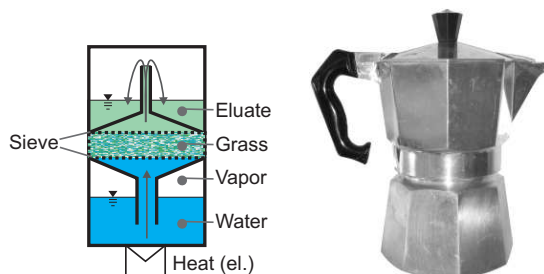
Figure 5.3: *Leaching setup (left: scheme, right: mocca express)*

(eluate) can be recovered in the upper chamber, whereas the moist fuel will stay in the sieve. Only small amounts of fines were dragged up into the upper chamber. The removed amount of alkalis were determined by an ICP-OES measurement of the eluate (table 5.2). The grass was dried after the processing. The amount of leached potassium was $72\,\%$. This is about the same amount, which is given in literature for other leaching

Element	Amount, %
K	72
Na	21
Ca	NQ
Mg	NQ
Cl	NQ
P	NQ
S	NQ
Sr	NQ

Table 5.2: *Extracted elements (NQ: verified; not quantified)*

types like rinsing. For our small samples the mocca extraction method was best suited showing simmilar or even better results within much shorter time and less effort. The other elements listed in table 5.2 were not quantified but found in the eluate in significant concentrations. At least chlorine is known to be responsible for the volatilisation of inorganic constituents such as potassium [274].

Doping with alkalis: Doping of the grass was done by soaking the grass sample with an aqueous solution of KNO_3 and $NaNO_3$ at ambient conditions. The grass was subsequently dried at $40\,°C$ assuming the nitrates were entirely adsorbed. The amounts of the alkalis in the nitrate were chosen at concentrations to double the alkali concentrations in the used grass.

Drying of the grass: Drying grass completely is hardly achievable based on its highly hygroscopic behaviour. Drying for 150 minutes at $105\,°C$ reduced the water content to less than $0.5\,\%$. Two pellets were produced from the dried grass and transported to the reactor. One pellet was gasified and the other pellet was analysed for its water content being $4\,\%$ again. In a second try the grass was first pressed into pellets and then dried. This resulted in only $2\,\%$ water content of the gasified pellet. Compared to a water content of normally $8\,\%$ this was assumed to be low enough to see a difference in the volatilisation behaviour.

Pelletising of the grass: After the pretreatments the fuel was weighed and manually pressed into a pellet to a constant volume and density under elevated temperature ($80\,°C$) as described in [284]. The density for a commercial grass pellet was measured to be around $1.3\,kg/l$. The pellets were produced accordingly. The resulting pellets had a diameter of $5\,mm$ and a height of $20\,mm$. This corresponds to a pellet weighing approx. $500\,mg$– ten times as much as used in a TGA. The pellet pressing device is depicted in figure 5.4. The resulting pellets proved to be quite strong.

Sampling of the gas stream: Sampling respectively gas cleaning was conducted with the pressurised scrubber, exactly like the procedure for the fluidised bed experiments. The solvent was identical.

1 heated cylinder
2 Piston
3 Guiding piston
4 Press holder
5 Space for pellet
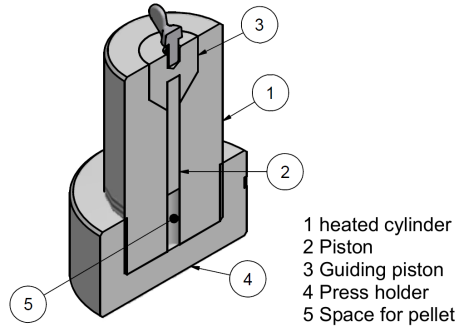
Figure 5.4: *Pellet pressing device*

5.6 Results and discussion of the basic behaviour

The first test was conducted in order to determine the slip-stream of the alkalis through the sampling system. The test was done only for standard grass pellets. Maintaining a constant flow, the SID was positioned once upstream of and once downstream of the sampling system. Each time a grass pellet was dropped into the reactor. The difference of the signal is assumed to be the part being removed by the sampling system. The integral was evaluated for the slip as illustrated in equation (5.1)

$$\text{Alkali slip} = \frac{\int_t I_{SID}(\text{outlet of the scrubber})}{\int_t I_{SID}(\text{inlet of the scrubber})} \qquad (5.1)$$

Since the SID always showed a tailing, the signal was cropped at around $30\,min$ but only when the signal was below 10 % of its peak value.

Graph 5.5 depicts results for the slip stream. The total retention of the particles containing alkalis is about 99.9 %. This test was repeated once to ensure reproducibility. From the mechanistic principle of the sampling system it can be said, that the fraction that can pass the system are the particles with sizes presumably between 30 and 100 nm. This conclusion is based on two phenomena, particles in gas streams are subject to. Large particles are separated easily based on their large inertia. Very small particles ($<30\,nm$) are subject to difusion. For long linings this means that those particles are separated as well. In Hinds [212] it is described that $1\,nm$ particles will be lost to 97.8 % in a $1\,m$ tubing for a laminar flow due to difusion. $10\,nm$ particles will be lost to a degree of 10.8 %, wheras $100\,nm$ particles will only lose 0.6 % due

to difusion. The used lining was $11\,m$ long. Thus it can be assumed, that all the smallest particles will be removed as well.

Based on this experiment a second conclusion can be drawn. The alkalis, which form the first peaks in the signal are likely in the discussed range.
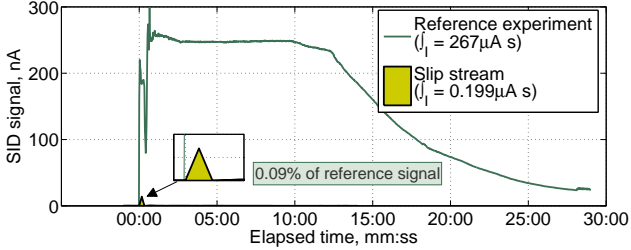
Figure 5.5: *Measurement of alkali slip-stream through the sampling system compared to a typical alkali signal during gasification and char combustion*

In figure 5.6 the reference experiment is illustrated. It was conducted with an untreated grass pellet and air as gasification agent. The upper graph shows the temperature that was measured in the direct vicinity of the pellet (⑨ figure 5.1). The middle graph depicts the alkali signal by means of the current, produced by the ionized potassium and sodium molecules. In the lower graph the MS intensities for the main species CO_2, H_2 and CH_4 are plotted. The existence of CH_4 and H_2 proves that after the pellet drops immediate pyrolysis and gasification takes place. At the same time the temperature drops significantly due to the endothermic processes during volatilisation. A small portion of the temperature drop results from the energy transfer into the pellet. This was tested by a stainless steel pellet of the same size. The steel pellet shows a higher specific heat as well as a higher mass and hence should even enhance this effect. But the temperature drop caused by the pellet itself is much less significant. After the pyrolysis and gasification is finished the char combustion takes place. This can be seen by means of the temperature, which rises above the original furnace temperature and the MS signal that only shows CO_2 during the combustion phase. The combustion is considered to be finished, when the temperature reaches its set point again.

The alkali signal (second graph) shows two very distinct and fast peaks followed by a wider shoulder holding most of the volatilised alkali portion. This general characteristic is constant for all tests. Similar results were obtained by Dayton and Milne [274] who showed that the main alkali compound (KCl) volatilised primarily during the combustion phase by means of a MS. The fast peak during the pyrolysis phase was not detected by those experiments.
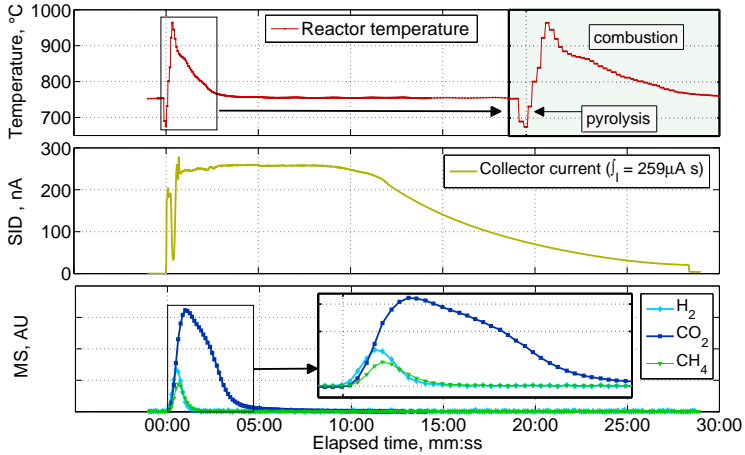
Figure 5.6: *Test with untreated grass pellet (reference)*

The CO_2 concentrations take slightly more time to come down after combustion is finished. This can be explained by combustion of remaining carbon that is more difficult to access. It may not be detectable by a temperature increase any more. A second explanation is the sampling system tends to blur the concentration changes (see section 3.5). The alkali signal takes much longer to return to its background level.

The MS measurement shows by using a rough calibration that the CO_2 concentration peaks at 19 %, H_2 and CH_4 at 6 % and 5 % respectively. This is similar to the concentrations from the fluidised bed experiments just above the fuel feed inlet (figure 4.22), where the pyrolysis takes place. It thus can be assumed, that the conditions during the pyrolysis much resemble those in the fluidised bed.

In order to evaluate the hypothesis of the two processes pyrolysis phase versus the combustion phase, further experiments were conducted (fi-

gure 5.7) to separate the two stages. In this case the reactor was firstly run on pure nitrogen until pyrolysis was over and then the nitrogen flow was replaced by an equivalent air flow. The graphs show very nicely that the first temperature drop and the first alkali intensity increase can be allocated to the volatilisation of the fuel, whereas the second part – showing the much bigger portion of alkali emission – can be connected to the combustion phase. The second peak (char combustion) holds 92 % of the alkali signal (area).
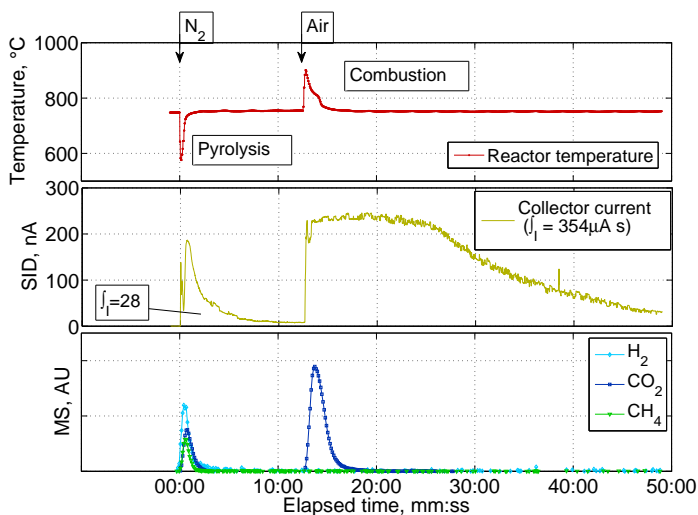
Figure 5.7: *Test with untreated grass pellet: pyrolysis - combustion separated*

For this test the alkali signal also takes much longer to return to the background than the other signals. There could be several explanations for this effect:

◇ The SID sensor is saturated by the amount or type of the alkali components. The ionisation of the alkalis takes place bit by bit until the filament is blank again. The integral of the curve is equivalent to the overall airborne alkalis.

◇ The alkalis are deposited in the lining and eventually resuspended.

◇ It could be a combined deposition of tars and alkalis during the pyrolysis phase.

The first suggestion could not be tested with this set up. The approach would be to increase the dilution by changing the flow at Q2. Dilutions lower than 4 % of sample gas in nitrogen were technically not possible with the installed mass flow controllers. Nevertheless it could be verified, that the integral of the signal changes according to the weight of the pellets introduced. This means that the alkali signal corresponds to the absolut amount of the alkalis in the pellets.

Resuspension by vaporisation can be excluded because the temperature in the lining does not exceed 400 °C. There are a number of other reasons why particles detach [212], from which only resuspension by jets can be relevant. This effect depends on the accessibility of the air jet to the particle, and the force the jet can apply onto the particle. Usually the force of a laminar gas stream at $10\,m/s$ can not detach particles with sizes less than $10\,\mu m$ [212]. But the maximum gas flow in the lining did not exceed $4\,m/s$ (Re≈ 500). Such a process would also result in a decreasing alkali signal, whereas the measured signal stays very constant for some time.

The last thesis was tested by an appropriate experiment, in which the lining between the reactor and the SID was flushed with air between the gasification and combustion sequence (figure 5.7). This did not produce a significant signal. The combustion was initiated by letting air through the reactor until the temperature dropped but the SID signal was still high.The SID did hold its signal even after that the reactor gas and quench gases were switched off. This proves the tailing in the SID signal is not produced by depositions in the lining. It can be concluded from the described test, that the signal characteristic of the SID must be due to surface phenomena at the filament of the sensor.

5.7 Results and discussion of the pretreated grass

The SID signal responds to the absolute amount of alkalis. A Linear tendency between the absolute alkali content and alkali emission was derived from the experiments. Quantification is not possible with the sensor until the mentioned phenomena can be explanation.

5.7.1 The dried pellet

Dried pellets were tested to analyse the first intensive peak of the alkali signal. It was thought to result from the sudden evaporation of the water and entrained alkalis during this step. The first peak did not change its shape or amplitude ratio of the first to the second peak dependent on the water content. This leads to the conclusion, that the described phenomenon is not due to the evaporation of water. Figure 5.8 displays the comparison between a standard run (see figure 5.6) and the test with the dried pellet. The dried pellet emitted less than the normal pellet. This is rather based on the smaller absolute alkali content of the pellet not on the emission behaviour of the drier fuel.
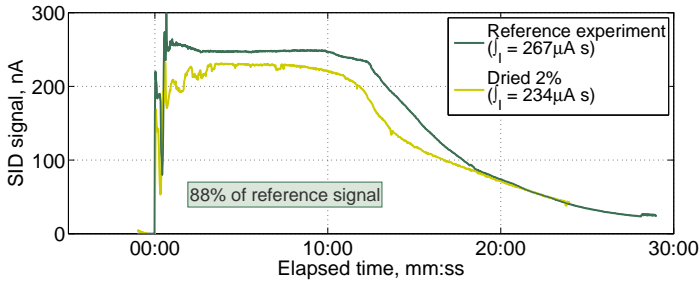
Figure 5.8: *Comparison of dried grass pellet ($\xi = 2\%$) with reference pellet ($\xi = 8.8\%$)*

5.7.2 The leached pellet

The leached pellet emitted about 40 % less alkalis then the reference (figure 5.9). This is rather surprising, since the extraction removed 72 % of the alkalis from the grass. One reason may be the mechanism of partial melting as explained by Andersson et al. [280]. For large particles only the outer layers of the particle melt. This means, that the particle size distribution has an effect on the effective signal. It is by all means possible that the leached pellet is more brittle causing a higher fines entrainment than the natural pellet. Another reason may be due to the formation of potassium hydroxide and potassium cyanate as reported by [274]. These compounds are formed if chlorine is not present in sifficient amounts to form chlorides.
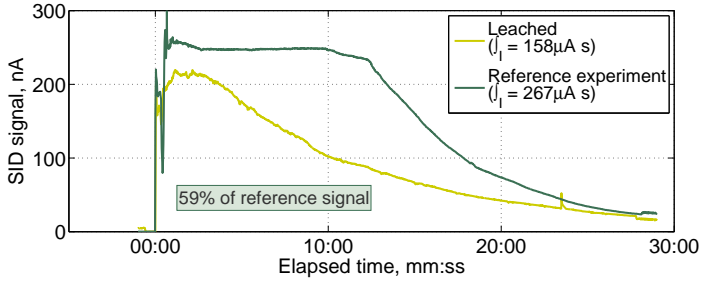
Figure 5.9: *Comparison of leached grass pellet with reference pellet*

5.7.3 The doped pellet

The gasification and combustion of doped grass revealed an increase of around 80 % alkali emission, though the doping doubled the amount of potassium and sodium in the grass. But is has to be noted that the doping was perfomed with alkali nitrate and no additional chlorine was introduced. As mentioned earlier chlorine is one of the main elements responsible for the volatilisation of inorganic elements.
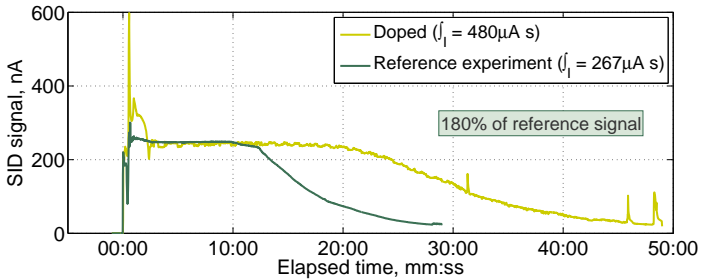
Figure 5.10: *Comparison of doped grass pellet with reference pellet*

The additional alkalis seem to volatilise primarily in the combustion phase. A smaller portion is detected right at the beginning, whereas the main part adds to the combustion resulting in a much longer tailing. The peaks at the end of the signal are signal distortions.

Running the leached and doped pellets in the separated gasification-combustion mode (as in figure 5.7) revealed that the manipulation effected the combustion phase much more than the gasification phase.

5.7.4 Summary of the tests with the pretreated fuel

The results show that leaching the grass as pretreatment will unlikely be relevant for industrial applications. The influence on the alkali emission by leaching affects only the char combustion, which is equally covered by the hot gas filtration. The results for the doped pellets indicate that the alkali emission corresponds to the alkali content. The dependency on chlorine seems to be of minor influence as it was already found by Dayton and Milne [274] for biomass combustion.

5.7.5 The influence of hot gas filtration

A final set of experiments was performed by introducing a hot gas filter into the gas line after the reactor exit. The hot gas filter has a pore size of 5 μm and was operated at 400 °C. The filter area was very large compared to the gas volume, so no dynamic influence of a filter cake could distort the measurement. The filter was identical with the hot gas filter used in the fluidised bed experiments. The result is presented in figure 5.11. The response was around 1 % of the reference signal. The alkalis passing the 5 μm filter were found to volatilise during the pysrolysis and gasification phase. This is in excellent agreement with the slip-stream, since for both systems only the smallest particles can pass. Normally a hot gas filter acumulates a filter cake, which results in a very efficent filter enhancement. In such a case, even less alkalis would pass.

As it can be seen in figure 5.12, the ash still shows the shape of the former pellet. The figure shows three gasified pellets. The last one lays on the top. This means the gasification and subsequent combustion is following the shrinking core model at a constant particle size [272; 273]. It is also an indication, that the particle size is a parameter that can not be neglected. From the shape of the ash it can be derived, that the pellets did not break, or explode when being dropped into the reactor. This is an important issue since the entrainment of mechanically suspended particles would distort the measurements.
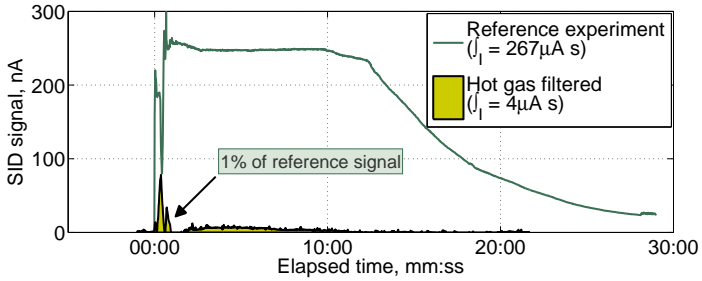
Figure 5.11: *Comparison of the alkali emission with and without hot gas filtration at 400°C*

Figure 5.12: *Pellet before (left) and after (right) gasification and combustion in the reactor grate*

The above described results show two reproducible but unexpected behaviours of the SID sensor: firstly there is a tailing of the alkali signal and secondly there is a stable plateau during the combustion phase. Both phenomena can not be explained by means of the conducted experiments, but both are thought to be connected to surface phenomena on the filament, triggered by too many or too large particles.

Chapter

6

Conclusions

6.1 Fuel review

✧ The stability of the fluidised bed process depends on the ash melting behaviour, which mainly depends on the formation of low melting alkali silicates. Besides grass, agricultural residues and energy crops show similar amounts of silicon and alkalis in the fuel. The ash deformation and sintering temperature (see figure 2.14 and 2.15) is comparable to each other. Figure 6.1 displays a ternary plot for the main ash influencing elements. The arrows indicate the composition change with increasing ash melting risk based on the formation of the alkali silicates (K_2SiO_3 and $K_2Si_2O_5$) given by Kosminski et al. [285]. Since the first compound is reported to be dominating, grass may be expected to be the more difficult fuel. Every fuel below the lines have excess silicon, which means the fuel with more alkalis is expected to show higher risks of ash melting.

Unless a specific fuel shows higher levels of silicon and alkalis than grass, any of the mentioned solid fuels is expected to behave stable with the reported settings.

✧ The review revealed minor amounts of the earth alkalis barium and strontium. These elements are of similar or higher corrosiveness than the usually mentioned alkalis potassium and sodium.
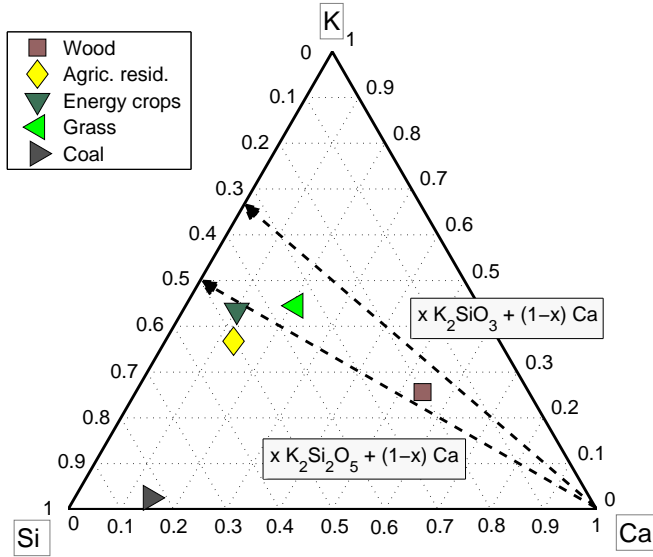
Figure 6.1: *Molar ternary diagram of the main bio-ash influencing elements*

They are not restricted by the gas turbine manufacturers but must be observed as well. The corrosion potential of all relevant elements must meet the limitation.

6.2 Sampling system

The continuous monitoring of the contaminants required the development of an appropriate sampling system. Such a system was developed at PSI and optimised in this work.

✧ The sampling system proved to run very reliable during wood gasification showing an excellent separation of fines and condensables. It also proved to be able to measure contaminant concentrations in the gas phase continuously in ranges down to *µg/kg*. This is a major progress in continuous monitoring of contaminants in product gases from gasification units.

✧ Using the system in grass gasification resulted in the formation of NH_4CO_3H, which corresponds to the high ammonia concen-

tration in the gas phase and the operation parameters (pressure, temperature) of the sampling system. Acidification and water addition of respectively to the solvent improved the situation but did not prevent the formation. The formation did mainly interfere with the ICP-OES measurements, whereas the sampling system could cope with the solid NH_4CO_3H fairly well.

6.3 Fluidised bed gasification

A 5kW bubbling fluidised bed gasifier was designed and operated on grass. Temperature, bed material and air to fuel ratio were varied to discover the gasification behaviour regarding the stability and contaminant emission.

- ✧ The fluidised bed gasifier is by any means very suitable to gasify grass at slightly lower temperatures than for wood and coal. This is required due to the lower ash melting point of grass. The temperature can be as high as $750\,°C$, if alumina is used as bed material. For silica sand the temperature should not exceed $700\,°C$, unless secondary measures are taken to prevent ash agglomeration. Dolomite as sole bed material should be avoided due to its low material strength and consequent bed material loss.

- ✧ The carbon conversion was around $90\,\%$. To reach a better carbon conversion, secondary air or steam injection should be considered. The char produced during the volatilisation was found to float on top of the fluidised bed. The steam injector should be adjusted to this position. A second possibility could be employing a circulating fluidised bed, where most of the particles can be recycled to the feed. The recycled char would be introduced into an oxygen rich zone.

- ✧ The heating values are good and slightly lower than for wood gasification. This is mainly because of the lower carbon fraction in the fuel since the product gas shows a lower CO concentration compared to wood gas. The concentrations of the other permanent gases are similar.

- ✧ Despite the lower temperatures in comparison with usual fluidised bed gasification the tar concentration is very low. This corresponds to the generally lower lignin content of grass compared to wood. This is in agreement with DeGroot and Richards

[92]; von Scala [93] that for biomass with a higher alkali content less tar but more char can be expected.

◇ The concentration of fines in the raw gas stream is higher, owing to the high fluidisation, which was chosen to lower the risk of ash agglomeration. The entrainment can be reduced by lowering the fluidisation.

◇ The analysis of the used alumina bed by XPS revealed potassium attachments together with silica and calcium. This indicates that reactions between the bed material and alkali silicates is possible.

◇ In spite of the low temperature of the hot gas particle filter (400 °C), the concentration of sodium in the clean gas is too high for direct application in a mono-fuel power plant. The concentration of potassium could not be verified at sufficiently low concentrations. The concentration of the other relevant contaminants (Mg, Ca, Pb, V) are low enough for the direct application.

◇ After hot gas clean up, the gas with a cofiring fraction of 10 % LHV is clean enough to be used without secondary measures for cofiring with NG. This is valid unless the combustion air contains alkalis as it is the case for sites close to the sea.

6.4 Single pellet gasifier M_iV

A novel reactor was built to process entire pellets of 500 mg compared to TGA studies, which process about a tenth of this amount. Especially if the fuel is characterised by a shrinking-core-model during volatilisation and combustion, the size of the fuel plays an important role. The reactor was used to examine the gasification and contaminant emission of a single pellet in more detail.

◇ The reactor allows heating rates as shown in gasification units, where the fuel experiences volatilisation within seconds.

◇ With the reactor it is possible to represent the pyrolysis and gasification phase during the volatilisation. The volatilised gas shows a similar composition as the gas from the fluidised bed gasification in the lower part near the feed inlet. The char combustion as the second phase was conducted with air, whereas the char reactions in the fluidised bed are mainly due to steam and CO_2 gasification. This part would be better simulated by changing the gasification

agent entering the M_iV to the corresponding concentrations. This gas composition can be derived from the axial profiles. Since the volatilising pellet provides exactly the gas composition, which it would experience when rising in the reactor through the following volatilising pellet, a back loop of the produced gas into the reactor could be a good option to simulate real gas conditions.

✧ With the reactor it is possible to monitor the qualitative alkali emission from single grass pellets during gasification and subsequent combustion by means of a surface ionisation detector. First alkali emissions takes place very fast during drying and volatilisation, whereas the main alkali emission takes place during char combustion. This is in agreement with tests by Dayton and Milne [274] and Porbatzki [276].

✧ Additional tests showed that smaller particles are emitted during the volatilisation than during combustion. Larger particles can be removed by filtration, whereas small particles pass the filter. This again shows, that small particles can not be neglected and must be retained by secondary measures e. g. feeding solid adsorbents together with the feed.

✧ Since leaching mainly influences the alkali emission from the char combustion, but the hot gas filtration removes this fraction efficiently, the effort to leach the grass in advance is most likely not justified. There is a strong evidence derived from the leaching experiments and the HGF experiment, that the effort to leach the grass in advance is most likely not justified. Furthermore the pellets made of leached grass are less stable during handling compared to the natural grass.

✧ The alkali emission primarily corresponds to the alkali content. The dependency on chlorine seems to be of minor influence, not less but rather other alkali species such as KOH must be expected when chlorine is absent. The manipulation of the alkali content affects the emission during the char combustion much more the one during volatilisation.

✧ Alkali emission characteristics proved to be quite different from standard TGA experiments. The ratio between the alkalis emitted during volatilisation and the alkalis emitted during combustion is lower for the used setup compared to TGA tests [286].

✧ The SID showed a phenomenon, which can not be explained by the conducted tests alone. The signal stayed at the peak level for much longer time then the pellets needed to fully react (tailing). Furthermore the signal was constant at this level indicating a steady state. This behaviour most likely corresponds to surface physics taking place during the operation.

Outlook

7.1 Fluidised bed gasification

✧ Both alumina and silica are commercially available for fluidised bed applications. Silica is a natural product, whereas alumina must be produced through e. g. the Bayer-Process. Pure alumina was used in this study to provide the process with a non silica bed material showing a high hardness. In real applications alumina of this grade will unlikely be used because of its higher costs compared to silica. Additionally chemical degradation of the bed material as well as abrasion must be expected. This leads to the need to periodically replace a part of the bed material. A native alumina or alumina silicate based bed material e. g. bauxite or kaolinite that can be transported from nearby, will always be preferred. The low Moh's hardness (2-3) of the native materials suggests a pre-treatment like calcination. Calcined kaolinite e. g. shows an increased Moh's hardness of 6-8 [287]. Pure silica based materials should be avoided due to increased risks of ash melting. The important factor when discussing the costs of the bed material, is the distance between the power plant site and the mining site of the qualified material. For this reason prices depend strongly on the transportation and can only be calculated if those sites are determined.

⬥ Based on the results it is necessary to test secondary measures to remove the remaining alkalis from the gas if the gas is applied in a mono-fuel plant. This can be done by introducing reactive bed materials like bauxite, kaolinite $(Al_2Si_2O_5(OH)_4)$ or dolomite (natural materials) together with the fuel into the reactor or by placing a fixed bed absorber downstream of the particle filter. The named materials are known to have binding effects on alkalis from biomass and coal. A preliminary literature review reveals alkali alumina silicates such as $KAlSiO_4$ as the major resulting components for aluminium containing additives [288; 180; 4; 265; 289–293]. The addition of dolomite was reported to form solid $MgCa(SiO_3)_2$ [265]. The removed silicon increased the ash melting temperature. The additives were introduced to bind either alkalis or silicon into higher melting minerals such as alkali alumino silicates or alkali oxides. Tests should be conducted to find the most suitable for grass.

⬥ Steam injection should be tried to increase the heating value of the gas and increase the carbon conversion. Steam could be taken from the steam cycle in the IGCC plant.

⬥ CO_2 gasification may be a possible way to increase the overall efficiency, since the future CC power plants will be equipped with CO_2-sequestration. A partial stream could be looped back to the gasifier.

⬥ If higher filter temperatures than $400\,°C$ are required, a dual bed gasifier like the Battelle/Ferco or FICFB type should be considered for grass gasification. In the first reactor (allothermal) the pyrolysis and gasification takes place. The bed material and the char is entrained to the second reactor (exothermal), where the char is combusted. The heated bed material is entrained to the first reactor, where the heat is used for the endothermic pyrolysis. Since most of the alkalis are released from the char, they would be permanently removed from the gas turbine cycle.

⬥ Sulphur and ammonia species should be quantified to get information about the requirements of the sulphur removal unit. Organic sulphur species are relevant for catalytic applications of the gas. Recognition and quantification of those organic sulphur species are crucial for fuels with a high sulphur content such as grass.

⬦ Profile measurements in gasification units are very rare but reveal much phenomena. More such measurements should be conducted to get information about the kinetics in the fluidised bed. This includes steam as well as alkali, ammonia and sulphur profiles. It would much improve the fundamental knowledge needed to model the fluidised bed gasification process.

7.2 The single pellet gasifier M_iV

⬦ MS analysis should be employed to get further information about the compounds such as alkali chlorides, hydroxides or cyanides emitted during the gasification process.

⬦ The behaviour of the gasification should be tested for different gasification agents such as steam or CO_2, which both are available in an IGCC power plant especially with regard to CO_2 sequestration.

⬦ Further and more profound identification of the general alkali emission characteristic obtained from the first tests is a very important task to be able to link the signal to species or particle size. It should include MS analysis as well as particles size distributions.

⬦ M_iV experiments are suitable to produce data to model the gasification of a single pellet. The appropriate approach derived from the experiments would be the shrinking core constant size model for grass. For wood the approach must also include a shrinking shell [294].

Epilogue

Bibliography

[1] Nuon, Nuon Magnum infographic, Tech. Rep., Nuon, 2009.

[2] M. Franken, Teures Holz bremst Boom der Pelletöfen, VDI nachrichten (2006) 18.

[3] H. W. Gudenau, G. Schauermann, W. Hahn, Vergasung von Weidelgras in der Zirkulierenden Wirbelschicht, BWK 45 (1993) 491–494.

[4] M. M. DeLong, M. Onishak, M. Schmid, B. Wiant, E. Oelke, Alfalfa stem feedstock for IGCC power system fuel, Symposium on biomass fuels (ACS Division of Fuel Chemistry) 40 (1995) 699–703.

[5] J.-L. Hersener, E. Meister, V. Mediavilla, A. Lips, J. Rüeg, T. Nussbaumer, U. Baserga, D. Müller, F. Dinkel, B. Waldeck, T. T. Müller, B. Hirs, Schlussbericht Energiegras/ Feldholz, Tech. Rep., Eidg. Forschungsanstalt für Agrarwirtschaft und Landtechnik Tänikon, 1997.

[6] K. Wiegmann, A. Heintzmann, W. Peters, A. Scheuermann, C. Thoss, Bioenergie und Naturschutz: Sind Synergien durch die Energienutzung von Landschaftspflegeresten möglich? Endbericht, Tech. Rep., Öko-Institut e.V. Berlin, 2007.

[7] K. Buchgraber, G. Gindl, Zeitgemässe Grünlandbewirtschaftung, Leopold Stocker Verlag, 2 edn., 2004.

[8] J. Kort, M. Collins, D. Ditsch, A review of soil erosion potential associated with biomass crops, Biomass Bioenergy 14 (1998) 351–359.

[9] D. Christian, A. Riche, Nitrate leaching losses under miscanthus grass planted on a silty clay loam soil, Soil Use and Management 14 (1998) 131–135.

[10] F. Thériault, H. Javorská, K. Cásová, M. Tucker, T. GulholmHansen, The potential for perennial grasses as energy crops in organic agriculture, Tech. Rep., The Royal Veterinary and Agricultural University Denmark Department of Agricultural Sciences, 2003.

[11] J.-F. Soussana, P. Loiseau, N. Vuichard, E. Ceschia, J. Balesdent, T. Chevallier, D. Arrouays, Carbon cycling and sequestration opportunities in temperate grasslands, Soil Use and Management 20 (2004) 219–230.

[12] D. Tilman, J. Hill, C. Lehman, Carbon-negative biofuels from low-input high-diversity grassland biomass, Science 314 (2006) 1598–1600.

[13] S. Steinbeiss, H. Beßler, C. Engels, V. M. Temperton, N. Buchmann, C. Roscher, Y. Kreutziger, J. Baade, M. Habekost, G. Gleixner, Plant diversity positively affects short-term soil carbon storage in experimental grasslands, Global Change Biology 14 (2008) 2937–2949.

[14] C. Keller, C. Ludwig, F. Davoli, J. Wochele, Thermal treatment of metal-enriched biomass produced from heavy metal phytoextraction, Environ. Sci. Technol 39 (2005) 3359–3367.

[15] A. Prochnow, M. Heiermann, M. Plöchl, B. Linke, C. Idler, T. Amon, P. Hobbs, Bioenergy from permanent grassland - a review: 1. biogas, Bioresour. Technol. 100 (2009) 4931–4944.

[16] J. Judex, S. Biollaz, U. Baier, S. Baum, Biogas-Aufbereitung: Methanverlust von 1 % technisch möglich, GWA 10 (2009) 803–809.

[17] U. R. Fritsche, G. Dehoust, W. Jenseit, K. Hünecke, L. Rausch, D. Schüler, K. Wiegmann, Stoffstromanalyse zur nachhaltigen energetsichen Nutzung von Biomasse, Tech. Rep., ÖkoInstitut, 2004.

[18] A. Prochnow, M. Heiermann, M. Plöchl, T. Amon, P. Hobbs, Bioenergy from permanent grassland - a review: 2. combustion, Bioresour. Technol. 100 (2009) 4945–4954.

[19] B. Sander, Properties of Danish biofuels and the requirements for power production, Biomass Bioenergy 12 (1997) 177–183.

[20] H. Hartmann, T. Böhm, L. Maier, Naturbelassene biogene Festbrennstoffe umweltrelevante Eigenschaften und Einflussmöglichkeiten, Tech. Rep., Bayrisches Staatsministerium für Landesentwicklung und Umweltfragen, 2000.

[21] T. Launhardt, Umweltrelevante Einflüsse bei der thermischen Nutzung fester Biomasse in Kleinanlagen (Schadstoffemissionen, Aschequalität und Wirkungsgrad), Ph.D. thesis, Department für Biogene Rohstoffe und Technologie der Landnutzung, 2002.

[22] P. McKendry, Energy production from biomass (part 1): overview of biomass, Bioresour. Technol. 83 (2002) 37–46.

[23] I. Obernberger, G. Thek, Physical characterisation and chemical composition of densified biomass fuels with regard to their combustion behaviour, Biomass Bioenergy 27 (2004) 653–669.

[24] T. von Puttkamer, Charakterisierung biogener Festbrennstoffe, Ph.D. thesis, Universität Stuttgart, 2005.

[25] B. Strömberg, Fuel Handbook, VÄRMEFORSK Service AB, 2006.

[26] I. Obernberger, T. Brunner, G. Barnthaler, Chemical properties of solid biofuels–significance and impact, Biomass Bioenergy 30 (2006) 973–982.

[27] A. Boateng, G. Banowetz, J. Steiner, T. Barton, D. Taylor, K. Hicks, H. ElNashaar, V. Sethi, Gasification of Kentucky bluegrass (Poa pratensis l.) straw in a farmscale reactor, Biomass Bioenergy 31 (2007) 153–161.

[28] L. Cuipinga, W. Chuangzhi, Yanyongjie, H. Haitao, Chemical elemental characteristics of biomass fuels in China, Biomass Bioenergy 27 (2004) 119–130.

[29] W. de Jong, A. Pironea, M. Wojtowicz, Pyrolysis of miscanthus giganteus and wood pellets: TG-FTIR analysis and reaction kinetics, Fuel 82 (2003) 1139–1147.

[30] S. E. Florine, K. J. Moore, S. L. Fales, T. A. White, C. L. Burras, Yield and composition of herbaceous biomass harvested from naturalized grassland in southern Iowa, Biomass Bioenergy 30 (2006) 522–528.

[31] A. Faaij, R. van Ree, L. Waldheim, E. Olsson, A. Oudhuis, A. van Wijk, C. DaeyOuwens, W. Turkenburg, Gasification of biomass wastes and residues for electricity production, Biomass Bioenergy 12 (1997) 387–407.

[32] N. A. H. Holt, S. B. Alpert, Integrated gasification combinedcycle power plants, Elsevier Science Ltd., 3 edn., 897–923, 2004.

[33] R. Lundqvist, The IGCC demonstration plant at Värnamo, Bioresour. Technol. 46 (1993) 49–53.

[34] R. D. Brdar, R. M. Jones, GE IGCC technology and experience with advanced gas turbines, Tech. Rep., GE Power Systems, 2000.

[35] K. Brun, R. M. Jones, Economic viability and experience of IGCC from a gas turbine manufacturers perspective, 2001.

[36] F. Hannemann, B. Koestlin, G. Zimmermann, H. Morehead, F. G. Peña, Pushing Forward IGCC Technology at Siemens, 2003.

[37] H. Morehead, F. Hannemann, B. Koestlin, G. Zimmermann, J. Karg, Improving IGCC flexibility through gas turbine enhancements, 2004.

[38] RWE, Programm Klimaschutz: IGCC-Kraftwerk Mit CO2-Abtrennung und -Speicherung, 2008.

[39] H. Morehead, Siemens gasification and IGCC update, 2008.

9

[40] W. C. Kok, R. W. Smit, Startnotiz Umweltverträglichkeitsbericht Multi-Brensstoff-Kraftwerk, Tech. Rep., Nuon, 2005.

[41] K. Stahl, Värnamo: demonstration plant, 2001.

[42] S. Daniele, P. Jansohn, K. Boulouchos, Experimental investigation of lean premixed syngas combustion at gas turbine relevant conditions: lean blow out limits, emissions and turbulent flame speed, 2009.

[43] S. Gadde, J. Wu, A. Gulati, G. McQuiggan, B. Koestlin, B. Prade, Syngas capable combustion systems development for advanced gas turbines, in: Power for Land, Sea and Air, 2006.

[44] Alstom, Method and device for the combustion of hydrogen in a premix burner, 2009.

[45] J. Judex, S. Daniele, S. Biollaz, P. Jansohn, Investigations about cofiring of herbaceous biomass in an integrated gasification combined cycle, 2009.

[46] A. Foster, H. von Doering, M. Hilt, Fuels flexibility in heavy-duty gas turbines, Tech. Rep., GE Company, 1983.

[47] A. Beenackers, K. Maniatis, Gasification technologies for heat and power from biomass, in: EuroSun'96, 1311, 1996.

[48] F. Engstrom, Hot gas cleanup bioflow ceramic filter experience, Biomass Bioenergy 15 (1998) 259–262.

[49] I. G. Wright, C. Leyens, B. A. Pint, An analysis of the potential for deposition, erosion, or corrosion in gas turbines fueled by the products of biomass gasification or combustion, Tech. Rep., Oak Ridge National Laboratory, 2000.

[50] H. Spliethoff, Status of biomass gasification for power production, IFRF Combustion Journal .

[51] S. Skoblja, J. Malecha, B. Koutsky, P. Buryan, Hot gas cleaning for biomass gasification for clean gas production, 2005.

[52] GE, Specifications for fuel gases for combustion in heavy-duty gas turbines, Tech. Rep., GE Power Systems, 2005.

[53] G. A. Energy, LM2500 Gas Turbine, 2003.

[54] P. Roberge, Handbook of Corrosion Engineering, McGrawHill, 2000.

[55] C. Leyens, I. G. Wright, B. A. Pint, Hot corrosion of nickel-base alloys in biomass derived fuel simulated atmosphere, in: J. M. H. und N. B. Dahotre (Ed.), Elevated Temperature Coating: Science and Technology III, Warrendale, TMS, 79–90, 1999.

[56] S. M. DeCorso, R. A. Newby, D. Anson, R. A. Wenglarz, I. G. Wright, Coal/biomass fuels and the gas turbine: utilization of solid fuels and their derivatives, in: Intl. Gas Turbine and Aero-engine Congress & Exhibition, 1996.

[57] N. S. Bornstein, M. A. DeCrescente, H. A. Roth, The relationship between V_2O_5, Na_2SO_4 and sulphidation attack, in: Deposition and Corrosion in Gas Turbines, 1973.

[58] J. P. Gutierrez, T. B. Sullivan, G. J. Feller, Turning NGCC into IGCC: cycle retrofitting issues, in: Proceedings of PWR2006, 2006.

[59] GTW, Gas Turbine World 2008 Performance Specs, Pequot Publishing Inc., 25 edn., 2008.

[60] J. v. Belle, A model to estimate fossil CO2 emissions during the harvesting of forest residues for energywith an application on the case of chipping, Biomass Bioenergy 30 (2006) 1067–1075.

[61] N. E. Bassam, Energy plant species, James & James Ltd., 1998.

[62] W. Dietl, J. Lehmann, Ökologischer Wiesenbau, Österreichischer Agrarverlag, 2004.

[63] ECN, Phyllis the composition of biomass and waste, 2006.

[64] B. Oettli, M. Blum, M. Peter, O. S. D. Bedniaguine, A. Dauriat, E. Gnansounou, J. Chételat, F. G. J.-L. Hersener, U. Meier, K. Schleiss, Potentiale zur energetischen Nutzung von Biomasse in der Schweiz, Tech. Rep., Swiss Federal Office of Energy (BfE), 2004.

[65] K. Raab, C. Rösch, V. Stelzer, Perspektiven einer Nachhaltigen Grünlandnutzung zur Energieerzeugung, 2005.

[66] M. Bötsch, Agrarbericht 2005, Tech. Rep., Bundesamt für Landwirtschaft BWL, 2005.

[67] M. Bötsch, Agrarbericht 2006, Tech. Rep., Bundesamt für Landwirtschaft BWL, 2006.

[68] C. Rösch, K. Raab, Ökonomische Betrachtung der energetischen Nutzung von Grünschnitt, 2006.

[69] L. Eltrop, K. Raab, S. Deimling, M. Kaltschmitt, B. Schneider, C. Rösch, B. Jahraus, P. Heinrich, H. Hartmann, I. Lewandowski, V. Siegle, H. Spliethoff, I. Obernberger, Leitfaden Bioenergie: Planung, Betrieb Und Wirtschaftlichkeit Von Bioenergieanlagen, Fachagentur Nachwachsende Rohstoffe e. V., 2005.

[70] A. A. Rentizelas, A. J. Tolis, I. P. Tatsiopoulos, Logistics issues of biomass: the storage problem and the multi-biomass supply chain, Renew. Sust. Energy Rev. 13 (2009) 887–894.

9

[71] J. W. Worley, J. S. Cundiff, Comparison of harvesting and transport issues when biomass crops are handled as hay vs silage, Bioresour. Technol. 56 (1996) 69–75.

[72] J. S. Cundiff, N. Dias, H. D. Sherali, A linear programming approach for designing a herbaceous biomass delivery system, Bioresour. Technol. 59 (1997) 47–55.

[73] J. S. Cundiff, L. S. Marsh, Harvest and storage costs for bales of switchgrass in the south-eastern United States, Bioresour. Technol. 56 (1996) 95–101.

[74] H. Hochberg, Eignung unterschiedlicher Grünlandtypen für eine energetische Nutzung, 2006.

[75] G. Voigtländer, P. Boeker, Grünlandwirtschaft und Futterbau, Stuttgart : Verlag Eugen Ulmer, 1987.

[76] H. Ellenberg, Vegetation Mitteleuropas mit den Alpen, UTB Ulmer, 1996.

[77] W. O. von Boberfeld, Grünlandlehre, Eugen Ulmer Stuttgart, 1994.

[78] M. Benke, Ackerfuttergräser als Biogassubstrat, 2007.

[79] E. Ganko, L. Jaworski, F. M. D. Thrän, Renewable fuels for advanced powertrains – Review on existing studies and definitions of biomass provision chains, Tech. Rep., EC BREC and Institute for Energy and Environment, 2006.

[80] J.-L. Hersener, S. Biollaz, J. Judex, R. Meyer, Verfügbarkeit von Gras für Kombi-Kraftwerke in der Schweiz, Final Report prepared for the Swiss Federal Office of Energy (BfE), Ingenieurbüro HERSENER and Paul Scherrer Institut and Ernst Basler und Partner AG, to be published.

[81] R. Overend, Biomass for Energy, Energy Studies Review: 1 (1989) 16–27.

[82] S. Wolff, Anleger setzen auf Körnerrallye, VDI nachrichten (2008) 33.

[83] T. Searchinger, R. Heimlich, R. A. Houghton, F. Dong, A. Elobeid, J. Fabiosa, S. Tokgoz, D. Hayes, T. Yu, Use of U.S. croplands for biofuels increases greenhouse gases through emissions from land use change, Science 319 (2008) 1238 –1240.

[84] P. J. Crutzen, A. R. Mosier, K. A. Smith, W. Winiwarter, N2O release from agrobiofuel production negates global warming reduction by replacing fossil fuels, Atmos. Chem. Phys. 8 (2008) 389–395.

[85] J. Fargione, J. Hill, D. Tilman, S. Polasky, P. Hawthorne, Land Clearing and the Biofuel Carbon Debt, Science 2 (2008) 1.

[86] K. Stroh, Treibhausgase, Tech. Rep., LfU Bayern, 2004.

[87] C. Higman, M. van der Burgt, Gasification, Elsevier Amsterdam, 1 edn., 2008.

[88] P. Ghetti, L. Ricca, L. Angelini, Thermal analysis of biomass and corresponding pyrolysis products, Fuel 75 (1996) 565–573.

[89] P. T. Williams, S. Besler, The influence of temperature and heating rate on the slow pyrolysis of biomass, Renewable Energy 7 (1996) 233–250.

[90] K. Raveendran, A. Ganesh, K. C. Khilar, Influence of mineral matter on biomass pyrolysis characteristics, Fuel 74 (1995) 1812–1822.

[91] J. A. Moulijn, F. Kapteijn, Towards a unified theory of reactions of carbon with oxygen-containing molecules, Carbon 33 (1995) 1155–1165.

[92] W. F. DeGroot, G. Richards, Influence of pyrolysis conditions and ion-exchanged catalysts on the gasification of cottonwood chars by carbon dioxide, Fuel 67 (1988) 352 – 360.

[93] C. von Scala, The influence of contaminants on the gasification of waste wood, Ph.D. thesis, ETH-Zürich., 1998.

[94] A. Gani, I. Naruse, Effect of cellulose and lignin content on pyrolysis and combustion characteristics for several types of biomass, Renewable Energy 32 (2007) 649–661.

[95] R. Fahmi, A. Bridgwater, I. Donnison, N. Yates, J. Jones, The effect of lignin and inorganic species in biomass on pyrolysis oil yields, quality and stability, Fuel 87 (2008) 1230–1240.

[96] E. Luger, Rohstoffbereitstellung pflanzlicher Biomasse, 2005.

[97] F. Rabier, M. Temmerman, T. Bohm, H. Hartmann, P. Daugbjerg Jensen, J. Rathbauer, J. Carrasco, M. Fernandez, Particle density determination of pellets and briquettes, Biomass Bioenergy 30 (2006) 954–963.

[98] Topell, Torrepellets, 2008.

[99] K. Reisinger, H. Sporrer, D. H. Hartmann, Die Energiedichte biogener Energieträger im Vergleich zu Heizöl und Steinkohle, 2006.

[100] A. Oasmaa, E. Leppämäki, P. Koponen, J. Levander, E. Tapola, Physical characterisation of biomass based pyrolysis liquids application of standard fuel oil analyses physical characterisation, Tech. Rep., VTT, Espoo Finland, 1997.

[101] P. Lehtikangas, Storage effects on pelletised sawdust, logging residues and bark, Biomass Bioenergy 19 (2000) 287–293.

9

[102] A. Hopkins, Grass its production and utilization, Blackwell Science, 2000.

[103] J. P. Diebold, A review of the chemical and physical mechanisms of the storage stability of fast pyrolysis biooils, Tech. Rep., NREL, 2000.

[104] J. Blin, G. Volle, P. Girard, T. Bridgwater, D. Meier, Biodegradability of biomass pyrolysis oils: comparison to conventional petroleum fuels and alternatives fuels in current use, Fuel 86 (2007) 2679–2686.

[105] G. Bisio, A. Bisio, Thermodynamic anaylsis of photosynthesis, in: 29th Intersocietey Energy Conversion Engeneering Conference, 1994.

[106] K. Tennakone, S. Wickramanayake, S. Punchihewa, K. Weerasena, A theoretical and experimental study of the energy harvest efficiency of an energy crop, Solar Energy 39 (1987) 291–295.

[107] S. A. Channiwala, P. P. Parikh, A unified correlation for estimating HHV of solid, liquid and gaseous fuels, Fuel 81 (2002) 1051–1063.

[108] D. I. for Physical Properties, DIPPR Project 801, 2005.

[109] R. H. Williams, E. D. Larson, Aeroderivative turbines for stationary power, Ann. Rev. Energy 13 (1988) 429–489.

[110] B. Adouane, P. Hoppesteyn, W. de Jong, M. van der Wel, K. R. G. Hein, H. Spliethoff, Gas turbine combustor for biomass derived LCV gas, a first approach towards fuel–NOx modelling and experimental validation, Appl. Therm. Eng. 22 (2002) 959–970.

[111] D. W. van Krevelen, J. Schuyer, Coal science, Elsevier publishing company, 1957.

[112] U. Kutschera, Prinzipien der Pflanzenphysiologie, Spektrum, Akademischer Verlag, 2002.

[113] DIN, DIN–51720 Bestimmung des Gehaltes an flüchtigen Bestandteilen, 1988.

[114] Tampella, Westinghouse, GTI, Sustainable biomass energy production: Alfagas fesability study conversion technology, Tech. Rep., Tampella Power Corporation; Westinghouse Electric Corporation and Institute of Gas Technology, 1995.

[115] Gaderer, Aschen aus Biomassefeuerungen, 2003.

[116] S. Bajohr, C. Higman, R. Reimert, The distribution of heavy metals during biomass gasification, in: 6th European Gasification Conference, 2004.

[117] M. Schingnitz, F. Melhose, Mega–GSP process, 2005.

[118] DIN, DIN–51730 Bestimmung des Asche Schmelzverhaltens, 1998.

[119] M. Öhman, L. Pommer, A. Nordin, Bed agglomeration characteristics and mechanisms during gasification and combustion of biomass fuels, Energy Fuels 19 (2005) 1742–1748.

[120] D. R. Lide (Ed.), Physical constants of inorganic compounds, CRC Press, 56 edn., 4.43–4.101, 2008.

[121] A. Moilanen, Thermogravimetric characterisations of biomass and waste for gasification processes, VTT Finland, 2006.

[122] I. Mills, T. Cvita, K. Homann, N. K. K. Kuchitsu, Quantities, units and symbols in physical chemistry, International Union Of Pure And Applied Chemistry, 1993.

[123] G. Baernthaler, M. Zischka, C. Haraldsson, I. Obernberger, Determination of major and minor ashforming elements in solid biofuels, Biomass Bioenergy 30 (2006) 983–997.

[124] A. B. Hart, A. J. B. Cutler (Eds.), Deposition and Corrosion in Gas Turbines, Applied Science Publishers LTD, London, 1973.

[125] V. Thien, F. Schmitz, W. Slotty, W. Voss, Metallkundlich-mikroanalytische Untersuchungen der Wirkung von Schutzschichten gegen Hochtemperaturkorrosion von Gasturbinenschaufelwerkstoffen, Fresenius J. Anal. Chem. 319 (1984) 646–654.

[126] NACE, Corrosion Survey Database, The Corrosion Society, 2002.

[127] P. Basu, Combustion and Gasification in Fluidized Beds, Taylor & Francis Group, LLC, 2006.

[128] P. A. Schweitzer, Fundamentals of metallic corrosion, Taylor & Francis, 2007.

[129] C. J. Zygarlicke, D. P. McCollor, K. E. Eylands, M. D. Hetland, M. A. Musich, C. R. Crocker, J. Dahl, S. Laducer, Task 3.4 impacts of cofiring biomass with fossil fuels, Tech. Rep., Energy & Environmental Research Center University of North Dakota, 2001.

[130] J. Houghton, Y. Ding, D. Griggs, M. Noguer, P. van der Linden, X. Dai, K. Maskell, C. Johnson, Climate change 2001: the scientific basis, Cambridge-university Press, 2001.

[131] G. Y. Lai, High temperature corrosion of engineering alloys, ASM International, 1990.

[132] P. von Sengbusch, Botanik online The Internet Hypertextbook, 2003.

9

[133] W. de Jong, Ömer Ünal, K. R. G. Hein, H. Spliethoff, Pressurised flui-
dised bed gasification experiments of biomass and fossil fuels, Thermal
Science 5 (2001) 69–81.

[134] W. de Jong, Nitrogen compounds in pressurised fluidised bed gasifica-
tion of biomass and fossil fuels, Ph.D. thesis, Technische Universiteit
Delft, 2005.

[135] Uniterra, Rutherford Lexikon der Elemente, 2006.

[136] E. J. Erekson, C. H. Bartholomew, Sulfur poisoning of nickel methana-
tion catalysts : II. Effects of H2S concentration, CO and H2O partial
pressures and temperature on reactivation rates, Appl. Cat. 5 (1983)
323–336.

[137] BASF, Hydrodesulfurization catalyst Sulfur conversion for feedstock
purification 2 (2007) 1–2.

[138] E. Schulze, E. Beck, K. Müller-Hohenstein, Plant Ecology, Springer,
2005.

[139] Lenntech, Periodic elements, 2006.

[140] L. Helsen, E. V. den Bulck, J. S. Hery, Low-temperature pyrolysis of
CCA-treated wood: thermogravimetric analysis, J. Anal. Appl. Pyro-
lysis 52 (1999) 65–86.

[141] L. Helsen, E. V. den Bulck, J. S. Hery, Total recycling of CCA treated
wood waste by lowtemperature pyrolysis, Waste Management 18 (1998)
571–578.

[142] D. Thompson, B. B. Argent, Prediction of the distribution of trace
elements between the product streams of the Prenflo gasifier and com-
parison with reported data, Fuel 81 (2002) 555–570.

[143] B. B. Miller, D. R. Dugwell, R. Kandiyoti, Partitioning of trace elements
during the combustion of coal and biomass in a suspensionfiring reactor,
Fuel 81 (2002) 159–171.

[144] M. Díaz-Somoano, M. R. Martínez-Tarazona, Retention of trace ele-
ments using fly ash in a coal gasification flue gas, J. Chem. Technol.
Biotechnol. 77 (2002) 396–402.

[145] S. N. Kartal, W. Hwang, Y. Imamura, Evaluation of effect of leaching
medium on the release of copper, chromium, and arsenic from treated
wood, Building and Environment 42 (2007) 1188–1193.

[146] M. Lopez-Anton, M. Diaz-Somoano, J. Fierro, M. Martinez-Tarazona,
Retention of arsenic and selenium compounds present in coal combus-
tion and gasification flue gases using activated carbons, Fuel Process.
Technol. 88 (2007) 799–805.

[147] N. D. Kuznetsov, S. I. Veselov, N. D. Stepanenko, Use of composites in the construction of gas turbine engines, Strength Mater. 6 (1974) 211–217.

[148] A. Iwashita, Y. Sakaguchi, T. Nakajima, H. Takanashi, A. Ohki, S. Kambara, Leaching characteristics of boron and selenium for various coal fly ashes, Fuel 84 (2005) 479–485.

[149] S. Schorn, E. Hock, C. Linde, V. Annacker, P. Seroka, Mineralienatlas, 2007.

[150] M. Kannan, G. Richards, Gasification of biomass chars in carbon dioxide: dependence of gasification rate on the indigenous metal content, Fuel 69 (1990) 747–753.

[151] R. Pappas, G. Polzin, L. Zhang, C. Watson, D. Paschal, D. Ashley, Cadmium, lead, and thallium in mainstream tobacco smoke particulate, Food Chem. Toxicol. 44 (2006) 714–723.

[152] K. Fridley, B. D. Berven, N. Thiex, Fertilizer program, Tech. Rep., The South Dakota Department of Agriculture, 2001.

[153] M. Narodoslawsky, I. Obernberger, From waste to raw materialthe route from biomass to wood ash for cadmium and other heavy metals, J. Hazard. Mater. 50 (1996) 157–168.

[154] H. Küpper, A. Parameswaran, B. Leitenmaier, M. Trtílek, I. Setlik, Cadmium-induced inhibition of photosynthesis and long-term acclimation to cadmium stress in the hyperaccumulator thlaspi caerulescens, New Phytologist 175 (2007) 655–674.

[155] K. Jamil, Aquatic plants for removal of metal contamination, 1999.

[156] L. Hellstrom, B. Persson, L. Brudin, K. P. Grawe, I. Oborn, L. Jarup, Cadmium exposure pathways in a population living near a battery plant, Sci. Total Environ. 373 (2007) 447–455.

[157] M. Diaz-Somoano, M. R. Martinez-Tarazona, Hightemperature removal of cadmium from a gasification flue gas using solid sorbents, Fuel 84 (2005) 717–721.

[158] E. Björkman, B. Strömberg, Release of chlorine from biomass at pyrolysis and gasification conditions, Energy Fuels 11 (1997) 1026–1032.

[159] H. Boettger, F. Umland, Untersuchungen zur Hochtemperaturkorrosion durch Chloride, Werkst. Korros. 24 (1974) 805–816.

[160] H. J. Grabke, E. Reese, M. Spiegel, The effects of chlorides, hydrogen chloride, and sulfur dioxide in the oxidation of steels below deposits, Corros. Sci. 37 (1995) 1023–1043.

9

[161] G. McKay, Dioxin characterisation, formation and minimisation during municipal solid waste (MSW) incineration: review, Chem. Eng. J. 86 (2002) 343–368.

[162] J. Burvall, Influence of harvest time and soil type on fuel quality in reed canary grass (Phalaris arundinacea L.), Biomass Bioenergy 12 (1997) 149–154.

[163] R. Fahmi, A. Bridgwater, L. Darvell, J. Jones, N. Yates, S. Thain, I. Donnison, The effect of alkali metals on combustion and pyrolysis of Lolium and Festuca grasses, switchgrass and willow, Fuel 86 (2007) 1560–1569.

[164] F. Frandsen, K. DamJohansen, P. Rasmussen, Trace elements from combustion and gasification of coal an equilibrium approach, Prog. Energy Combust. Sci. 20 (1994) 115–138.

[165] I. Alstrup, M. T. Tavares, C. A. Bernardo, O. Sörensen, J. R. Rostrup-Nielsen, Carbon formation on nickel and nickel-copper alloy catalysts, Mater. Corros. 49 (1998) 367–372.

[166] W. Li, H. Lu, H. Chen, B. Li, Volatilization behavior of fluorine in coal during fluidizedbed pyrolysis and CO2–gasification, Fuel 84 (2005) 353–357.

[167] M. Takeda, A. Ueda, H. Hashimoto, T. Yamada, N. Suzuki, M. Sato, N. Tsubouchi, Y. Nakazato, Y. Ohtsuka, Fate of the chlorine and fluorine in a sub-bituminous coal during pyrolysis and gasification, Fuel 85 (2006) 235–242.

[168] M. Grigore, R. Sakurovs, D. French, V. Sahajwalla, Coke gasification: the influence and behavior of inherent catalytic mineral matter, Energy Fuels 23 (2009) 2075–2085.

[169] S. Q. Turn, C. M. Kinoshita, D. M. Ishimura, J. Zhou, The fate of inorganic constituents of biomass in fluidized bed gasification, Fuel 77 (1998) 135–146.

[170] L. S. Morf, P. H. Brunner, MVA als Schadstoffsenke: Stoffflussanalyse für Quecksilber im MHKW Würzburg, Tech. Rep., GEO Partner AG Umweltmanagement and Technische Universität Wien, 2005.

[171] M. G. Klett, R. C. Maxwell, M. D. Rutowski, The cost of Mercury removal in an IGCC plant, Tech. Rep., Parsons, 2002.

[172] H. El-Nashaar, S. Griffith, J. Steiner, G. Banowetz, Mineral concentration in selected native temperate grasses with potential use as biofuel feedstock, Bioresour. Technol. 100 (2009) 3526–3531.

[173] M. Anke, M. Seifert, A. Regius-Möcseyi, E. Lösch, The importance of potassium in the food chain of plants, animal and man: part one: the potassium concentration of the plants as a function of the geological origin, and of age, part and species, 2006.

[174] D. Thompson, B. Argent, The mobilisation of sodium and potassium during coal combustion and gasification, Fuel 78 (1999) 1679–1689.

[175] W. Mojtahedi, E. Kurkela, M. Nieminen, Release of sodium and potassium in the P.F.B. gasification of peat, Journal of the Institute of Energy 63 (1990) 95–100.

[176] X. Wei, U. Schnell, K. R. Hein, Behaviour of gaseous chlorine and alkali metals during biomass thermal utilisation, Fuel 84 (2005) 841–848.

[177] E. Kurkela, M. Kurkela, A. Moilanen, Science in Thermal and Chemical Biomass Conversion, vol. 1, CPL Press. Newbury, 662–676, 2006.

[178] C. Leyens, B. Pint, P. Tortorelli, I. Wright, Significance of experimental procedures on the hot corrosion behavior of nickel-base alloys under cyclic conditions, 1999.

[179] S. Turn, C. Kinoshita, D. Ishirnura, J. Zhou, Gasification characteristics of high alkali biomass subjected to mechanical dewatering and leaching processes, Tech. Rep., Hawaii Natural Energy institute School of Ocean and Earth Science and Technology University of Hawaii at Manoa, 1997.

[180] S. Pintsch, H. W. Gudenau, Alkalienheissgasreinigung beim GUD-Prozess. III, Praktische Versuche, VGB Kraftwerkstechnik 71 (1991) 469–474.

[181] S. Pintsch, H. W. Gudenau, Alkalienheissgasreinigung beim GUD-Prozess. I, Kenntnissatnd der Literatur, VGB Kraftwerkstechnik 71 (1991) 42–47.

[182] S. Pintsch, H. W. Gudenau, Alkalienheissgasreinigung beim GUD-Prozess. II, Thermodynaische Berechnungen, VGB Kraftwerkstechnik 71 (1991) 469–474.

[183] A. L. Hallgren, Hot gas particulate and alkali removal in PCFB gasification of biomass, in: 29th Intersocietey Energy Conversion Engeneering Conference, 1994.

[184] T. Novakov, C. E. Corrigan, Thermal characterization of biomass smoke particles, Microchim. Acta 119 (1995) 157–166.

[185] R. Zevenhoven, P. Kilpinen, Control of pollutants in flue gases and fuel gases, The Nordic Energy Research Programme Solid Fuel Committee, 2004.

9

[186] M. Johansson, Catalytic combustion of gasified biomass for gas turbine applications, Ph.D. thesis, Royal Institute of Technology Department of Chemical Engineering and Technology Chemical Technology, 1998.

[187] R. Bunshah, Handbook of Hard Coatings, William Andrew Publishing/Noyes, 2001.

[188] J. Konttinen, R. Backman, M. Hupa, A. Moilanen, E. Kurkela, Trace element behavior in the fluidized bed gasification of solid recovered fuels a thermodynamic study, Tech. Rep., VTT, 2005.

[189] L. Zhang, M. Masui, H. Mizukoshi, Y. Ninomiya, C. Kanaoka, Formation of submicron particulates (PM1) from the oxygen-enriched combustion of dried sewage sludge and their properties, Energy Fuels 21 (2006) 88–98.

[190] R. W. Joyner, P. Meehan, J. M. MacLaren, J. B. Pendry, Poisoning of the methanation reaction on the Ni(100) surface; theoretical calculations compared with the results of Goodman et al, Appl. Cat. 25 (1986) 9–17.

[191] C. Erber, P. F. Henningsen, Heavy metal contents and mobility of artificially inundated grasslands along River Weser, Germany, Water Sci. Technol. 44 (2001) 507–514.

[192] G. P. Reed, D. R. Dugwell, R. Kandiyoti, Control of trace elements in a gasifier hot gas filter: a comparison with predictions from a thermodynamic equilibrium model, Energy Fuels 15 (2001) 1480–1487.

[193] R. Samson, B. Mehdi, Strategies to reduce the ash. content in perennial-grasses, 1998.

[194] K. L. Luthra, H. S. Spacil, Impurity deposits in gas turbines from fuels containing sodium and vanadium, J. Electrochem. Soc. 129 (1982) 649–656.

[195] R. A. Newby, E. E. Smeltzer, T. E. Lippert, R. B. Slimane, O. M. Akpolat, K. Pandya, F. S. Lau, J. Abbasian, B. E. Williams, D. Leppin, Novel gas cleaning/ conditioning for integrated gasification combined cycle base program final report, Tech. Rep., Siemens Westinghouse Power Corporation and Gas Technology Institute, 2001.

[196] N.-K. Park, D.-H. Lee, J. H. Jun, J. D. Lee, S. O. Ryu, T. J. Lee, J.-C. Kim, C. H. Chang, Two-stage desulfurization process for hot gas ultra cleanup in IGCC, Fuel 85 (2006) 227–234.

[197] H. W. Elbersen, E. R. P. Keijsersa, J. van Doornb, Biorefinery of verge grass to produce biofuel, Tech. Rep., Agrotechnological Research Institute, 2001.

[198] S. Q. Turn, C. M. Kinoshita, D. M. Ishimura, Removal of inorganic constituents of biomass feedstocks by mechanical dewatering and leaching, Biomass Bioenergy 12 (1997) 241–252.

[199] S. Turn, C. Kinoshita, D. Ishimura, Removal of alkali from banagrass using mechanical dewatering and leaching processes, Tech. Rep., Ocean and Earth Science and Technology University of Hawaii at Manoa, 1997.

[200] S. Q. Turn, C. M. Kinoshita, L. A. Jakeway, B. M. Jenkins, L. L. Baxter, B. C. Wu, L. G. Blevins, Fuel characteristics of processed, highfiber sugarcane, Fuel Process. Technol. 81 (2003) 35–55.

[201] T. Radiotis, J. Li, K. Goel, R. Eisner, Fiber characteristics, pulpability, and bleachability of switchgrass, Tappi J. 82 (1999) 100–105.

[202] P. C. Bergman, J. H. Kiel, Torrefaction for biomass upgrading torrefaction for biomass cofiring in existing coalfired power stations, Tech. Rep., ECN, 2005.

[203] T. Bridgeman, L. Darvell, J. Jones, P. Williams, R. Fahmi, A. Bridgwater, T. Barraclough, I. Shield, N. Yates, S. Thain, I. Donnison, Influence of particle size on the analytical and chemical properties of two energy crops, Fuel 86 (2007) 60–72.

[204] P. Bergman, A. Boersma, J. Kiel, M. Prins, K. Ptasinski, F. Janssen, Torrefaction for entrained–flow gasification of biomass, Tech. Rep., ECN, 2005.

[205] J.-L. Hersener, U. Baserga, Energetische Nutzung Landwirtschaftlicher Biomasse Band 1 (Wärme und Strom aus Energiegras unf Feldholz), Tech. Rep., Ingenierubüro HERSENER, 1998.

[206] T. R. Miles, L. Baxter, R. W. Bryers, B. M. Jenkins, L. L. Oden, Alkali deposit found in biomass power plants, Tech. Rep., NREL National Renewable Energy Laboratory, 1995.

[207] O. Moersch, H. Spliethoff, K. R. G. Hein, Tar quantification with a new online analyzing method, Biomass Bioenergy 18 (2000) 79–86.

[208] S. van Paasen, J. Kiel, J. Neeft, H. Knoef, G. Buffinga, U. Zielke, K. Sjostrom, C. Brage, P. Hasler, P. Simell, M. Suomalainen, M. Dorrington, L. Thomas, Guideline for sampling and analysis of tar and particles in biomass producer gases, Protocol, ECN, 2002.

[209] S. van Paasen, J. Kiel, Tar formation in a fluidisedbed gasifier, Tech. Rep., ECN, 2004.

[210] D. Carpenter, S. Deutch, R. French, Quantitative Measurement of Biomass Gasifier Tars Using a Molecular Beam Mass Spectrometer: Comparison with Traditional Impinger Sampling, Energy Fuels 21 (2007) 3036–3043.

9

[211] Y. Neubauer, Online-Analyse von Teer aus der Biomassevergasung mit Lasermassenspektrometrie, Ph.D. thesis, Prozesswissenschaften der Technischen Universität Berlin, 2008.

[212] W. C. Hinds, Aerosol Technology, John Wiley & Sons, 2 edn., 1999.

[213] P. G. Griffin, R. J. S. Morrison, A. Campisi, B. L. Chadwick, Apparatus for the detection and removal of vapor phase alkali species from coalderived gases at high temperature and pressure, Rev. Sci. Instrum. 69 (1998) 3674–3677.

[214] P. Monkhouse, Online diagnostic methods for metal species in industrial process gas, Prog. Energy Combust. Sci. 28 (2002) 331–381.

[215] VDI, VDI 2268 Stoffbestimmung an Partikeln: Bestimmung der Elemente Ba, Be, Cd, Co, Cr, Cu, Ni, Pb, Sr, V, Zn, 1987.

[216] P. Stahlberg, M. Lappi, E. Kurkela, P. Simell, P. Oesch, M. Nieminen, Sampling of contaminants from product gases of biomass gasifiers, Technical Research Centre of Finland, 1998.

[217] C. Ludwig, J. Wochele, U. Jorimann, Measuring evaporation rates of metal compounds from solid samples, Anal. Chem. 79 (2007) 2992–2996.

[218] T. Kowalski, Evaluating a surface ionisation detector for measuring alkalis in biomass gasification, Ph.D. thesis, ETH Zürich, 2007.

[219] K. Davidsson, K. Engvall, M. Hagstrom, J. Korsgren, B. Lonn, J. Pettersson, A Surface Ionization Instrument for OnLine Measurements of Alkali Metal Components in Combustion: Instrument Description and Applications, Energy Fuels 16 (2002) 13691377.

[220] M. Svane, M. Hagstrom, K. Davidsson, J. Boman, J. Pettersson, Cesium as a tracer for alkali processes in a circulating fluidized bed reactor, Energy Fuels 20 (2006) 979985.

[221] S. Kinugasa, K. Tanabe, T. Tamura, SDBS spectral database for organic compounds, 2009.

[222] R. Peltier, Alstom's chilled ammonia CO2-capture process advances toward commercialization, 2008.

[223] M. Kaltschmitt, H. Hartmann, Grundlagen, Techniken und Verfahren, Springer, 1 edn., 2001.

[224] J. Zhou, S. M. Masutani, D. M. Ishimura, S. Q. Turn, C. M. Kinoshita, Release of fuel-bound nitrogen during biomass gasification, Ind. Eng. Chem. Res. 39 (2000) 626–634.

[225] R. . C. Wood, Mond gas, R. D. Wood & Co, 1903.

[226] S. S. Wyer, A treatise on producer-gas and gas-producer, McGraw-Hill, 1906.

[227] J. E. Dowson, Producer gas, Longmans, Green, 1907.

[228] A. Horace, Modern Power Gas Producer - Practice and Applications, D. Van Nostrand Company, 1908.

[229] F. Fischer, The conversion of coal into oils, Ernest Benn Limited, 1925.

[230] W. Gumz, Vergasung fester Brennstoffe, Springer, 1 edn., 1952.

[231] A. Schütte, Biomasse–Vergasung Der Königsweg für eine effiziente Strom und Kraftstoff Bereitstellung?, tangram documents, Landwirt-schaftsverlag, 2004.

[232] H. D. Baehr, Thermodynamik, Springer, 3 edn., 2000.

[233] M. Farris, M. A. P. J. Irving, R. P. Overend, The biomass gasifica-tion process by battelle/ferco: design, engineering, construction, and startup, 1998.

[234] T. Sonntag, H. Mühlen, C. Schmid, Energie und Wasserstoff aus Bio-masse Die Gestufte Reformierung, Tech. Rep., Dr. Mühlen GmbH & Co. KG, 2002.

[235] K. Maniatis, Progress in biomass gasification: an overview, Tech. Rep., Directorate General for Energy & Transport , European Comission, 2001.

[236] H. D. Baehr, Thermodynamik Grundlagen und technische Anwendun-gen, Springer, 3 edn., 2006.

[237] H. Kaufmann, Vergasung von Holz und Gras in Festbettvergasern, in: Tagungsband, 1994.

[238] P. D'Jesus, N. Boukis, B. KraushaarCzarnetzki, E. Dinjus, Gasification of corn and clover grass in supercritical water, Fuel 85 (2006) 1032–1038.

[239] W. C. Yang, Handbook of Fluidization and Fluid-Particle Systems, Marcel Dekker, 1 edn., 2003.

[240] VDI, VDI-Wärmeatlas, VDI-Verlag, 6 edn., 2006.

[241] Bibus, Datenblatt: INCONEL® Alloy 600, 2008.

[242] R. H. Perry, D. W. Green, Perry's Chemical Engineers' Handbook, McGrawHill, 7 edn., 1997.

[243] VDI, VDI 2066 Gravimetrische Bestimmung der Staubbeladung, 2006.

[244] WITT, Sicherheitsventile: SV805/808, 2009.

9

[245] TC, Handbuch zur Temperaturmessung mit Thermoelementen und Widerstandsthermometern, 2003.

[246] TecSis, Drucksensoren OEM: mit innenliegender Membran für Überdruck und Absolutdruck, 2009.

[247] Gems, Turbine Flow Rate Sensor FT-110 Series, 2008.

[248] Varian, CP4900 Micro GC Techview, 2006.

[249] DIN, DIN–51719 Bestimmung des Aschegehaltes, 1978.

[250] H.-D. Baehr, K. Stephan, Wärme- und Stoffübertragung, Springer, 5 edn., 2009.

[251] A. Bejan, A. D. Kraus, Heat transfer handbook, John Wiley & Sons, 2003.

[252] M. Toledo, Infrared Dryer LP16, 1999.

[253] Retsch, Hochleistungs-Schneidemühle SM 2000, 2009.

[254] J. G. Yates, Fundamentals of Fluidized-bed Chemical Processes (Monographs in Chemical Engineering), Butterworth-Heinemann Ltd, 1 edn., 1983.

[255] D. Kunii, O. Levenspiel, Fluidization Engineering, Butterworth-Heinemann, 2 edn., 1991.

[256] G. Hu, S. Xu, S. Li, C. Xiao, S. Liu, Steam gasification of apricot stones with olivine and dolomite as downstream catalysts, Fuel Process. Technol. 87 (2006) 375–382.

[257] A. Ergüdenler, A. Ghaly, Agglomeration of silica sand in a fluidized bed gasifier operating on wheat straw, Biomass Bioenergy 4 (1993) 135–147.

[258] M. Öhman, A. Nordin, The role of kaolin in prevention of bed agglomeration during fluidized bed combustion of biomass fuels, Energy Fuels 14 (2000) 618–624.

[259] S. Arvelakis, H. Gehrmann, M. Beckmann, E. G. Koukios, Effect of leaching on the ash behavior of olive residue during fluidized bed gasification, Biomass Bioenergy 22 (2002) 55–69.

[260] W. B. . Badger, F. A. . Hummel, Phase Equilibrium in the System $Li_20 - Na_20 - Al_2 - Si_2O$, J. Am. Ceram. Soc. 68 (1985) C48–C51.

[261] J. Kopyscinski, T. J. Schildhauer, S. M. A. Biollaz, Employing catalyst fluidization to enable carbon management in the SNG–production from biomass, Chem. Eng. Technol. 32 (2009) 343–347.

[262] J. Bilodeau, N. Therien, P. Proulx, S. Czernik, E. Chornet, A mathematical model of fluidized bed biomass gasification, Can. J. Chem. Eng. 1 (1993) 549–557.

[263] L. Waldheim, GREVE Arbre and CHRISGAS, 2006.

[264] Sasol, Datasheet coarse alumina, 2009.

[265] B. M. Steenari, O. Lindqvist, High-temperature reactions of straw ash and the anti-sintering additives kaolin and dolomite, Biomass Bioenergy 14 (1998) 67–76.

[266] A. Ghaly, A. Ergüdenler, A. Al Taweel, Determination of the kinetic parameters of oat straw using thermogravimetric analysis, Biomass Bioenergy 5 (1993) 457–465.

[267] L. Helsen, E. Van den Bulck, Kinetics of the lowtemperature pyrolysis of chromated copper arsenate treated wood, J. Anal. Appl. Pyrolysis 53 (2000) 51–79.

[268] M. Gronli, G. Varhegyi, C. Di Blasi, Thermogravimetric analysis and devolatilization kinetics of wood, Ind. Eng. Chem. Res. 41 (2002) 4201–4208.

[269] P. Haselbacher, F. Lettner, C. Kirilowitsch, G. Em, Investigation of the effective kinetics of gas char reactions in biomass gasification, 2007.

[270] M. Jeguirim, G. Trouvé, Pyrolysis characteristics and kinetics of Arundo donax using thermogravimetric analysis, Bioresour. Technol. 100 (2009) 4026–4031.

[271] D. M. Keown, G. Favas, J. Hayashi, C. Li, Volatilisation of alkali and alkaline earth metallic species during the pyrolysis of biomass: differences between sugar cane bagasse and cane trash, Bioresour. Technol. 96 (2005) 1570–1577.

[272] M. Ishida, C. Wen, Comparison of zone-reaction model and unreacted-core shrinking model in solid–gas reactions–I isothermal analysis, Chem. Eng. Sci. 26 (1971) 1031–1041.

[273] M. Ishida, C. Wen, T. Shirai, Comparison of zone-reaction model and unreacted-core shrinking model in solid–gas reactions–II non-isothermal analysis, Chem. Eng. Sci. 26 (1971) 1043–1048.

[274] D. C. Dayton, T. A. Milne, Mechanisms of alkali metal release during biomass combustion, in: Symposium on biomass fuels, vol. 17, 758–762, 1995.

[275] A. Moilanen, J. Vepsäläinen, E. Kurkela, J. Konttinen, Gasification reactivity of large biomass pieces, in: A. Bridgwater, D. Boocock (Eds.), Science in Thermal and Chemical Biomass Conversion, vol. 2, CPL Press, 2006.

9

[276] D. Porbatzki, Freisetzung anorganischer Spezies bei der thermochemischen Umwandlung biogener Festbrennstoffe, Ph.D. thesis, Fakultät für Maschinenwesen der Rheinisch-Westfälischen Technischen Hochschule Aachen, 2008.

[277] Thermo Onix, VG ProLab, 2001.

[278] U. Jäglid, J. G. Olsson, J. B. C. Pettersson, Detection of sodium and potassium salt particles using surface ionization at atmospheric pressure, J. Aerosol Sci. 27 (1996) 967–977.

[279] G. D. Alton, G. D. Mills, A positive (negative) surface ionization source concept for RIB generation, Tech. Rep., Oak Ridge National Laboratory, 1995.

[280] L. Andersson, J. Olsson, L. Holmlid, Surface ionization at atmospheric pressure: partial melting of alkali salt particles, Langmuir 2 (1986) 594–599.

[281] B. M. Jenkins, R. R. Bakker, J. B. Wei, On the properties of washed straw, Biomass Bioenergy 10 (1996) 177–200.

[282] S. Turn, C. Kinoshita, D. Ishimura, B. M. Jenkins, , S. Turn, C. Kinoshita, D. Ishirnura, J. Zhou, Leaching of alkalis in biomass using banagrass as a prototype herbaceous species, Tech. Rep., Hawaii Natural Energy Institute University of Hawaii and University of California and Sandia National Laboratories, 1997.

[283] D. Dayton, B. Jenkins, S. Turn, R. Bakker, R. Williams, D. BelleOudry, L. Hill, Release of inorganic constituents from leached biomass during thermal conversion, Energy Fuels 13 (1999) 860–870.

[284] P. Gilbert, C. Ryu, V. Sharifi, J. Swithenbank, Effect of process parameters on pelletisation of herbaceous crops, Fuel 88 (2009) 1491–1497.

[285] A. Kosminski, D. Ross, J. Agnew, Reactions between sodium and silica during gasification of a low-rank coal, Fuel Processing Technology 87 (2006) 1037 – 1049.

[286] K. O. Davidsson, J. G. Korsgren, J. B. C. Pettersson, U. Jäglid, The effects of fuel washing techniques on alkali release from biomass, Fuel 81 (2002) 137–142.

[287] Omya, Mineralische Zusatzstoffe für die Kunststoff-Industrie, Tech. Rep., Omya AG, 2001.

[288] M. Uberoi, W. A. Punjak, F. Shadman, The kinetics and mechanism of alkali removal from flue gases by solid sorbents, Prog. Energy Combust. Sci. 16 (1990) 205–211.

[289] S. Q. Turn, C. M. Kinoshita, D. M. Ishimura, T. T. Hiraki, J. Zhou, S. M. Masutani, An experimental investigation of alkali removal from biomass producer gas using a fixed bed of solid sorbent, Ind. Eng. Chem. Res. 40 (2001) 1960–1967.

[290] K. Wolf, M. Muller, K. Hilpert, L. Singheiser, Alkali sorption in second-generation pressurized fluidized bed combustion, Energy Fuels 18 (2004) 1841–1850.

[291] K. Q. Tran, K. Iisa, B. M. Steenari, O. Lindqvist, A kinetic study of gaseous alkali capture by kaolin in the fixed bed reactor equipped with an alkali detector, Fuel 84 (2005) 169175.

[292] A. Kosminski, D. Ross, J. Agnew, Reactions between sodium and kaolin during gasification of a low-rank coal, Fuel Process. Technol. 87 (2006) 1051–1062.

[293] M. F. Llorente, P. D. Arocas, L. G. Nebot, J. C. García, The effect of the addition of chemical materials on the sintering of biomass ash, Fuel 87 (2008) 2651–2658.

[294] M. Bellais, K. O. Davidsson, T. Liliedahl, K. Sjostrom, J. B. C. Pettersson, Pyrolysis of large wood particles: a study of shrinkage importance in simulations, Fuel 82 (2003) 1541–1548.

9

Appendix α

Additional analysis

α .1 Preliminary test with wood

The two diagrams in figure α .1 present an experiment for wood at $800\,°C$ with SiO_2 as bed material. The concentration axis of the permanent gases is logarithmic to give access to the low concentrations of the higher C_XH_Y species. The test was performed in order to evaluate the newly built fluidised bed test rig. The data is in excellent agreement with the expected data for fluidised bed wood gasification [223]. The test was conducted without any problems of the feeding mechanism or fluidisation. The sampling system worked fine as well. The lower heating value was $6.8\,MJ/kg$ for an air to fuel ratio of 0.22. The blank in the permanent gas data occurred due to general problems with the sampling system.
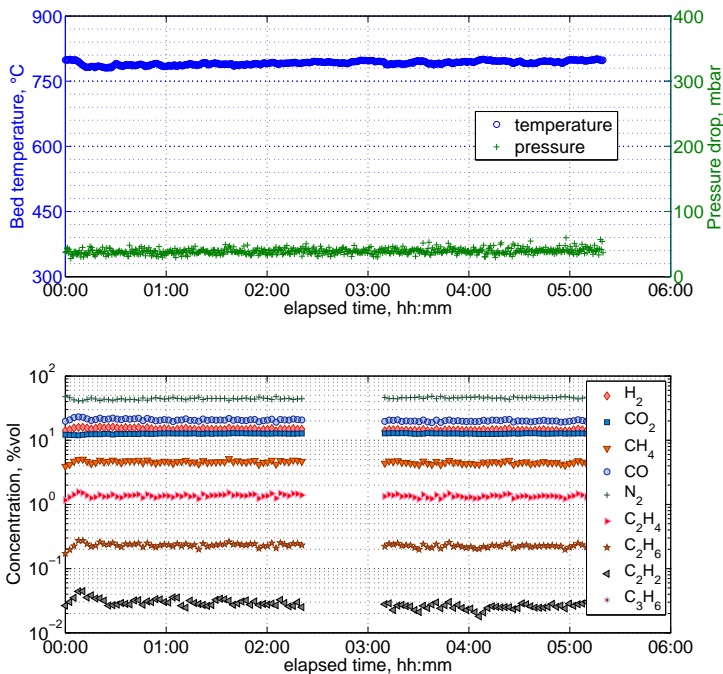
Figure α .1: *Process data for the reference experiment with wood for $\lambda = 0.22$ in a silica bed*

α .2 TGA for grass

α
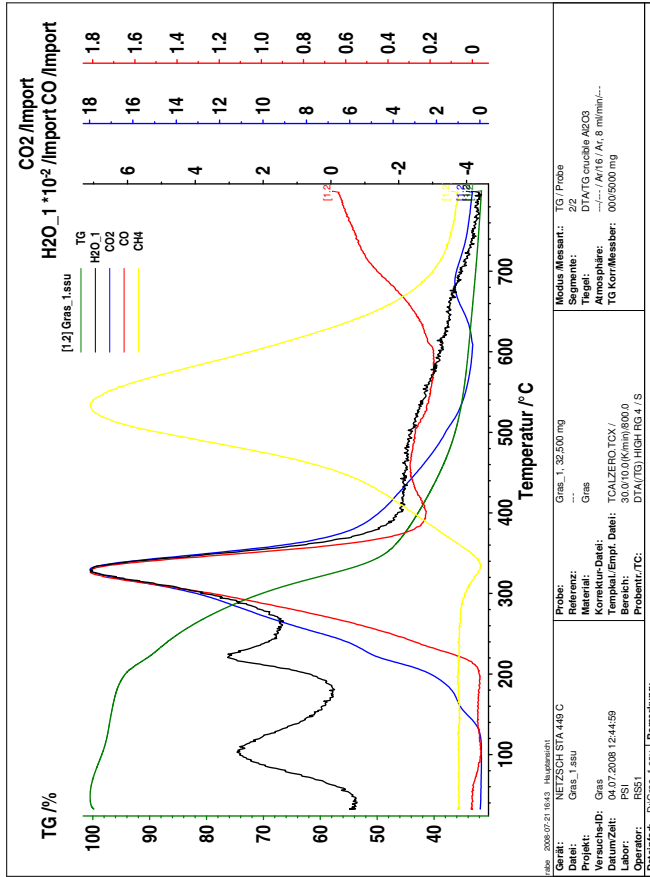
Figure α .2: *TGA for a untreated grass sample*

α .3 GC/MS tar analysis

...
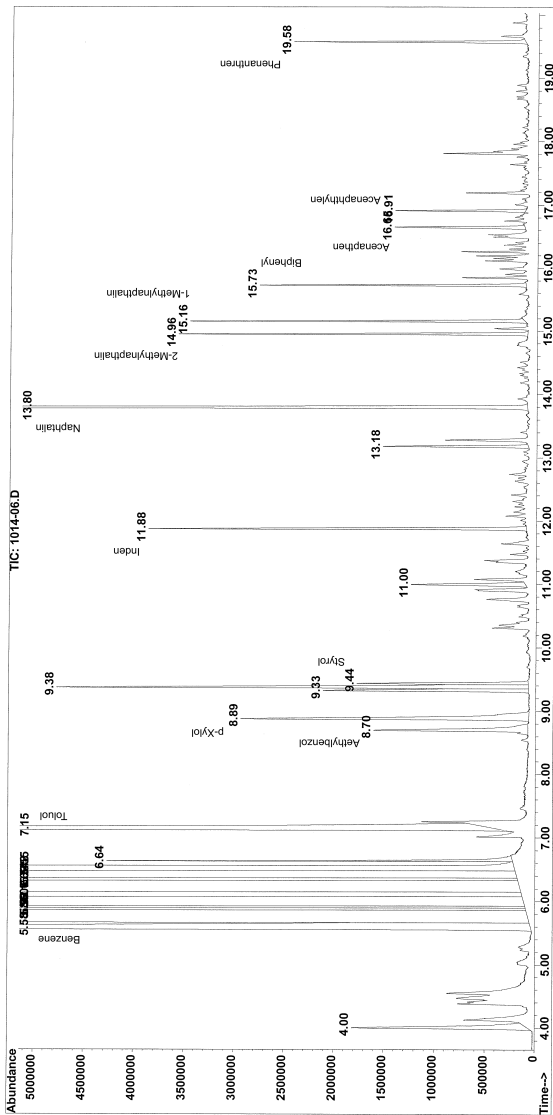
Figure α .3: GC/MS analysis of light tars: fluidised bed experiment at 750 °C, λ=0.26
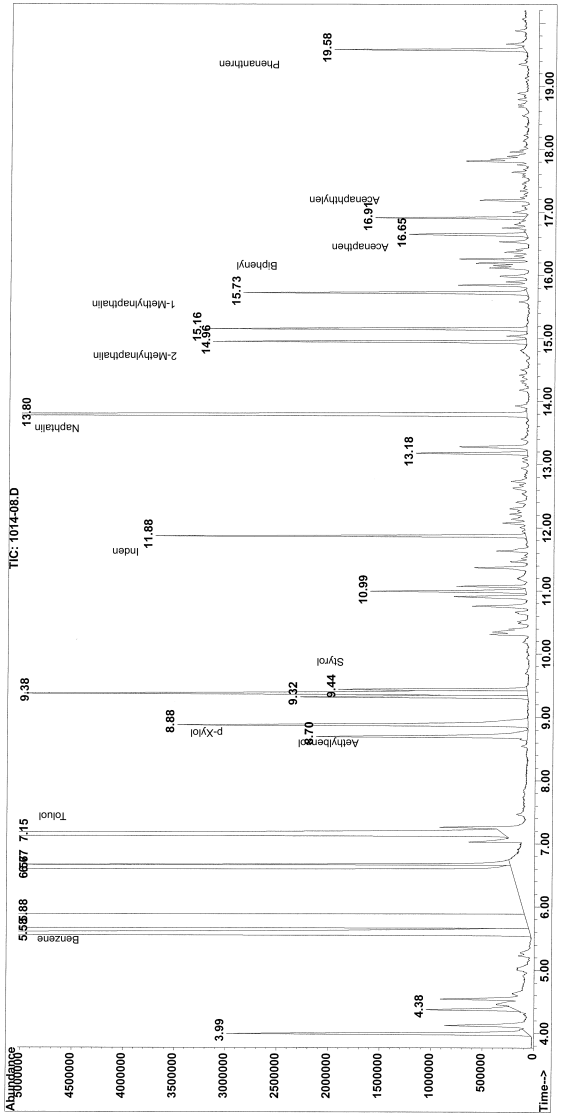
Figure α .4: GC/MS analysis of light tars: fluidised bed experiment at 750°C, λ=0.21

Appendix β

Photographs from the set ups
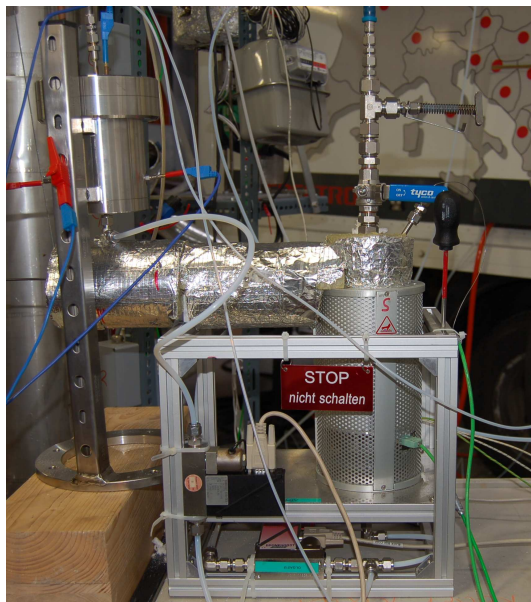
Figure β .1: *Setup of the M_iV experiments*
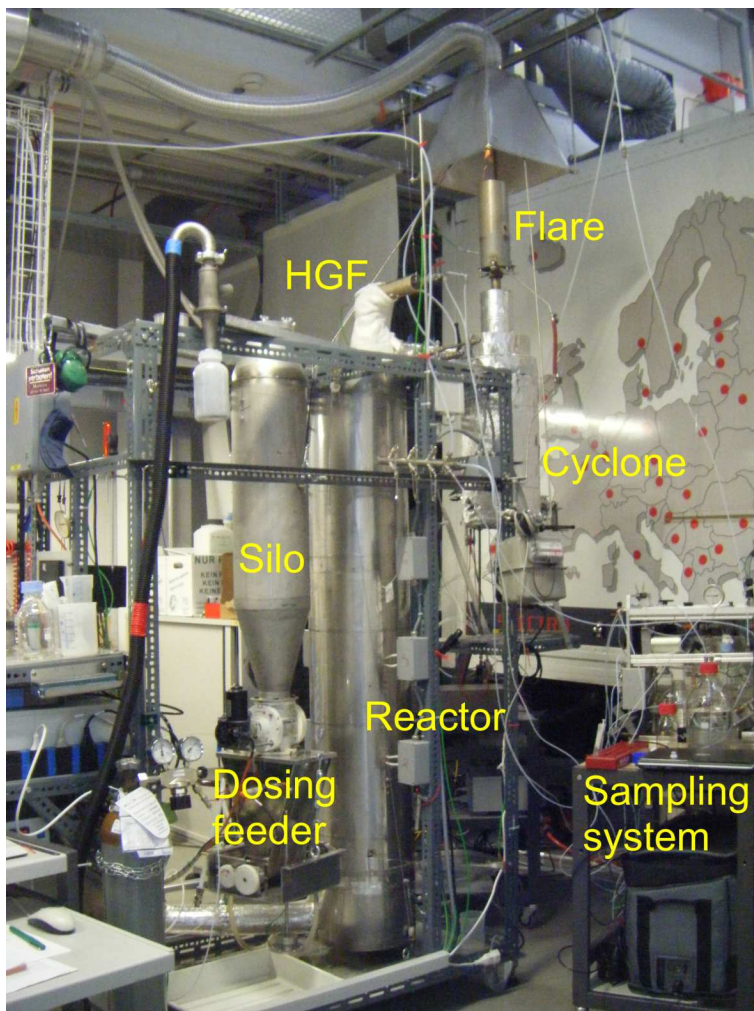
Figure β .2: *Bubbling fluidised bed test rig*

Appendix γ

Methane slip stream in a biogas plant with PSA operated CO_2 sequestration

The methane loss project was realised as a mandate of the BFE under the contract ID 101718[1]. The project name is: »*Methanverluste bei der Biogas-Aufbereitung*«.

The goal was to evaluate the loss of methane during the conditioning of the biogas from the fermentation process by means of a PSA[2] plant. The result is depicted in figure γ .1. Around 2.3 % of the methane (inlet) is released into the environment.
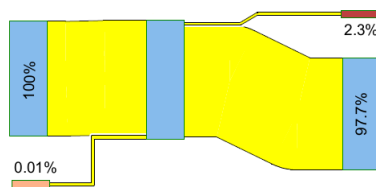
Figure γ .1: *Methane flows to and from the PSA unit*

The final report is online available at the information platform aramis.

---

[1] http://www.aramis.admin.ch/Default.aspx?page=Texte&ProjectID=21120
[2] Pressure Swing Adsorption

Index

δ

δ